A BIPHASIC ROLE FOR THE VOLTAGE-GATED SODIUM CHANNEL *SCN5LAB* IN CARDIAC DEVELOPMENT OF ZEBRAFISH

By

Jeffrey Scott Bennett

Dissertation

Submitted to the Faculty of the

Graduate School of Vanderbilt University

in partial fulfillment of the requirements

for the degree of

DOCTOR OF PHILOSOPHY

in

Human Genetics

August, 2013

Nashville, TN

Approved:

H. Scott Baldwin, M.D.

Dan Roden, M.D.

Al George, M.D.

Doug Mortlock, Ph.D.

Charles Hong, M.D., Ph.D.

To those who came before me, on whose shoulders I stand,

and

Amanda, on whose shoulders I lean.

ACKNOWLEDGEMENTS

This work would not have been possible without the assistance and support of many people and departments throughout the Vanderbilt community. I'd like to particularly thank Terry Dermody, and the leaders and administration of the Medical Scientist Training Program for years of support and encouragement, as well as the Graduate Program in Human Genetics, for providing me an academic home for these years.

So much of my academic success, present and future, is owed to the many people who got me to where I am today, and prepared me for tomorrow. My career never could have gotten started without the unfailing support of my mentor, Dan Roden. I am blessed to have been welcomed into a laboratory which truly values science and discovery, and given all I needed to be put in a position to succeed. I hope my future success reflects upon the training and commitment I received from him. Additionally, much of the assistance after I first joined lab, as well as my knowledge of developmental biology and the zebrafish model system comes from Dina Myers Stroud, who graciously served as a day-to-day mentor, teaching skills and techniques I would use over the rest of my career.

I'd also like to thank the members of my thesis committee, Al George, Charles Hong, Doug Mortlock, and the chair, Scott Baldwin. Their interest in my research and career are reflected heavily in my thesis. Leaving each committee meeting inspired and enthusiastic about my project was always encouraging, and their thoughtfulness helped shape my dissertation research, as well as my knowledge of genetics.

Much collaboration has made my life easier, and facilitated many of the findings below. Jason Becker and the members of his laboratory provided a great amount of advice and reagents, and served as a valuable co-author in the publication of many findings here. The laboratories of Josh Gamse, Charles Hong, and Jason Jessen in particular, as well as the entire zebrafish community unfailingly provided

reagents, facilities, expertise and advice. I'd like to also thank the Vanderbilt zebrafish core, led by Amanda Goodrich, for their dedication to the care and health of our research model.

This work was supported in part by Public Health Service award T32 GM07347 from the National Institute of General Medical Studies for the Vanderbilt Medical Scientist Training Program. Experiments were performed in part through the use of the VUMC Cell Imaging Shared Resource (supported by NIH grants CA68485, DK20593, DK58404, HD15052, DK59637 and EY08126).

Lastly, I'd like to thank the loved ones who inspired and pushed me along the way. My parents Wayne and Roberta always inspired me to seek answers to my questions, and instilled in me a drive and value for academic success. Amanda, my beautiful wife, partner-in-crime, and confidante, provided love and support throughout all the ups and downs of graduate training. None of this would have been possible without the three of them, their love, and their guidance.

TABLE OF CONTENTS

LIST OF TABLES

LIST OF FIGURES

CHAPTER I

INTRODUCTION

Overview

Voltage-gated ion channels play a critical role in human biology. They are largely responsible for mediating depolarization and repolarization in excitable tissues, initiating and responding to electrical signals. As a result of ion flux through voltage-gated channels, the nervous system can transmit signals throughout the body, and muscle tissue can respond to signals, producing coordinated movement and systemic circulation of blood. The bulk of the ion channel protein forms the pore and membrane spanning domains, determining gating and ion selectivity. Other conserved regions function in mediating interactions with subunits and other protein partners. Many of these relationships are required for the proper function and localization of the channel. While voltage-gated sodium channels are well-characterized in the production and propagation of action potentials in nervous and cardiac tissue, less is known of possible structural or signaling functions. Mouse knockout and zebrafish knockdown models suggest the cardiac voltage-gated sodium channel is required for development of the heart, as well playing a canonical role in action potential generation. Here I investigate the requirement for the zebrafish voltage-gated sodium channel *scn5Lab* in multiple phases of cardiac development.

Ions in Human Physiology

Ion homeostasis and human disease

Voltage-gated sodium channels (VGSCs) are a family of highly-conserved genes prominently expressed in excitable tissues. The channel proteins are complex membrane-spanning ‘alpha’ subunits,

requiring multiple binding partners to function properly in their responsibilities in mediating sodium ion flux, among other purposes. In the heart, VGSCs are required for action potential initiation and propagation, by contributing to depolarization of the myocardium. Sodium ion homeostasis is a critical component of neural and cardiac physiology, and altered function of VGSCs has been implicated in multiple human disease states, including epilepsy and cardiac arrhythmias. Recent evidence has shown ion channels to be involved in wide-ranging phenotypes from tumor invasion and metastasis, to structural disease of the myocardium.

Ion homeostasis is important in human physiology beyond the cardiovascular and nervous systems. Pore-forming proteins regulating intra- and extra-cellular concentrations of specific ions are found on the plasma membrane of nearly every tissue in the body [1]. In epithelial cells, ion flux across the membrane is required for release of hormones of the endocrine system, as well as absorption and secretion events. Activation of ion channels in the nervous system mediates response to sensory inputs such as taste and pain. Action potential generation in nerve fibers allows the central nervous system to act and react to the body's environment. Rapid transmission of electrical signals among myocytes creates the synchronous contraction of muscle fibers needed for coordinated contraction. In the cardiovascular system, regulated conduction of action potentials through each chamber is necessary for rhythm homeostasis as well as coordinated myocardial contraction. Ion channels have evolved to selectively regulate passage of charged molecules into and out of the cell in response to ligands, changes in electric potential, or mechanical stimuli [2]. In addition, the pore-forming subunit is modified through binding partners and post-translational modifications, forming a complex membrane-spanning protein which must be correctly folded and trafficked in order to function properly [2]. As a result, a change in just a single nucleotide of the coding gene can dramatically disrupt ion homeostasis and manifest in severe human disease (Table 1.1).

One well-characterized disease caused by ion channel dysfunction is cystic fibrosis, the most common lethal inherited disease among Caucasians [3]. In the most common form of this disease, the ligand-gated channel encoded by CFTR has a single amino acid deletion which disrupts folding of the channel and impairs trafficking of the protein to the cell surface [4]. Degradation of the channel results in an inability of epithelial tissue to resorb chloride ions from secretions, and the production of secretions with high salinity [5]. In the lungs, loss of Cl^- efflux results in production of thick, dehydrated mucus, and leaves patients susceptible to ultimately fatal severe pulmonary infections [6]. Disruptions in gradients of other ions cause disease as well. As the regulator of systemic ion concentrations, the kidney is particularly sensitive to ion channel mutations. Mutations in the genes encoding channels such as the ligand-sensitive renal outer medullary potassium channel (ROMK) [7], the epithelial sodium channel (ENaC) [8], and voltage-gated chloride channels [9], have been demonstrated to cause disease ranging from salt wasting to hypertension. Alterations in ion channel activity in the inner ear have been identified in syndromes resulting in sensorineural hearing loss [10, 11].

Alterations of voltage-gated ion channels function are well-described in disorders of the nervous system. These channels respond to alterations in membrane potential by opening and closing, allowing the brain to coordinate ion channel activity in sending and receiving signals to and from tissues. When variants in ion channel function prevents normal signal generation or transduction, neural disorders such as epilepsy can occur. Mutations in any of a number of voltage-gated sodium channels and their subunits, in particular *SCN1A*, have been associated with the disease [12]. Mutations in *SCN1A* have been linked to febrile seizures, myoclonic epilepsy, and generalized tonic-clonic seizures [13], all resulting from coordinated misfiring of neurons and aberrant signals sent throughout the body [2]. In addition, neural voltage-gated potassium channels have been implicated in susceptibility or onset of epilepsy [14, 15].

Table 1.1 Selected Ion Channels and Disease: Mutations in ion channel genes result in a wide variety of human disease. Phenotypes occur in many different tissues, from alterations in channels with a wide variety of ion selectivity and gating. Below is a list of selected genes encoding ion channels and exchangers, and some phenotypes resulting from their dysfunction.

Gene	Ion(s)	Gating	Phenotype
CFTR	Chloride	ATP	Cystic fibrosis
SLC26A3	Chloride, Bicarbonate	Ion Exchanger	Congenital chloride diarrhea
GLRA1	Chloride	Glycine	Hyperekplexia
SLC4A1	Chloride, Bicarbonate	Ion Exchanger	Renal Tubular Acidosis
GABRA1A	Chloride	GABA	Myoclonic epilepsy
KCNQ1	Potassium	Voltage	Long QT Syndrome 1
KCNQ4	Potassium	Voltage	Deafness
HERG	Potassium	Voltage	Long QT Syndrome 2
ENAC	Sodium	Ligand	Pseudohypoaldosteronism
SCN4A	Sodium	Voltage	Paramyotonia Congenita
SCN5A	Sodium	Voltage	Long QT Syndrome 3
SCN5A	Sodium	Voltage	Dilated Cardiomyopathy
SCN5A	Sodium	Voltage	Brugada Syndrome 1
SCN9A	Sodium	Voltage	Paroxysmal extreme pain disorder
SCN9A	Sodium	Voltage	Congenital insensitivity to pain
CACNA1C	Calcium	Voltage	Brugada Syndrome 3
CACNA1C	Calcium	Voltage	Long QT Syndrome 8
CACNA1A	Calcium	Voltage	Episodic Ataxia
RYR	Calcium	Calcium	Sudden Cardiac Death [16]
CACNA1F	Calcium	Voltage	Retinitis Pigmentosa

Muscular contraction requires rapid, coordinated impulses and immediate shortening by muscle fibers in response. Through voltage-gated ion channels, local currents generated and propagated along the sarcolemma, creating an action potential [2]. In the heart, this process must be repeated over and over in a fast and efficient manner, allowing cardiac muscle to sense, propagate, and respond to the change in current, then re-set and prepare for the subsequent action potential. When a mutation in an ion channel disrupts this process, fatal arrhythmias can occur. Brugada syndrome is significant cause of sudden cardiac death in otherwise healthy young males [17]. The syndrome has a characteristic profile on an electrocardiogram, and responsible mutations have been identified in voltage-gated potassium channels and their subunits, and the L-type calcium channel, though the most common form results

from mutations in the voltage-gated sodium channel *SCN5A* [17, 18]. Another classification, Long QT Syndrome, results in slowed action potential conduction, and susceptibility to arrhythmias. Responsible mutations are often found in voltage-gated potassium channels, but have been identified in voltage-gated sodium channels as well as channel binding partners and subunits [19, 20]. These two diseases are discussed in more detail below.

Excitable membranes in human cardiac biology

Action potentials are generated by the time-dependent flow of ion currents across the membranes of individual cells. They represent the rapid depolarization of a cell's membrane, transmitted to its neighbor and so on, resulting in propagation of impulses along axons in neurons and from myocyte to myocyte in muscles, including the heart. All cells at rest have a resting membrane potential, usually between -40 and -80 millivolts (mV), determined by the intra- and extracellular concentrations of anions and cations, and their permeabilities through the cell membrane. Two important cations, potassium and sodium, are maintained at high gradients across the cell membrane, primarily by a sodium-potassium pump (Na^+-K^+ ATPase). Using adenosine triphosphate (ATP) as an energy source, the exchanger pumps potassium into the cell and sodium out of the cell, creating a concentration gradient for each. In addition, for every three molecules of Na^+ pumped into the extracellular space, only two K^+ ions are pumped in, creating a net negative charge inside the cell.

Membrane potential of a cell is determined by the electrical and chemical (electrochemical) gradients of each on in the cell, and the permeability of the membrane to each. The cell membranes of cardiomyocytes are highly permeable to potassium, largely due to the presence of potassium 'leak' channels called inward rectifiers (I_{Klr}). As a result, the resting membrane potential in myocardium is largely determined by the potassium gradient. The high intracellular concentration of K^+ would normally allow for diffusion of K^+ outside the cell; however the presence of negatively-charged molecules in the cell creates an electrical gradient opposing the diffusion loss of potassium. The measured voltage across

the membrane at the state where net membrane flux of an ion is zero is the equilibrium potential for that ion. The equilibrium potential of each ion of a cell can be described using the Nernst equation:

$$V = \frac{RT}{zF} * ln(\frac{C_o}{C_i})$$

where V= the equilibrium potential in voltage, R=the gas constant, T=temperature (K), F=Faraday's constant, z=valence charge of the electron, and C_o/C_i is the ratio of ion concentration outside/inside the cell [2]. At membrane potentials more positive than the equilibrium potential for a cation like potassium, the ions will exit the cell, according to the concentration gradient. In the case of potassium, the negative resting membrane potential of the cell inhibits the flow of potassium down its concentration gradient and out of the cell. The Nernst potential of each ion can be used to calculate the membrane potential of a cell. The Goldman–Hodgkin–Katz voltage equation is similar to the Nernst equation; however it takes into account permeability of each ion:

$$V_m = \frac{RT}{F} * \ln(\frac{p_K[K^+]_o + p_{Na}[Na^+]_o + p_{Cl}[Cl^-]_i}{p_K[K^+]_i + p_{Na}[Na^+]_i + p_{Cl}[Cl^-]_o})$$

where V_m=membrane potential, p_K=permeability of the membrane to potassium, and $[K^+]_i/[K^+]_o$ are the concentrations of K^+ inside and outside the cell, respectively [2].

In response to varying membrane potential, typical voltage-gated sodium channels have three states: open, closed, and inactive (Figure 1.1). The channel cycles through these states rapidly in response to a voltage stimulus. At resting membrane potential, channels typically exist in a closed state. Depolarization of the membrane results in a physical change in conformation of the channel to an open state, allowing in influx of Na^+ ions into the cell, along the electrochemical gradient. At rest, cardiomyocytes maintain a low intracellular concentration of sodium relative to the extracellular space resulting in a steep concentration gradient. In addition, the resting membrane potential of a ventricular cardiomyocyte is very negative (-90mV), resulting in an electric potential promoting the rapid entry of positively charged Na^+ ions into the negatively charged myocyte. Immediately following opening and Na^+

flux through the pore of the channel, VGSCs enter an inactivated conformation, where the pore is physically occluded by the inactivation domain of the protein. As the cell repolarizes towards resting membrane potential, the channels alter conformation yet again to recover from inactivation, entering the closed state from which they can again open in response to membrane depolarization.

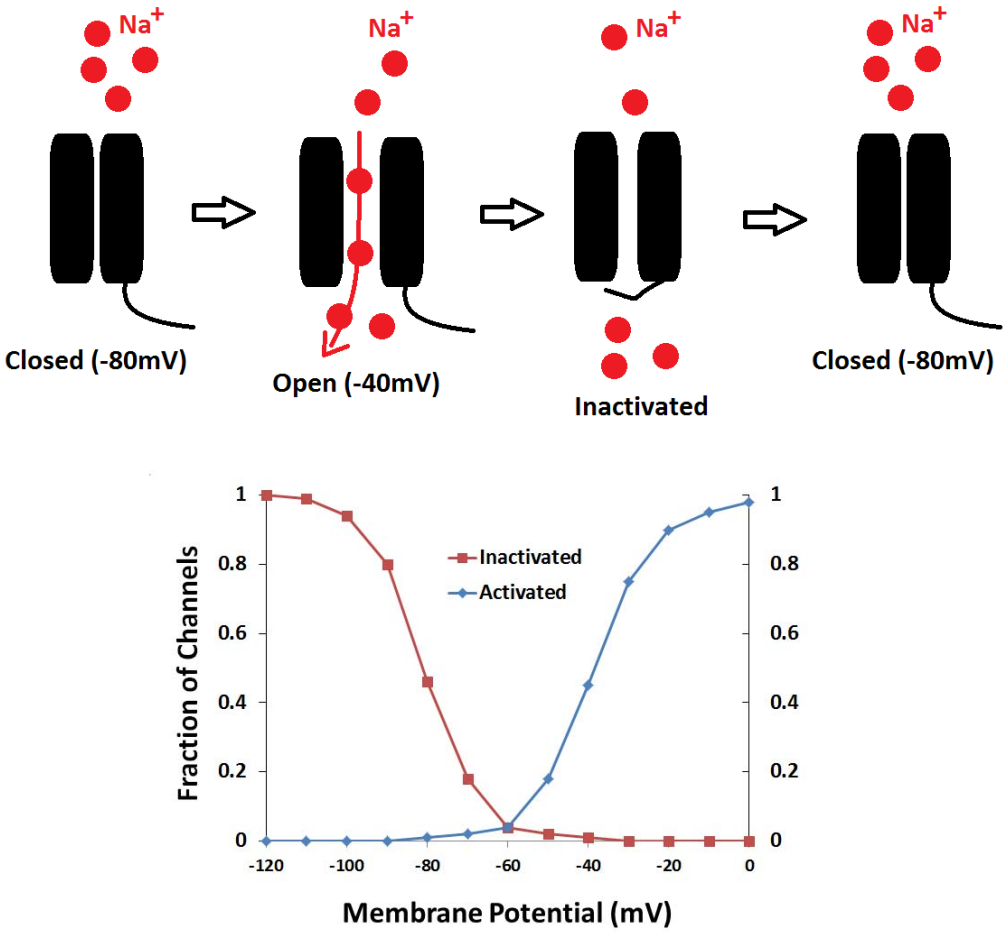

Figure 1.1: Gating states of voltage-gated sodium channels. At normal cardiac resting membrane potentials, most sodium channels are closed (top left). Depolarization of the membrane results in shifting of the voltage sensing domains, opening the channel and allowing sodium ion flux into the cell. Immediately following depolarization, the channel becomes fast inactivated by a hinged lid. As the cardiomyocyte repolarizes, the channel returns to a de-inactivated closed state, ready to open in response to a stimulus. *In vitro* studies have determined voltage-dependent activation and inactivation of voltage-gated sodium channels (bottom). At cardiomyocyte resting membrane potential (-90mV), very few sodium channels are open, while maximal sodium current is achieved at depolarized voltages (Data approximated from Amin *et al*, 2010 [21]).

At typical ventricular resting membrane potentials (-90mV), nearly 100% of voltage-gated sodium channels are closed, with very few in the inactivated state [21]. A ventricular action potential (Figure 1.2) is initiated by a depolarizing stimulus (most often from a neighboring cell), resulting in the rapid opening of voltage gated sodium current, and influx of Na^+ ions and depolarization of the myocyte (I_{Na}, action potential Phase 0). Very quickly after depolarization, Na^+ flux is complete and VGSCs become inactivated, while repolarizing transient outward potassium current (I_{TO}) is activated (Phase 1). Phase 2 of the action potential features a plateau, where opposing inward ($I_{Ca\text{-}L}$ current through L-type calcium channels) and outward potassium delayed rectifiers keep the membrane potential stable. Calcium ions are required for allosteric activation of the contractile apparatus. Ca^{2+} enters the cell from the extracellular space via $I_{Ca\text{-}L}$, and subsequent calcium-induced calcium release from the sarcoplasmic reticulum through the ryanodine receptor (RyR). Cardiomyocyte repolarization completes during Phase 3, as potassium continues to exit the cell through the slow (I_{Ks}) and the rapid (I_{Kr}) delayed rectifiers. In phase 4, the membrane potential has been restored, and the ion concentrations are re-established through the function of ion exchangers and pumps. Calcium is removed from the cytosol via the Na^+/Ca^{2+} exchanger, which allows three Na+ ions to flow down its concentration gradient into the cell, in exchange for removal of one Ca^{2+} ion [22]. The sarco/endoplasmic reticulum Ca^{2+} ATPase (SERCA) also removes Ca^{2+} from the cytosol, using ATP hydrolysis as an energy source [23]. Another ATPase, the Na^+/K^+ pump, removes three Na^+ ions from the cytosol, in exchange for two K^+ ions from the extracellular space, and also serves to repolarize the membrane. Additionally, the potassium inward rectifier helps to set the resting membrane potential during Phase 4, allowing K^+ ions into the cell at voltages more negative than the potassium equilibrium potential [24].

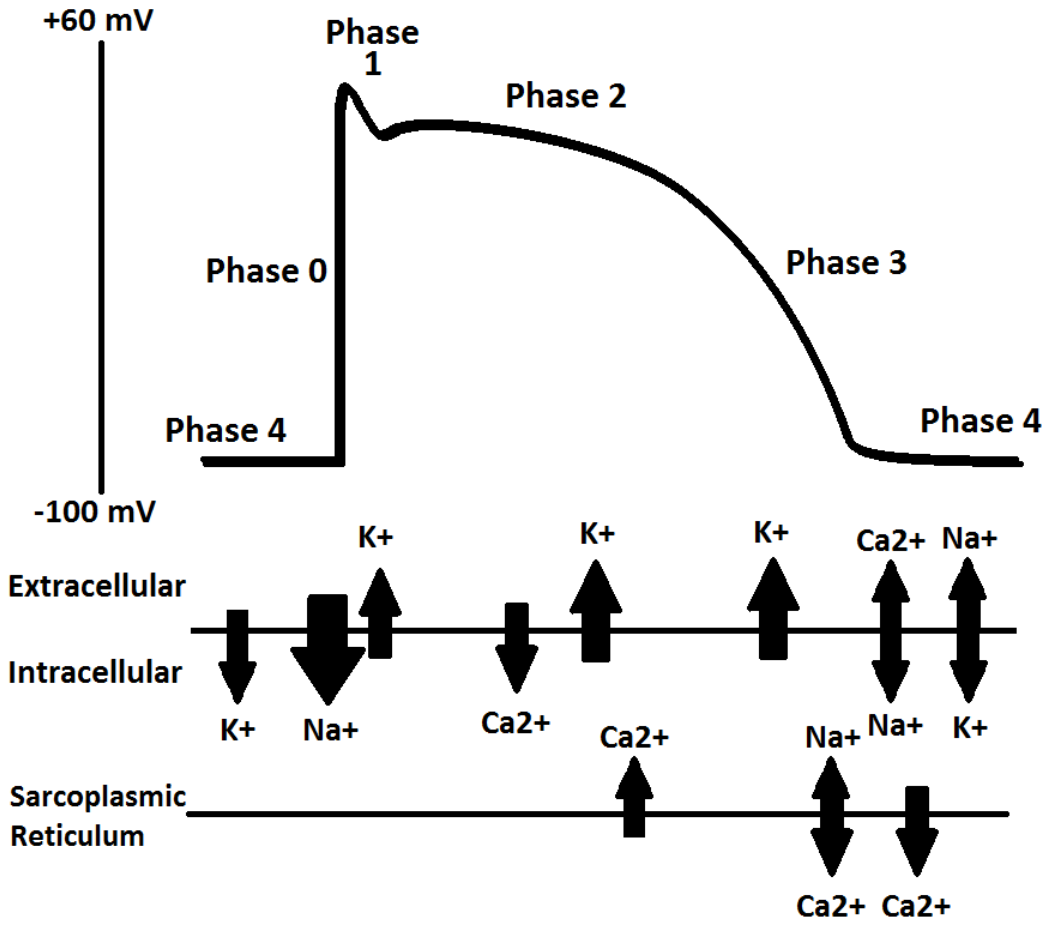

Figure 1.2: Ventricular cardiac action potential and ion currents. Ventricular myocytes have a resting potential (Phase 4) of -90mV, and rapidly depolarize in Phase 0 with influx of sodium current. Transient outward potassium current (I_{To}, Phase 1) and delayed rectifiers (I_{KS} and I_{KR}, Phase 2 and Phase 3) provide repolarizing currents, while inward calcium flux from the extracellular space (I_{Ca}) and the sarcoplasmic reticulum (RyR) is responsible for the plateau in Phase 2, as well as excitation-contraction coupling. Inward potassium current (I_{K1}) during Phase 3 is also responsible for restoring the resting membrane potential. In Phase 4, the sodium-calcium exchanger (NCX) and sodium-potassium pump are responsible for restoring ions to pre-excitation levels.

Evolution and Structure of Voltage-Gated Sodium Channels

Voltage-gated sodium channel genes: homology, and conservation

The earliest ion channels first appeared three billion years ago, as potassium inward rectifiers in early bacteria [25]. The channels consisted of two membrane-spanning helices (2TM), separated by a pore forming loop. Since then, potassium channels have evolved in eukaryotes to encode six membrane-spanning helices (6TM) in a single domain, which then associate *in vivo* as homotetramers to form functional channels. During evolution of the 6TM domain, a string of positively-charged residues in the fourth membrane-spanning helix (S4) evolved to function as a voltage sensor. A round of gene duplication produced a channel with two 6TM domains, which dimerized *in vivo* to form a complete channel. A second duplication event resulted in a gene encoding all four 6TM domains in a single channel protein, a voltage-gated calcium channel (VGCC). Much of the evolutionary evidence for this second round of duplication arises from the fact that the first and third, and second and fourth 6TM domains have a higher degree of similarity to each other, than to the other domains. VGCCs are commonly thought of as phylogenetic precursors of voltage-gated sodium channels [26], and functioned in early eukaryotes functioned as mediators of intracellular signaling. Homologs for voltage-gated sodium channels are thought to have evolved from voltage-gated calcium channels 800 million years ago, 150 million years before multicellular animals – and the muscles and nervous system which rely on their function today – appeared [27]. When early iterations of the nervous system evolved, sodium currents were used in action potential generation, to avoid interference with calcium signaling of the cell [27, 28].

Today, homologs of voltage-gated sodium channel genes (*SCNA*) found in lower organisms still have strong conservation to vertebrates in residues critical for ion selectivity and inactivation of the channel [27]. While early eukaryotes contained just one voltage-gated sodium channel gene, early

genome duplications in vertebrates gave teleosts (ray finned fishes) and tetrapods four phylogenetically-related genes/ families [29, 30]. The teleost genome underwent an additional duplication, giving its members four pairs of *SCNA* genes, eight in total. The four *SCNA* genes in mammals underwent additional duplications due to close association of the *SCNA* genes to HOX gene clusters [31, 32], giving the mammalian genome possesses nine voltage-gated sodium channel genes on four chromosomes, each corresponding to a unique protein and resulting current notated with $Na_V1.n$ [33] (Table 1.2). A tenth *SCNA* gene is phylogentically related to the largest *SCNA* family, but appears to have lost its voltage-gating mechanism.

The genes for voltage-gated sodium channels in humans generally contain between 24 and 28 exons, coding for anywhere from 1791 to 2016 amino acid residues (e!Ensembl Genome Browser [34]). The genes are very often differentially spliced, and the translation start site is generally located in the second exon, with a few exceptions. Regional duplications have resulted in 'families' of voltage-gated sodium channels in specific genomic locations. The genes are expressed in a wide range of tissues, with specific function and distribution possessing some correlation to phylogeny.

SCN1A, *SCN2A*, *SCN3A*, *SCN9A* are all located on chromosome 2, and expressed in the central or peripheral nervous system. They all function in action potential initiation and conduction in neurons [33]. In addition, the channels encoded by these genes all possess residues which confer sensitivity to nanomolar concentrations of the channel blocker tetrodotoxin (TTX), and Na_V1-3 are common targets for antiepileptic drugs [33]. Gain-of-function mutations in *SCN9A* ($Na_V1.7$) have been identified in paroxysmal extreme pain disorder, while homozygous loss-of-function renders patients insensitive to pain [35]. Thus the channel represents an important pharmacologic target for development of analgesics. Also located in this family on chromosome 2 is the more distantly-related *SCN7A* gene, encoding a channel Na_X (also known as Na2 and Na_G) which appears to be activated by increasing sodium ion concentration, rather than voltage [36, 37].

Two voltage-gated sodium channel genes lie independent of any gene clusters. On chromosome 12, *SCN8A* is expressed primarily in the nervous system. In 2006, a mutation resulting in early termination of SCN8A protein ($Na_V1.6$) has been identified in a patient with mental retardation and ataxia, however the genotype-phenotype relationship has not been firmly established [38]. Since then studies in a human family affected by epilepsy and ataxia [39] and mouse models of induced *SCN8A* mutations [40] have correlated loss of *SCN8A* function to those phenotypes. A second single gene, *SCN4A* (chromosome 17) is a mediator of action potential initiation and conduction in skeletal muscle [32, 33]. Mutations in *SCN4A* have been identified as causing hypokalemic and hyperkalemic periodic paralysis [41], and paramyotonia congenita, a disease of hyperexcitable muscles and impaired muscle relaxation which is worsened in cold or increased potassium levels [42, 43].

Table 1.2: Human voltage-gated sodium channel genes: Humans have nine voltage-gated sodium channel genes, and one related channel encoded by *SCN7A*. The genes have between 24-28 exons, with translation often starting in the second exon. ANS = autonomic nervous system. *= common alternatively spliced variants have been identified

Gene	Location	Channel	Primary Expression	Exons/Coding	Amino Acids*
SCN1A	2q24.3	$Na_V1.1$	Central Nervous System	26/26	2009*
SCN2A	2q24.3	$Na_V1.2$	Central Nervous System	27/26	2005
SCN3A	2q24	$Na_V1.3$	Central Nervous System	28/26	2000*
SCN4A	17q23.2	$Na_V1.4$	Skeletal muscle	24/24	1836
SCN5A	3p21	$Na_V1.5$	Heart	28/27	2016*
SCN7A	2q23	Na_X	Hippocampus	25/24	1682
SCN8A	12q13	$Na_V1.6$	Cerebellum, cortex	27/26	1980*
SCN9A	2q24	$Na_V1.7$	Dorsal root ganglia	27/26	1989*
SCN10A	3p22.2	$Na_V1.8$	Dorsal root ganglia, Heart	27/27	1956
SCN11A	3p22.2	$Na_V1.9$	Dorsal root ganglia	26/26	1791

The remaining three *SCNA* genes (SCN5A, SCN10A, SCN11A) reside in a cluster on chromosome 3p21, and all possess a residue in the S5-S6 loop of domain I conferring TTX-resistance [13, 33]. *SCN5A* is the predominant channel responsible for action potential generation in the heart (Phase 0 depolarization), though its protein $Na_V1.5$ is also expressed in skeletal muscle and nervous tissues [13, 18]. *SCN10A* and *SCN11A* are noted for expression in the peripheral nervous system, modulating action potentials through slowed inactivation and sub-threshold depolarization [33]. Recent evidence suggests that in addition to expression in the nervous system, $Na_V1.8$ (encoded by *SCN10A*) is expressed in the heart and contributes to arrhythmia susceptibility [44]. A genome-wide association study in European Americans identified four SNPs in linkage disequilibrium (LD) with the *SCN10A* gene which were associated with PR interval in patients with normal ECGs [45]. Further studies found the addition of A-803467, a specific blocker $Na_V1.8$ (and not $Na_V1.5$) to isolated mouse cardiomyocytes *in vitro* resulted in shortened action potential duration, and had an antiarrhythmic effect. $Na_V1.8$ expression is also detected in pre-cardiac ganglia, and despite the effect observed by inhibition of $Na_V1.8$ in cardiomyocytes, the possibility exists that the protein modulates cardiac electrophysiology through innervation of the heart. In addition, $Na_V1.1$ (*SCN1A*), $Na_V1.3$ (*SCN3A*) and $Na_V1.6$ (*SCN8A*) also have cardiac expression, likely in the T-tubules and may function in excitation-contraction coupling [46, 47].

The primary cardiac sodium channel gene in humans, *SCN5A* consists of 28 exons, encoding a protein of 2016 amino acids [48, 49]. The length of the mRNA varies with alternative splicing, but the most common cardiac isoform has a length of 8504 bases, including the 5' and 3' untranslated regions (UTRs) [50-52]. A 2.7 kb promoter has been cloned, with both strong positive and negative regulatory regions [53]. In addition, recent evidence has identified at least one regulatory region for the channel resides inside an intron [54]. The *SCN5A* gene is highly conserved among model systems (Table 1.3). Within primates, the gene is 95-99% conserved in primates, both at the DNA and protein levels [55].

Scn5a in the mouse *Mus musculus* consists of 2020 amino acid residues with 94.7% protein identity to human *SCN5A*, with 89.5% DNA identity [55].

Table 1.3: *SCN5A* Homology. The cardiac voltage-gated sodium channel is highly conserved across many species, at both the DNA and protein sequences. Identity of *SCN5A* in mammals at the protein level (AA%) is greater than 90% conserved, and nearly as high at the nucleotide level (DNA%) .

Species	Symbol	Amino Acids	AA%	DNA%
H.sapiens	SCN5A	2016		
vs. P.troglodytes (Chimpanzee)	SCN5A	2016	99.3	99.3
vs. M.mulatta (Macaque)	LOC695085	2003	94.8	95
vs. C.lupus (Gray wolf)	SCN5A	2013	94.1	90.6
vs. B.taurus (Cattle)	SCN5A	2022	92.5	90.2
vs. M.musculus (Mouse)	Scn5a	2020	94.7	89.5
vs. R.norvegicus (Rat)	Scn5a	2019	93.9	89.1
vs. G.gallus (Chicken)	SCN5A	2038	77.7	72
vs. D.rerio (Zebrafish, isoform b)	scn12ab	1954	68.4	67.7
vs. D.rerio (Zebrafish, isoform a)	scn12aa	1932	67.9	66.2

The genome of the zebrafish, *Danio rerio* encodes eight voltage-gated sodium channel genes, in four pairs as a result of the teleost genome duplication (Table 1.4) [32]. The genes are generally noted with the sodium channel designation “scn”, a number representing the most evolutionarily similar mammalian VGSC (with or without an “L” for ‘like’), “a” for alpha subunit, and an additional ‘a’ or ‘b’ denoting which duplicated homolog is being discussed [56]. A duplicated pair of genes may also be denoted by dropping the final letter, referring to the pair of homologs; *scn1Laa* and *scn1Lab* may be referred to as *scn1La* collectively.

A 2006 study of voltage-gated sodium channels in zebrafish identified the homology and expression patterns of the four pairs of genes (Figure 1.3) [56]. The orthologous genes to the *SCN1A*/*SCN2A*/*SCN3A*/*SCN9A* family in mammals, *scn1Laa* and *scn1Lab* (*scn1La*) have the least identity to each other of any VGSC pair in zebrafish, at 68%. The two channels have distinct embryonic expression patterns as well, with *scn1Laa* expressed in the dorsal (sensory) nervous system, and *scn1Lab*

expressed in the ventral (motor) nervous system [56]. A mutation in *scn1Lab* has been identified in the *double indemnity (didy)* zebrafish line, resulting in impaired generation of fast eye movements [57]. The *scn4aa*/*scn4ab* pair of genes is orthologous to *SCN4A* in mammals, and appears to have similar function in action potential generation in skeletal muscle. The two genes are expressed in anterior mesoderm, pharyngeal muscle, and in trunk somites in zebrafish embryos. The *scn8a* homologs (*scn8aa* and *scn8ab*) have a high degree of identity with each other, and like their ortholog *SCN8A*, are expressed in neural tissue. *Scn8aa* and *scn8ab* isoforms are required in the transdifferentiation of the sympathetic nervous system, motor neuron excitability, and tactile sensitivity and locomotor responses [58-60].

The zebrafish cardiac voltage-gated sodium channels, *scn5Laa* and *scn5Lab* are evolutionarily related to the SCN5A/SCN10A/SCN11A mammalian VGSC family located on chromosome 3 in humans [56]. The two homologs have 67.9% and 68.4% DNA identity to *SCN5A*, and 66.2% and 67.7% protein identity, respectively [55]. Consistent with the whole genome duplication in teleosts, *scn5Laa* (2) and *scn5Lab* (24) reside on separate chromosomes, and have 77% DNA identity, and 84% protein identity to each other [55, 56]. The two channels are slightly smaller than their mammalian counterparts, with 1932 (*scn5Laa*) and 1954 (*scn5Lab*) amino acids [55]. In the embryo, *scn5Laa* expression is detected as early as 24 hours post-fertilization (hpf) in the developing heart tube, while *scn5Lab* is observed in trunk somites and nervous tissue [56]. Other studies have detected diffuse expression of *scn5Laa* and *scn5Lab* in the heart at 2 days post fertilization (dpf) with increasing ventricular expression as development proceeds [61].

Table 1.4: Zebrafish voltage-gated sodium channel genes: The zebrafish genome possesses four pairs of voltage-gated sodium channel genes, with orthologous expression and function to human VGSCs. *Scn1Laa* and *scn1Lab* have the lowest amino acid sequence identity, and *scn8aa/scn8ab* have the highest pairwise identity. Expression listed below refers to embryonic and larval expression of mRNA. Chr. = chromosome number. *scn5Laa/scn5Lab are also referred to in literature as scn12aa/scn12ab.

Gene	Chr.	Primary Expression	Amino Acids	Identity/Similarity
scn1Laa	9	sensory neurons	1955	68%/79%
scn1Lab	6	motor neurons	1996	
scn4aa	12	skeletal muscle	1829	70%/80%
scn4ab	3	skeletal muscle	1784	
*scn5Laa**	2	heart	1932	77%/84%
*scn5Lab**	24	heart, mesoderm	1954	
scn8aa	23	dorsal root ganglia	1949	87%/92%
scn8ab	6	brain	1958	

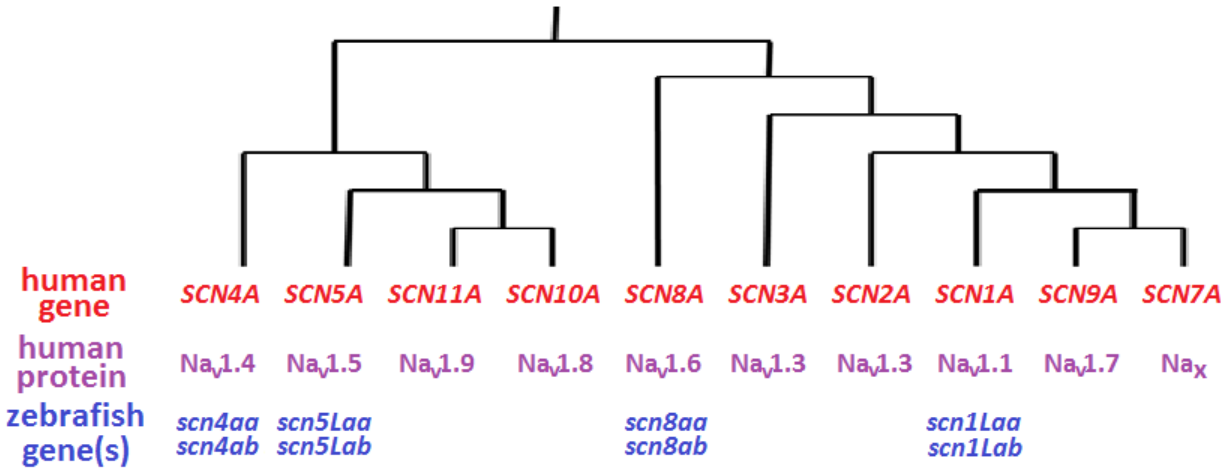

Figure 1.3: Phylogeny of human and zebrafish voltage-gated sodium channel genes. The human genome has two families of VGSC genes, and two other isolated genes on individual chromosomes: SCN4A, SCN5A/10A/11A, SCN8A, and SCN1A/2A/3A/7A/9A. Each gene has an $Na_V1.x$ protein designation, with the exception of *SCN7A* (not voltage-gated gated). The zebrafish genome possesses an orthologous pair of genes for each *SCNA* family, a result of whole genome duplication. (Note: line lengths not representative of evolutionary distance) [25, 31, 32].

Structure and function of cell biology of the sodium channel

Voltage-gated sodium channels have a stereotyped structure, with critical residues for ion selectivity, channel gating, and binding partners highly conserved from species to species. The channel consists of four transmembrane domains, each with six membrane-spanning helices (Figure 1.4). The fourth membrane-spanning helix of each domain contains a series of positively-charged residues spaced at three amino acid intervals, and functioning as a voltage-sensor for the channel [62]. In response to depolarization of the membrane, the positively-charged residues of each helix shift towards the extracellular aspect of the membrane and the helices rotate, opening the pore of channel and allowing sodium ion flux [1]. Connecting the 5^{th} and 6^{th} helix of each domain is a pore-forming loop [63]. Within each loop is a residue functioning in ion selectivity, aspartic acid (D, domain I), glutamic acid (E, domain II), lysine (K, domain III) and alanine (A, domain IV), forming the sodium ion-specific D-E-K-A ring [26] . A cysteine residue at the C-terminal position of the aspartate of the pore ring is responsible for tetrodotoxin resistance in some voltage-gated sodium channels, including $Na_V1.5$ [64].

In contrast to the potassium channels which feature a single six-segment domain and assemble as tetramers, the voltage-gated sodium channels are encoded as a single large protein with four domains [62]. Joining each domain is an intracellular linker, along with larger intracellular domains at the N- and C- terminus. The function of the N-terminal domain, despite regions of high conservation, is not well-classified, however disease-causing mutations in both neural channels (ataxia) and cardiac channels (Brugada syndrome) have been identified within the region [40, 65]. Evidence suggests the mechanism for N-terminal mutation diseases involve defective trafficking and binding partner associations [40, 65]. Transmembrane domains I and II are connected by a nearly 300 residue loop, containing highly-conserved residues for intracellular trafficking, with three endoplasmic reticulum (ER) retention motifs, as well as multiple serine residues serving as phosphorylation sites [66]. The intracellular loop connecting domains II and III in voltage-gated sodium channels contains a binding site

for ankyrin-G [67]. In $Na_V1.5$, this motif is required for membrane targeting of the channel, one of many protein interactions required to ensure normal spatial expression of the channel [68].

The region of residues connecting domains III and IV is thought to serve as an inactivating loop, blocking the channel pore from the intracellular side after Phase 0 of the action potential [33]. Accordingly, mutations in the region often contribute to cardiac channelopathies; diseases caused by mutations in ion channels themselves or their binding partners which result in perturbed function of the channels. Three residues (isoleucine-phenylalanine-methionine) in the III-IV linker form the IFM motif critical for fast inactivation of the channel [69]. The motif has been proposed to serve as a hydrophobic latch, stabilizing the channel in the inactivated state. Another three reside motif KPQ (lysine-phenylalanine-glutamate) is also involved in gating of the channel, playing an important role in determining the rate of inactivation, and recovery from inactivation [70]. Deletion of the nine bases coding for this tripeptide motif has been shown to result in a persistent inward sodium current, and was identified as causing some cases of congenital long QT syndrome [71]. Later studies have since identified deletions of single amino acids within the motifs in other cases of fatal arrhythmias [72].

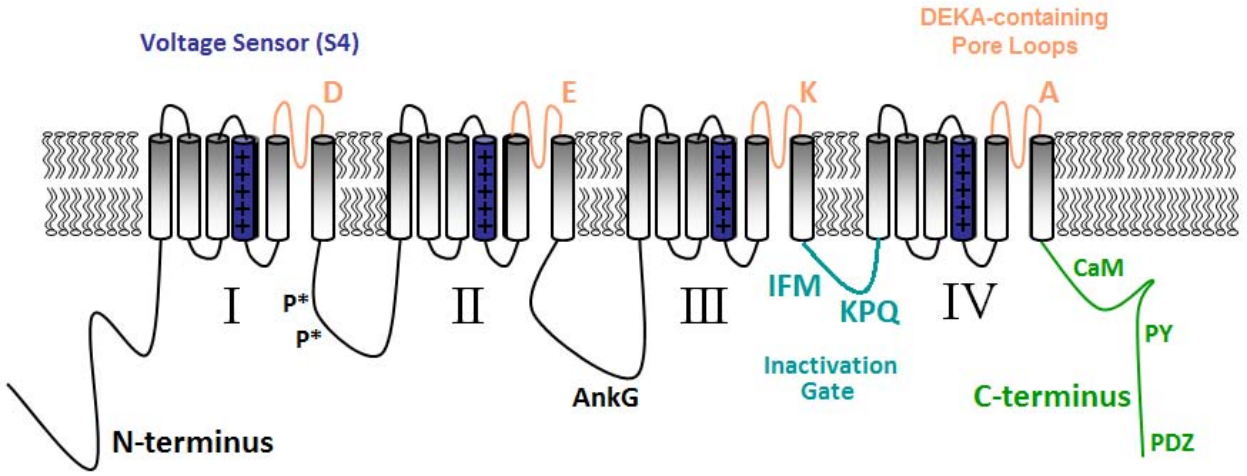

Figure 1.4: The cardiac voltage-gated sodium channel. Voltage-gated sodium channels are composed of four transmembrane domains, each with six membrane-spanning helices. The fourth helix in each domain functions as a voltage-sensor. The extracellular pore consists of residues in the loops joining the fifth and sixth helix, and each contains a conserved residue (D-E-K-A) functioning in ion selectivity. The intracellular inactivation gate between domains III and IV, with two highly conserved tripeptide motifs (I-F-M and K-P-Q), forms the inactivation gate of the channel. The N-terminus and C-terminus have multiple highly conserved motifs which function in binding of protein partners and alter the kinetics of the channel. P*=phosphorylation site, AnkG=binding site for AnkyrinG, CaM=binding site for Calmodulin, PY=interaction site for Nedd4 ubiquitin ligase, PDZ=binding motif for syntrophin [73-75].

The carboxy terminus of many voltage-gated ion channels contains multiple conserved regions that serve as binding sites for multiple channel interacting proteins; in some cases, these partners exert known effects on channel function while in others, the functional consequences of partnering are not well understood. In one channel, the L-type voltage-gated calcium channel, the C-terminus is actually cleaved and serves as a transcription factor for genes involved in neuronal signaling [76]. The C-terminus of voltage-gated sodium channels is less well-characterized, both in structure and function. Mutations in the C-terminus have been associated with impaired channel gating, and associated cardiac arrhythmia syndromes such as long QT syndrome [77], suggesting an auxiliary role (along with the DIII-DIV linker) in channel inactivation. Studies of $Na_V1.5$ have predicted the proximal half of the C-terminal contains six closely-spaced alpha helices, though the relative location of the 6^{th} is uncharacterized (Figure 1.5) [78]. The first and third helices function as EF Hand binding motifs for Ca^{2+} ions, possibly

providing a functional link intracellular calcium signals and modulation of $Na_V1.5$ gating [78, 79]. Within the region of the second alpha-helix is a binding site for fibroblast growth factor homologous factor 1B (FHF1B), which has also been shown to affect channel gating [80]. An aspartic acid reside (D1790) has been shown to be critical in FHF1B binding, and mutations at this position have been identified in *SCN5A*-related disease [48, 80]. The short 4^{th} and 5^{th} helices are highly conserved, but yet to have a functional characterization. The final alpha helix contains a calmodulin binding domain (IQ), identified by predictive models, and by the crystal structure of the $Na_V1.5$ C-terminal/FHF1B/Calmodulin complex [78, 81]. Calmodulin-dependent protein kinase II (CaMKII) is known to bind to the DI-DII linker, and modulates phosphorylation of residues within the loop, shifting voltage-dependent activation of the channel. Increased CaMKII activity has been observed in failing hearts, and produces complex alterations in VGSC gating which may contribute to acquired arrhythmias in heart failure patients [74].

The distal half of the C-terminus domain in $Na_V1.5$ is less well-conserved, however an interaction motif for Nedd4-like ubiquitin ligases resides in this region in almost all VGSCs [82]. This “PY” motif allows cells to regulate the membrane stability of the channel, controlling internalization of the protein [83]. The PDZ domain of the myocyte scaffolding protein syntrophin interacts with $Na_V1.5$, at the distal C-terminus, binding to the three residues at the immediate C-terminal end of the channel [84]. In addition to shifting the activation kinetics of the channel, and being implicated in long QT syndrome [84, 85], $Na_V1.5$ interactions with syntrophins have also been shown to mediate complex formation with other structural proteins, namely dystrophin [75]. Interestingly, the three residues (Serine, Isoleucine, Valine) at the distal C-terminus observed to be required for syntrophin association with *SCN5A* are not conserved in the zebrafish orthologs (Figure 1.5) [75].

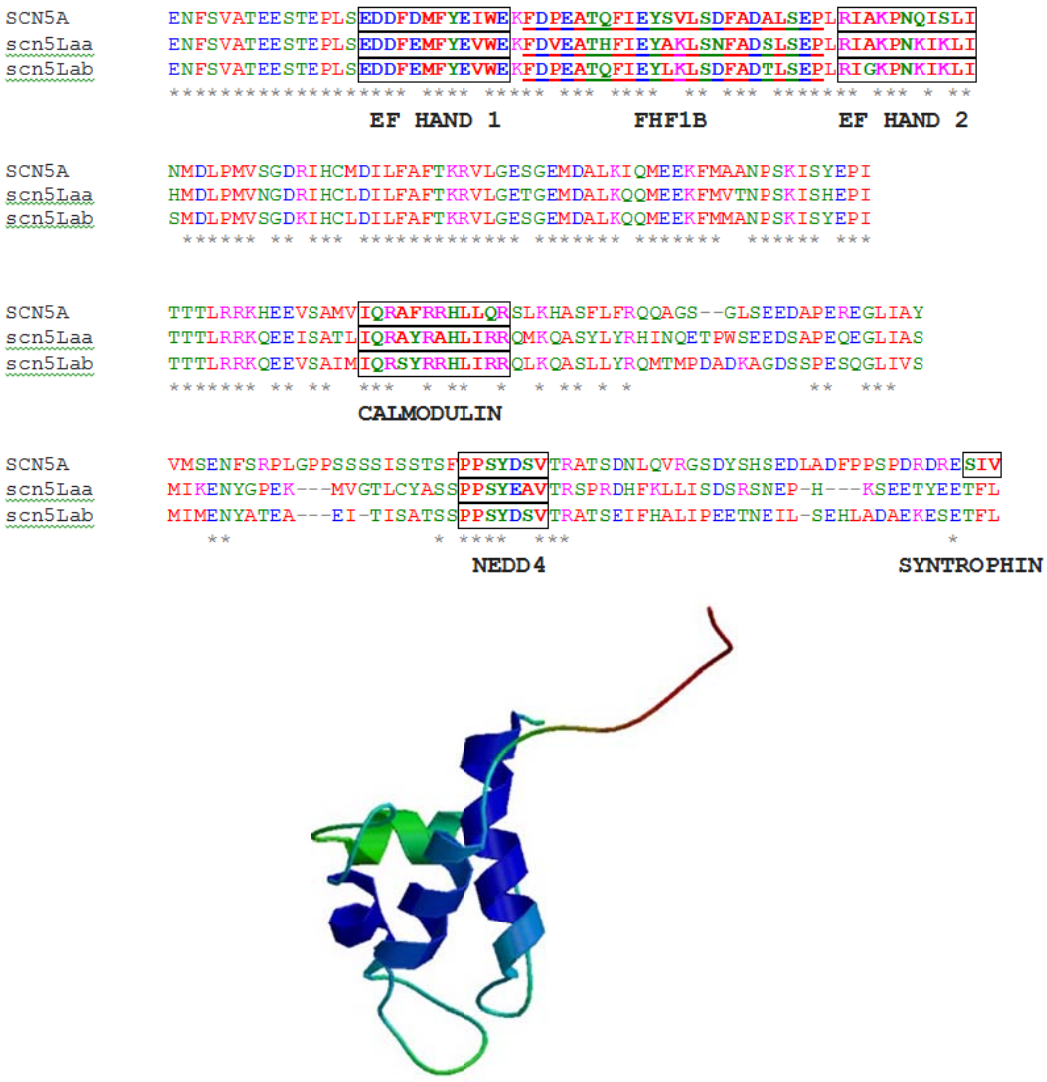

Figure 1.5: Conservation of the cardiac voltage-gated sodium channel C-terminus. The C-termini (Ct) of the channels encoded by *SCN5A* (human), and *scn5Laa*, and *scn5Lab* (zebrafish) contain multiple highly-conserved regions with predicted protein-binding functions (top). All three contain predicted two EF HAND (Ca^{2+} binding) motifs, an FHF1B binding motif, and a calmodulin binding motif. They also each possess a PY motif for the Nedd4 ubiquitin ligase, predicted to function in channel recycling and modulating membrane half-life. The C-terminus of *SCN5A* contains a syntrophin binding site (SIV), absent in *scn5Laa* and *scn5Lab. SCN5A-ct* (247 amino acids) has 62% and 65% identity to *scn5Laa-ct* (237 amino acids) and *scn5Lab-ct* (239 amino acids) respectively. The two zebrafish C-termini have 68% identity to each other. The secondary structure of the *scn5Lab* C-terminus (B) is predicted to have six closely-spaced alpha helices in the proximal portion, with little predicted secondary structure in the distal portion. Homology evaluated using Clustalw2 (The European Bioinformatics Institute, [86]). Structure predicted using SWISS-MODEL Workspace (SIB Bioinformatics Resource Portal, ExPASy [87]).

Physiologic function of voltage sodium channels often requires the association of one or more beta subunits with the alpha subunit pore-forming protein. The human genome encodes four beta subunits β1-β4 (genes *SCN1B* to *SCN4B*), with wide-ranging functions. β-subunits can promote cell adhesion and migration as members of the immunoglobulin superfamily. They are also important in modulating gating, voltage-dependence, and expression of the Na_V alpha subunits [88]. Accordingly, failure of β- and α- subunits to associate can result in phenotypes ranging from electrophysiological disease such as epilepsy and cardiac arrhythmias, to structural defects in cellular migration and axonal growth [88].

Certain Na_Vs preferentially associate with specific β-subunits. VGSCs in neurons and cardiac muscle generally associate with all βs, while the predominant skeletal muscle sodium channel $Na_V1.4$ interacts specifically with β1. The subunits encoded by *SCNB1* (brain, cardiac and skeletal muscle) and *SCNB3* (neuronal tissue) are non-covalently linked to the sodium channel alpha subunit, while *SCNB2* (CNS, heart) and *SCNB4* (many cell types) encode subunits which will be linked to the α-subunit through disulfide bonds [13]. Beta subunits have a single transmembrane domain, with the N-terminus oriented extracellularly, and the C-terminus as an intracellular domain [89]. The immunoglobulin-like extracellular domain assists in the function of the β-subunit as cell adhesion molecules [13], while the smaller intracellular C-terminus is responsible for association with the α- subunit, among other binding partners [90]. Less is known of the interaction between α- and β-subunits, however analysis of the long QT syndrome mutation D1790G in $Na_V1.5$ implicates that residue in the association of $Na_V1.5$ and β1 [91]. In zebrafish, all four VGSC beta subunits are conserved (as opposed to absence of the genes in invertebrate models), with β4 having a second duplicated homolog [92]. As with human *SCN5A*, β-subunits for voltage-gated sodium channels in teleosts have differentially-expressed splice variants, and have been shown to modulate gating properties of the channel *in vitro* [92].

Phenotypes resulting from disruption of cardiac $Na_V1.5$ function

Human phenotypes arising from SCN5A mutations

Dysfunction of the human cardiac sodium channel $Na_V1.5$ has been described in multiple arrhythmia syndromes and structural pathologies of the heart. Mutations in protein partners of the channels, such as *SCN1B*, have been associated with additional phenotypes as well. The Online Mendelian Inheritance in Man (OMIM) database lists nine established phenotype relationships for mutations in the *SCN5A* gene in humans, including atrial fibrillation, Brugada syndrome 1, dilated cardiomyopathy, long QT syndrome 3, susceptibility to Sudden Infant Death Syndrome, along with other forms of heart block and cardiac conduction disease. Many other non-Mendelian relationships have been identified from results of genome-wide association studies, which compare relative frequency of certain genotypes in cases and controls for a specific phenotype. The National Human Genome Research Institute (NHGRI) database dbSNP [93] cites five association studies correlating variation in *SCN5A* to increased or decreased PR interval, QRS interval, and cardiac conduction [94-98]. These studies identified single nucleotide polymorphisms in *SCN5A* which either have a functional impact on channel expression or function, or are in linkage disequilibrium (LD) with one that does. As a result, variation in a quantitative electrocardiographic trait is observed in patients possessing the polymorphic allele.

Sudden cardiac death (SCD) is responsible for 20% of deaths in adults; nearly half a million adults die each year in the United States from suspected cardiac disease [99]. The majority of these deaths are a result of ventricular fibrillation in (largely older) adults with coronary artery disease. However, mutations within ion channels are becoming increasingly identified in heritable cardiac channelopathies, a significant cause of SCD in young adults, particularly males [100]. Of these, some of the most common are the long QT syndromes (LQTS), a cluster of phenotypes characterized by inhibited repolarization of myocardium and lengthened action potential duration [101]. The result is an increased

QT interval on electrocardiogram (ECG), and susceptibility to ventricular arrhythmias. LQTS subtypes have diverse locus heterogeneity, having been mapped to multiple genes involved in cardiac arrhythmogenesis, including *SCN5A* (LQT Type 3, LQT3) [102, 103]. At least 77 unique LQT3 mutations, the vast majority of them missense mutations or small (in frame) deletions in coding regions of the channel, have been identified in *SCN5A* [13] (Inherited Arrhythmias Database: http://www.fsm.it/cardmoc/). The mutations in LQT3 are generally considered "gain-of-function" mutations, resulting from impaired inactivation causing persistent inward sodium current [104]. On the other hand, Brugada syndrome (discussed below), generally is caused by "loss-of-function" resulting in decreased sodium current. Additionally, mutations in voltage-gated potassium channels, ankyrin-B, L-type calcium channels, and multiple other ion channel β-subunits and interacting proteins have been identified in various long QT syndrome subtypes [105]. LQT3 was one of the first Mendelian channelopathies mapped to the 3p21 locus where SCN5A is found. LQT subtypes are often identified clinically; ECGs of patients with LQT3 feature peaked biphasic or asymmetric T waves following the long QT segment [106]. Electrophysiogic studies of mutations in $Na_V1.5$ causing LQT3 have revealed impaired channel inactivation, disrupting repolarization of the myocardium [71, 102]. As a result standard treatment for LQTS, β-adrenergic receptor antagonists, is less effective in patients with LQT3 [107]. These patients benefit from pharmacologic intervention with agents which inhibit sodium channels (such as mexiletine) and they often require surgical implantation of an implanted cardioverter-defibrillator (ICD) [101]. Fatal arrhythmias from LQT3 have increased occurrence during sleep, and post-mortem screening of sudden infant death syndrome (SIDS) victims has identified multiple candidate mutations in *SCN5A* [48, 108]. The S1103Y variant of $Na_V1.5$ appears to have normal electrophysiology *in vitro* at normal pH, however a sharp increase non-inactivating current appears when pH is reduced. It is hypothesized the decreased pH seen in respiratory acidosis or apnea alters the gating characteristics of the variant, resulting in potentially fatal arrhythmias and sudden death [109].

Brugada syndrome (BrS) is a congenital arrhythmia thought to be responsible for approximately 4% of all sudden deaths, and is a significant cause of sudden cardiac death (SCD) in young male patients with structurally normal hearts [17, 110]. The most common mutations responsible for the disease are found within *SCN5A*, with up to 30% of all patients testing positive for known *SCN5A* BrS mutations [111]. In addition to *SCN5A*, mutations in potassium channels, calcium channels and multiple ion channel subunits and interacting proteins have been implicated in BrS [17, 112]. To date, at least 300 unique mutations within *SCN5A*, including missense mutations, insertions, and deletions throughout each domain of the channel have been identified in BrS [13, 17, 111]. Brugada Syndrome often presents in middle age, and is characterized by right bundle branch block and ST segment elevation, along with T wave inversion on electrocardiography [113, 114]. The molecular mechanisms of Brugada Syndrome appear to be heterogeneous, with some combination of impaired activation, early repolarization, and reduced expression or maturation of $Na_V1.5$ likely responsible [110]. Administration of a sodium channel blocking drug (procainamide, flecainide) to elicit the characteristic ECG is used in the diagnosis of BrS [101].

Pathological implications of altered $Na_V1.5$ function and expression are not limited to cardiac conduction disorders. Nearly 30% of cases of dilated cardiomyopathy (DCM) have a familial component [115], with drug toxicity, nutritional deficiency, or viral exposure largely responsible for the rest of cases. Mutations in nearly 50 sarcomeric genes, including *SCN5A*, have been identified in DCM, nearly all with autosomal dominant inheritance [115]. In DCM, cardiomyocyte death and remodeling in response to either an intrinsic or extrinsic insult result in ventricular chamber enlargement, decreased ejection fraction, and eventual systolic failure. Another cardiomyopathy, left ventricular non-compaction cardiomyopathy (LVNC or NCC) has also been associated with mutations in *SCN5A* [116-118].

Mutations in *SCN5A* associated with dilated cardiomyopathy have divergent biophysical characteristics. A 2008 study by Nguyen *et al* examined two DCM mutations, R814W and D1595H [119].

While both mutations have been linked to structural and arrhythmogenic cardiac disease, R814W channels exhibit slower rise times and altered voltage dependence of activation resulting in increased window current (voltage-dependent overlap of activation and inactivation). On the other hand, D1595H channels feature impaired fast inactivation and a hyperpolarizaed inactivation curve. Another study performed linkage analysis on a family with DCM and cardiac conduction abnormalities, and identified a causal D1275N missense mutation with autosomal dominant inheritance and 75% penetrance [116]. *In vitro* studies on the heterologously-expressed mutated channel surprisingly yielded near-normal sodium currents [120]. Another missense mutation, R222Q, was identified in a second DCM family, also with cardiac conduction defects [117]. Electrophysiological follow-up found increased rate of activation and magnitude of sodium currents, and administration of a sodium channel blocker (flecainide) reduced ectopic ventricular beats and slowed the progression of DCM. The two mutations may produce DCM through different mechanisms, demonstrating the significant phenotypic and genotypic heterogeneity of cardiac disorders. Normal cardiac conduction in the heart requires not only electrophysiologically normal $Na_V1.5$, but multiple protein-protein interaction to promote proper localization of the channels. A mutation like D1275N may disrupt these interactions and cause protein mislocalization, leading to cardiac conduction abnormalities. Alternatively, R222Q channels may localize properly, and elicit their effects on DCM through altered activation. While pharmacologic evidence suggests the effects of *SCN5A* mutations on DCM are related to altered ion homeostasis, the two mutations demonstrate mechanistic heterogeneity, resulting in varied and overlapping phenotypes.

The difficulty in separating primary structural disease from electrophysiological is evident in other cardiomyopathies as well. At least seven different genes have been identified as having mutations associated with LVNC [121]. Diagnosis is often complicated by phenotypic heterogeneity as well, with the LVNC often appearing in the presence of other cardiomyopathies. The disease often appears early in life as a developmental abnormality, featuring deep trabeculation of the ventricular wall myocardium

which can increase the chances for heart failure and stroke [122]. Screens of families and idiopathic cases of LVNC have implicated polymorphisms in *SCN5A* in LVNC [118]. Patients whose disease was accompanied by arrhythmias and more significant heart failure were more likely to possess one of the *SCN5A* variants. As with DCM, little is known of the mechanisms through which an ion channel impacts cardiac structure and development, and whether altered $Na_V1.5$ function has a primary function in structural cardiac development in humans or a secondary effect where altered action potential characteristics and cellular electrophysiology produce a pathogenic response in myocardium. Additionally, variable penetrance of the phenotype suggests polymorphisms in other genes may further modulate the manifestation of the disease, and complicate the mechanisms involved.

Mouse models of $Na_V1.5$ loss-of-function

Multiple mutations discovered in human cardiac disease have been generated and studied *in vivo* in engineered mouse lines. Our lab has used recombinase-mediated cassette exchange to create a knockout-knockin line in which the endogenous mouse *Scn5a* is replaced with a human *SCN5A* allele [123]. Wildtype and mutated mouse lines with polymorphisms identified in human patients can be generated and studied in this manner. A patient with multiple arrhythmic diagnoses, including atrial flutter, slowed conduction, and sinus node dysfunction was discovered to have the same D1275N mutation in *SCN5A* found in the dilated cardiomyopathy family above [116]. Though the mutated channel had little electrophysiological differences detected *in* vitro, generation of a mouse line expressing this (human) allele in place of endogenous *Scn5a* resulted in a phenotype consisting of slowed conduction, atrial and ventricular dysrhythmias, and dilated cardiomyopathy [120]. Altered cell surface expression of the channel, or impaired interactions with protein partners, has been hypothesized as possible mechanisms for this phenotype.

The mouse model system has also allowed us to study *Scn5a* null alleles, and the results are especially relevant to the work I present here. Heterozygous deletion of the predominant cardiac

sodium channel in mice, Scn5a, results in a decrease in measurable voltage-gated sodium current in isolated cardiomyocytes, evidence of conduction slowing, and inducible ventricular tachycardia [124, 125]. No *Scn5a*$^{-/-}$ pups were detected in the study, indicating that homozygous knockout of the gene is embryolethal. *Scn5a*$^{-/-}$ embryos were identified up to embryonic day 10.5 (E10.5) with some uncoordinated weak cardiac contractions, with no embryo surviving to day E11.5 [124]. Ventricles in *Scn5a*$^{-/-}$ hearts were smaller than wildtype or heterozygous hearts, with reduced trabeculation. Other aspects of cardiac development appeared normal, as endocardial cushions, the atrium, and the primitive outflow tract region (truncus arteriosus) were all unaffected [124].

We and others have hypothesized that the failure in ventricular morphogenesis is unrelated to electrical signaling and thus directly due to loss of *Scn5a*/$Na_V1.5$, and not an effect on contractile function. One important argument supporting this contention is that robust current through sodium channels dramatically increases between E13 and E19, and appears unnecessary for action potentials at the time *Scn5a*$^{-/-}$ ventricles are affected [126]. Before E16, L-type calcium is significantly greater than sodium current in embryonic cardiomyocytes; by E19 the two are roughly equal, suggesting early fetal action potentials in the developing heart, similar to zebrafish [61, 127], are driven by inward calcium currents rather than sodium. Another is the finding, detailed below, that initial cardiac development occurs normally in the absence of a heartbeat in the developing zebrafish.

Knockdown of scn5Laa and scn5Lab in zebrafish

Rapid development, short generation time, external fertilization and optical transparency make the zebrafish *Danio rerio* an excellent model to study cardiac development. The zebrafish embryo can develop from an unfertilized ovum to an embryo with largely complete organogenesis in a matter of days [128]. External fertilization allows for easy collection of the embryos and manipulation of gene expression through microinjection of message sense RNA to express a gene product, or antisense oligonucleotides to inhibit expression [129]. These 'morpholinos' have proven an invaluable tool in the

exploration of loss-of-function phenotypes. Additionally, optical transparency of the embryo allows for easy characterization of such phenotypes during development, often with a simple dissecting microscope. In particular, visualization of the beating heart tube as early as 24 hpf allows for identification of mutations affecting cardiovascular development through forward genetic screens [130, 131]. External development in an aquatic environment allows the developing embryo to acquire oxygen systemically through diffusion, obviating the need for cardiac function in early embryonic development [132].

While extensive studies have explored the electrophysiological phenotypes resulting from alterations of $Na_V1.5$ function in the adult heart, evidence from mouse and zebrafish suggest Scn5a is required in the developing heart as well. A 2010 study by Chopra *et al* found the voltage-gated sodium channels denoted by *scn5La* (*scn5Laa* and *scn5Lab*) are required for normal cardiac development in the zebrafish embryo [61]. The study found cardiac expression of both sodium channel isoforms by in situ hybridization in 2 days post-fertilization (dpf) embryos, seemingly before I_{Na} is required for cardiac rhythm. Additionally, RT-PCR found expression of both channels early in development, well before a beating heart tube can be seen. Morpholino-knockdown of the two channels each resulted in a similar phenotype; the embryos developed with small hearts which failed to undergo normal atrio-ventricular looping and chamber hypertrophy (Figure 1.6). Circulation was compromised, and the embryos died by 5 dpf. This phenotype was evident in both *scn5Laa* and *scn5Lab* single gene knockdowns, as well as in a double (*scn5La*) morpholino knockdown, which had the most severe phenotype.

A further look at early cardiac development in morpholino-injected (morphant) embryos revealed a defect in the gene expression of cardiac precursors [61]. The expression of the cardiac specification transcription factor, *nkx2.5*, was dramatically reduced in the bilateral fields of cardiac progenitors in the anterior lateral plate mesoderm (ALPM) at 12 hpf. Other cardiac transcription factors, *hand2* and *gata4* also appeared reduced in the ALPM of both *scn5Laa* and *scn5Lab* morphant embryos.

As will be discussed below, the effect of the morpholino on *nkx2.5* expression was both dose-dependent, and not mitigated by co-injection of morpholino inhibiting the translation of the pro-apoptotic protein p53.

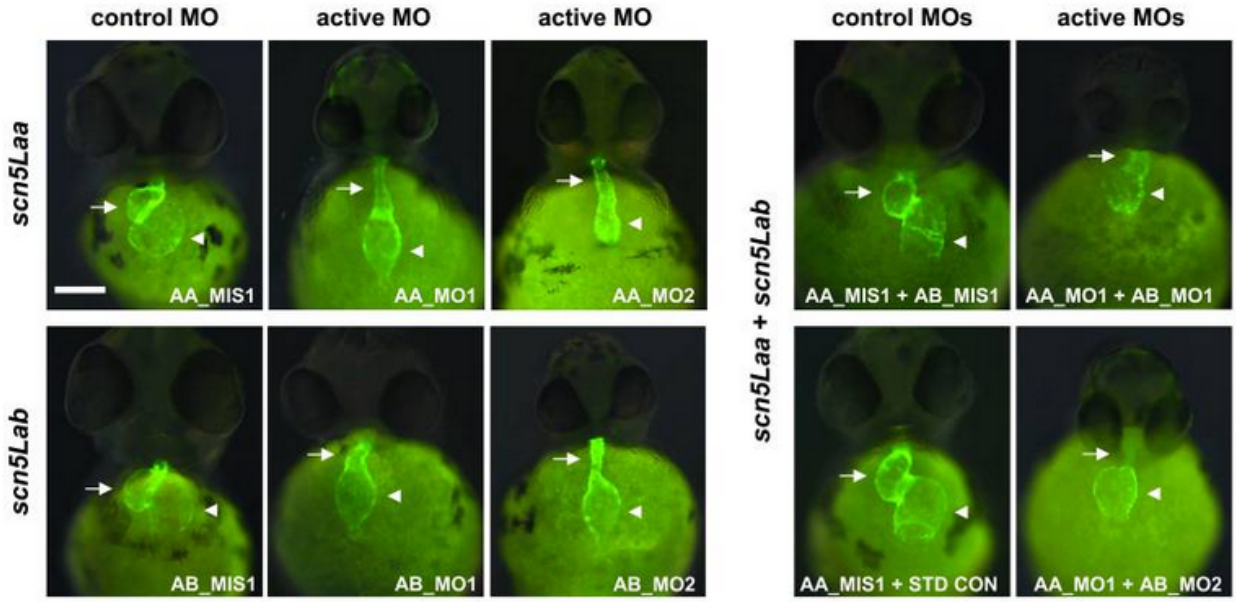

Figure 1.6 Morpholino knockdown of scn5Laa and scn5Lab results in defects in cardiac development of zebrafish. (from Chopra *et al* 2010). Zebrafish embryos were injected with control morpholino (MO) or active MO against *scn5Laa*, *scn5Lab*, or both genes. Defects in cardiogenesis were readily apparent at 48 hours post-fertilization with knockdown of either gene, in the form of small single layer ventricles (arrows). Hearts failed to loop, resulting in failure to establish robust circulation, pericardial edema, and lethality by 5 dpf. Injection of active MOs against *scn5Laa* and *scn5Lab* resulted in a severe form of the phenotype, with small ventricles and failure to maintain systemic circulation.

The heart tube at 20 hpf in morphant embryos had fewer *cmlc2*+ cardiomyocytes, suggesting the primary defect in *nkx2.5* expression resulted in a smaller heart tube and impaired primary differentiation [61]. The heart tubes in morphant embryos then failed to grow and loop appropriately, and the ventricles had fewer cells later in development, in particular from 58-104 hpf, failing to thicken concentrically. Interestingly, growth of wildtype embryos in pharmacologic blockers of voltage-gated sodium channels (TTX), and L-type calcium channels (nisoldipine) inhibited heartbeat but had no effect on early heart development consistent with observations by others. A zebrafish mutant line named

silent heart displays normal cardiac development through 2 dpf despite troponin T mutations which completely prevent the heart from beating. Thus, early cardiac development appears to not be dependent on cardiac contraction or a physiologic circulation [133]. Furthermore, it was shown that despite *in situ* data showing the expression of *scn5La* at 3 dpf, injection of TTX into the pericardium had no effect on cardiac rhythm at this stage [61], demonstrating again that permeation through sodium channels is required to support the early heartbeat. Consistent with expression data, the sea anemone toxin ATX II, a potent inhibitor of VGSC inactivation, was able to induce arrhythmias at 3 dpf, indicating that *scn5La* is present, but electrophysiologically silent (by the TTX data), during the early stages of cardiogenesis [61].

These findings then pose questions that I address in this research. I study the mechanisms through which *scn5La* influences heart development in zebrafish. Embryonic heart development requires multiple phases of differentiation, growth, and proliferation, and I present here data on the functions of cardiac voltage-gated sodium channels in development, and the effects of morpholino knockdown of *scn5La* these processes.

CHAPTER II

GENETIC PHENOTYPES OF LOSS OF SCN5LAB

Introduction: Genetics of heart development in zebrafish

Induction of pre-cardiac mesoderm in gastrulation

The cardiovascular system of the zebrafish develops rapidly; the fertilized ovum develops into an embryo with robust systemic circulation in a matter of days. The single cell at the animal pole rapidly divides following fertilization, undergoing successive rounds of doubling during the cleavage and blastula stages. The mass of cells (blastodisc) sitting on the yolk appears spherical by 4 hpf (sphere stage), at the onset of epiboly. During epiboly, the blastodisc envelops the yolk, migrating from animal pole (pictured top) to vegetal pole (bottom). At 40% completion of epiboly, cardiac development has already begun, five hours after fertilization. Here, fate-mapping has identified a region enriched for cardiac progenitors residing 60-120 degrees from dorsal, bilaterally in the first four tiers of blastomeres from the epiboly margin (Figure 2.1) [134].

With the onset of gastrulation, epiboly movement of the blastodisc towards the vegetal pole is accompanied by involution of the germ layers. As epiboly and gastrulation are completed, the region of cardiac precursors migrates dorsally towards the developing embryo, into a region known as the lateral plate mesoderm. The embryo, now undergoing somitogenesis, is defined according to the number of somites visible. Towards the original animal pole is the anterior lateral plate mesoderm (ALPM), where bilateral stripes of cardiac progenitors can be identified through genetic markers, 12 hours post-

fertilization. Though the ALPM represents an early window into the specified cardiomyocyte population, multiple pathways are known to play an early role in adoption of cardiac fate, during epiboly and gastrulation.

Induction of cardiac fate is temporally regulated, as well as spatially. A 2007 study identified a biphasic role for Wnt signaling in cardiac fate of zebrafish [135]. The study used heat shock inducible expression of *wnt8* (Wnt signaling activator) and *Dickkopf1 (dkk1*). Expression of *wnt8* before 50% epiboly resulted in a dramatic increase in the pre-cardiac mesoderm population (expressing *nkx2.5*) at 8 somites, as well as differentiating cardiomyocytes at 18 somites. Inhibition of Wnt signaling by expression of *dkk1* had the opposite effect, with significant reduction of future cardiomyocytes. Interestingly, an opposite effect was seen during gastrulation. From 6 hpf to 9 hpf, inhibition of Wnt signaling promoted cardiac fate, while Wnt agonists reduced it. A later study identified a third phase, in which atrial cardiomyocytes require Wnt signals to fully differentiate [136]. Not only is expression of pro-cardiac pathways required for differentiation of the heart, the timing of onset and repression of these pathways is critical as well.

Expression of additional signaling pathways, such as Bmp and Fgf, has also been implicated in adoption of cardiac fate. Bmp signaling is similar to Wnt signaling in heart development in that is plays a biphasic role in which both activation and inhibition of the pathway is required for cardiac differentiation. Zebrafish lacking *Bmp receptor 1a* had no differentiated cardiomyocytes [137]. The study identified a requirement for Bmp signaling during somitogenesis to induce cardiac differentiation. Interestingly, differentiating cardiomyocytes require the expression of *smad6a*, which inhibits Bmp signaling.

A mutation in *fgf8* generates the *acerebellar* (*ace*) line which displays abnormal development of the brain and heart. Initial studies found expression of *fgf8* during gastrulation, persisting through somitogenesis. Homozygous mutants deficient in fgf8, had perturbed expression of critical neural

transcription factors, and lack of a cerebellum [138]. These mutants also have dramatic disruption of cardiac development and function, featuring small hearts with dramatically reduced numbers of ventricular myocytes [139]. Cardiac specification in these embryos was disrupted, with loss of ALPM expression of both *nkx2.5* and *gata4*. Additionally, loss of fgf8 after the onset of cardiac differentiation can dramatically impact ventricular cell number as well [140].

At early stages of specification, overexpression of certain pathways modulates the size of the cardiac progenitor fields, rather than affecting cell fate in a chamber-specific, or even tissue-specific manner. In mice, the cardiac BAF complex (cBAF) has been shown to induce differentiation of myocardium from mouse embryonic mesoderm when ectopically expressed [141]. In zebrafish, the complex is formed by *scmarcd3b*, *gata5* and *tbx5* [142]. *Smarcd3b*, a member of the SWI/SNF chromatin-remodeling complex, is known to be required in the development of skeletal muscle. *Smarcd3b* expression can be detected in the marginal zone during mid-epiboly, preceding the onset of expression of *myod* and *myf5*. Evidence obtained using morpholino knockdown of *scmarcd3b* suggests the protein coordinates signals from *fgf8* and *ntl* to promote the onset of myogenesis [143]. Overexpression of cBAF components were shown in a more recent study to result in enlarged hearts during development, while combinatorial loss of the *smarcd3b*, *tbx5* and *gata5* resulted in impaired differentiation of cardiomyocytes [142]. Interestingly, overexpression of the cBAF complex resulted in an increase in both cardiomyocytes and endoderm, with modulation by other components such as Fgf, determining cell fate.

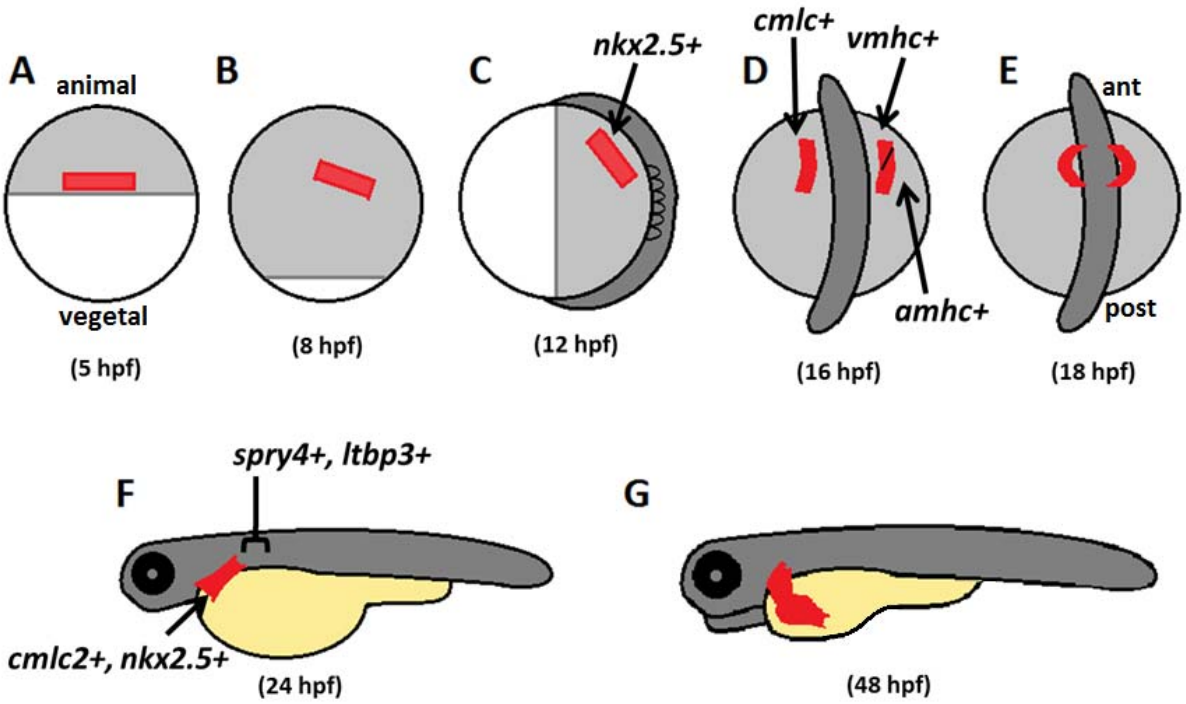

Figure 2.1 : Genetics of cardiac development of zebrafish. Bilateral regions enriched for cardiac precursors can be identified by fate-mapping near the margin at 40% epiboly (A). The regions migrate dorsally and anteriorly during development (B). Integration of Wnt, Fgf, and Bmp signaling are responsible for cardiac specification. By 12 hpf (C), cardiac precursors can be identified in the anterior lateral plate mesoderm, and expression *nkx2.5*, as well as other cardiac transcription factors (*gata4*). At 16, differentiation has begun (D), with cardiomyocytes expressing cardiac myosin light chain (*cmlc2*) as well as chamber-specific heavy chain (*vmhc*, *amhc*) with future ventricular myocytes residing anteromedial to the atrial cells. The bilateral stripes fuse medially (E) to form a cardiac cone, and elongates into the hear tube by 24 hpf (F). At 24 hpf, the second heart field (SHF) can be identified distal to the ventricle by expression of *spry4*, *ltbp3*, and *nkx2.5*, among other genes.

Specification of the ALPM

By the onset of somitogenesis, the integration of multiple cardiac specification pathways in gastrulation has resulted in a population of pre-cardiac mesoderm in the anterior lateral plate (Figure 2.1). The NK2 homeobox genes *nkx2.5* and *nkx2.7* function as an early readout of cardiac fate in the ALPM [144], as well as being required to maintain cardiac fate throughout heart development. A third NK2 gene *nkx2.3* has been identified in zebrafish, but is not expressed in pre-cardiac or cardiac cells [144]. Homologs of *nkx2.5* are required for cardiac development across model systems. In *drosophila*,

absence of the ortholog *tinman* results in failure of the heart to form [145]. By contrast, mouse embryos are able to form hearts in the absence of *Nkx2.5*(*Csx*), although cardiac development is arrested following looping of the heart tube with lethality by E10.5 [146]. Mutations in *NKX2.5* in humans have been linked to congenital heart defects such as atrial septal defects (ASD), tetralogy of fallot (TOF), and hypoplastic left heart syndrome (HLHS) [147-149].

In zebrafish, *nkx2.5* marks the cardiac fields in the ALPM at 12 hpf, with prominent expression of *nkx2.7* also in the region [144]. The related genes have overlapping, but not completely redundant roles in heart tube extension and growth, with *nkx2.7* expression preceding *nkx2.5*, and extending beyond the bilateral stripes of cardiac precursors [144, 150]. Other studies have demonstrated morpholino knockdown of *nkx2.5* alone has a mild cardiac phenotype: a slightly smaller ventricular chamber [151], while knockdown of *nkx2.7* results in failure of the developing heart to loop correctly [150]. Both studies observed dramatic phenotype on double knockdown, including reduced ventricular chamber size, impaired looping and weaker contractions [150, 151]. *Nkx2.7* in particular was observed to modulate the expression of *tbx5*, *tbx20*, and Bmp signals, to promote proliferation of myocardium [150].Taken together, the data suggest that *nkx2.5* and *nkx2.7* work together to direct cardiac differentiation and growth.

A number of other factors mark the pre-cardiac region of the ALPM during early somitogenesis. One is the GATA family of zinc-finger transcription factors that has many functions in zebrafish organogenesis, from gut endoderm-derived organs, to the heart and vasculature [152]. Though each factor is often expressed in multiple tissues, the roles for Gata transcription factors can vary. For example, *gata4* and *gata6* have redundant functions in liver development, as well as a requirement in pancreas and swim bladder development [153]. In the heart however, the two transcription factors have specific functions. Morpholino knockdown of *gata4* results in small, un-looped heart tubes and growth arrest following differentiation [154]. Zebrafish lacking *gata6* expression are unable to maintain normal

expression of *bmp2b* and *nkx2.5*, and have dramatically reduced expression of cardiac myosin genes critical to contractile function [155].

A third GATA transcription factor expressed during gastrulation, *gata5*, has been shown to be required for ALPM expression of *nkx2.5*, fusion of the bilateral cardiac primordial, ventricular growth following differentiation [153]. Interestingly, overexpression of *gata5* is sufficient to produce ectopic expression of *nkx2.5*, as well as ectopic foci of contracting myocardium. The effect of *gata5* on *nkx2.5* expression was shown to be at least partly regulated by two factors involved in dorsoventral patterning; *bmp2b*, and *one-eye pinhead* (*oep*), a growth factor involved in nodal signaling [156]. Further studies have since shown that *gata5* interacts with other genes including *smarcd3b* and *gridlock* to regulate the size of the developing heart [142, 157]. Cardiac precursors in the ALPM are also marked by the basic helix-loop-helix transcription factor *hand2* [158]. While *hand2* is not required for other early specification genes, disruption of *hand2* expression impairs cardiac fusion, as well as differentiation [159].

Differentiation of myocardium

Cardiomyocyte differentiation represents a transition from specification, in which transcription factors determine cell fate, to differentiation, during which cascades of pathways establish the expression of genes required for functions of the mature cell, as well as maintenance of cardiac fate. Differentiation of the myocardium begins in the bilateral stripes of cardiac precursors in the ALPM, by 16 hpf (14 somites) [160]. Future myocardium can be identified with *in situ* hybridization for *cardiac myosin light chain 2* (*cmlc2, myl7*) [161]. Within the bilateral cardiac fields, chambers have already become spatially and genetically distinct, with future ventricular myocardium expressing *ventricular myosin heavy chain* (*vmhc*), in the cells residing anterior and medial to the future atrial cells within the ALPM (Figure 2.1) [160]. The two stripes of future myocardium continue to migrate dorsally, where they fuse to form the cardiac cone, eventually elongating into the primary differentiated heart tube [162].

The interplay of multiple transcription factors is necessary for the expression of genes critical to cardiac contractility. Myocyte enhancing factors *mef2cb* and *mef2ca* are critical in both primary differentiation of the bilateral ALPM cardiac fields and in differentiation of the secondary heart field [163]. Double knockdown of the two genes has no effect on cardiac specification genes (*gata4*, *nkx2.5*), but results in loss of sarcomeric differentiation genes, including *cmlc2*and *vmhc*. Chamber specificity is induced by a number of factors. The promoter for *vmhc* contains *nkx2.5* binding elements, which when deleted results in de-repression of atrial *vmhc* expression, as well as binding sites for the homeobox transcription factor *prx2*, which promotes ventricular expression [164].

Other sarcomeric proteins appear to play both structural and regulatory roles in myocardial differentiation. The *early cardiac connexin* (*ecx*) is a gap junction protein which has been identified as being required in the developing heart for cardiac morphogenesis and myofibril organization. *Ecx* is expressed during gastrulation and somitogenesis and has shown to be required in maintaining ALPM expression of *nkx2.5*, as well as playing a role in the structural refinement of myocardium [165]. Interestingly, the role for *ecx* in development appears to be specific to the specification and differentiation of myocardium, as homozygote *futka* (*ecx* loss-of-function) mutants possess normal skeletal muscle development and structure.

Additionally, maintained expression of some transcription factors is required throughout development. Regulated expression of both *nkx2.5* and *tbx5* is required throughout the first 48 hours of development, as the two interact to promote cardiac-specific gene expression and growth of the heart. *Tbx5* binds to the promoters of both *connexin 40*, a gap-junction protein required for propagation of action potentials, and *atrial natriuretic factor* (*anf*), a hormone important for cardiac growth [166, 167]. In humans, *TBX5* mutations cause Holt-Oram syndrome, in which cardiac and limb development are both affected [168]. Hearts of Holt-Oram patients commonly have atrial or ventricular septal defects, as

well as abnormalities in cardiac conduction. Evidence in mice suggests *Tbx5* promotes conduction system development through the expression of *Scn5A* [169].

By 22-24 hpf, the heart tube has begun to undergo peristaltic contractions [127]. Recent evidence from our lab and others has shown that while cardiac voltage-gated sodium channels are not required for cardiac action potential early in development, they are required for specification and differentiation of the heart tube [56, 61]. Analysis of the *SCN5A* promoter in humans has revealed binding elements for multiple genes expressed during cardiac differentiation, including *MYOD* and *GATA* factors [53]. It is unknown if the requirement *scn5La* in the development of the heart tube is limited to promoting specification during gastrulation, or if the channels are part of a pathway governing myocardial differentiation specifically as well.

Second heart field

Though there has been some debate historically whether cardiac differentiation in vertebrates proceeds in a continuous or phased manner [170], most lines of evidence suggest genetic and morphologic distinction between the first heart field (FHF) and second heart field (SHF) [171]. The SHF in both mammals and fish is derived from cells in the splanchnic mesoderm, and represents an extra-cardiac population of cardiac precursors, which differentiates after the heart tube has formed [171, 172]. In mice, cardiomyocytes derived from the SHF form the left ventricular outflow tract (LVOT), and a portion of the right ventricle [173]. Many of the same genes involved in FHF differentiation are required for SHF contribution to the heart, including *Nkx2.5*. Mutations in genes involving the SHF are responsible for multiple conotruncal congenital heart defects, including both atrial and ventricular septal defects [174].

In zebrafish, the second heart field contributes to the venous (atrial) and arterial (ventricular) poles in the developing heart, the inflow tract (IT) and outflow tract (OT). In 2009, a study by de Pater *et al* used cardiac-specific expression of the photoconvertible protein Kaede to identify the contributions

of the SHF to the heart (see chapter IV for detailed method) [175]. Upon ultraviolet irradiation, Kaede alters confirmation, permanently photoconverting from its native green, to red fluorescence [176]. Cardiomyocytes differentiated at the time of irradiation appear red, and continue to make green Kaede and thus appear yellow, while newly-added (SHF) cardiomyocytes appear green. It was discovered that both poles of the heart experience SHF differentiation; the venous pole between 19 and 26 hpf and the arterial pole between 28 hpf and 48 hpf. By 48 hpf, differentiation is largely complete. The study additionally identified expression of factors marking the extracardiac population of future cardiomyocytes. Atrial progenitors were marked by the LIM homeodomain transcription factor *islet1*, while the future OT myocardium was marked by Fgf signaling. Though *fgf8* expression was undetected by *in situ* hybridization, the authors identified peri-ventricular expression of the Fgf feedback inhibitor *sprouty4* (*spry4*) [177].

Further studies have identified additional genes expressed in the ventricular SHF. Lazic and Scott (2011) identified the SHF through extracardiac expression of both *mef2cb*, a necessary factor for SHF contribution to the heart. Interestingly, while the region expressed both *vmhc* and *nkx2.5*, expression of *myl7* (*cmlc2*) was notably absent [178]. Another group observed that morpholino knockdown of *latent tgf-β binding protein* (*ltbp3*) in zebrafish resulted in multilineage defects of the aorta, pharyngeal arch arteries, and particularly of the outflow tract [179]. *In situ* hybridization and fluorescence riboprobes revealed expression of *ltbp3* in the region of the SHF, along with *nkx2.5*. Loss of *ltbp3* resulted in both decreased contribution of the SHF to the heart, as well as defects in proliferation of SHF-derived cardiomyocytes.

Question

We have previously shown scn5Laa and scn5Lab are expressed early in the embryo, with evidence of maternal deposition and gastrulation-stage expression [61]. While *scn5La* has a known functional role in differentiated myocardium, there is evidence for a developmental role as well,

evidenced by impaired expression of *nkx2.5* in the ALPM of *scn5La*-depleted embryos. The morphant phenotype is more severe than seen in single morpholino knockdown of *nkx2.5*, but it is unknown what other gene expression is perturbed by loss of *scn5La*. Additionally, *nkx2.5* is required for SHF differentiation of the distal ventricle and outflow tract, and It is unknown what role *scn5La* plays in SHF differentiation, as well as FHF specification and differentiation. Here we further refine the genetic phenotype caused by loss of cardiac voltage-gated sodium channels during development.

Methods

Morpholinos

Previously-validated morpholinos against scn5Laa (*AA-MO1*) and *scn5Lab* (AA-MO3) were used as described [61]. Active morpholino was co-injected with 4.5 ng anti-p53 morpholino (3-GCGCCATTGCTTTGCAAGAATTG-5, GeneTools) to limit p53 activation, a non-specific toxicity induced by knockdown technologies [180]. A *scn5Lab* 5-base mismatch morpholino (5-ACTTTCTGCTGAGCGGTGCTCTGCG-3, GeneTools) was also used a control. Active and control morpholinos were injected into one-cell fertilized ova (Figure 2.2). For a complete list of morpholinos described here, refer to Appendix A.

Zebrafish Strains and Animal Care

Morpholino injections to assay gene expression were performed using a wildtype AB strain. Transgenesis was also performed in an AB background. Drug exposures were performed on an outcross crossed AB-Tu line of zebrafish. All strain backgrounds were kept consistent within each experiment across morphants and controls. Organisms were cared for in accordance with guidelines set by the Vanderbilt University Institutional Animal Care and Use Committee (IACUC) and the Office of Animal

Welfare Assurance (OAWA) as well as the National Institutes of Health (NIH) and National Research Council's publication "Guide for Care and Use of Laboratory Animals".

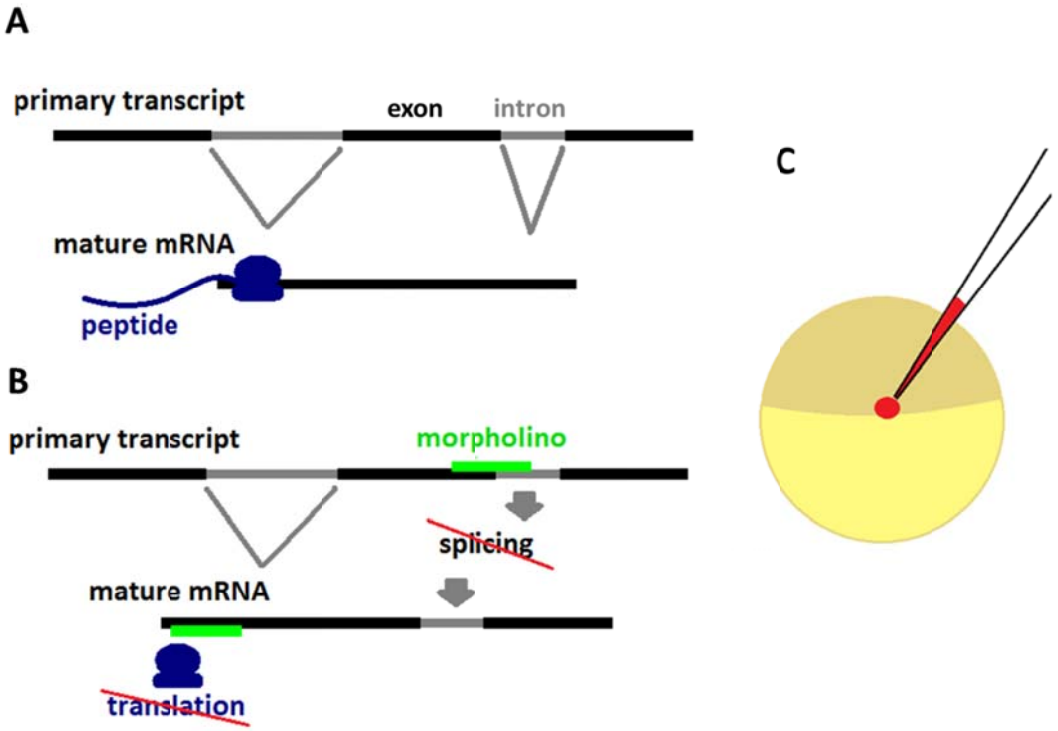

Figure 2.2: Morpholino injections. Immature mRNA (A) consists of exons, containing the ATG start site and protein coding message, along with non-coding introns in between, which must be spliced out for proper translation of the peptide. Morpholinos (B) bind to a splice site or ATG start codon to inhibit proper translation. Morpholinos are pressure injected (C) into a fertilized ovum using a micropipette.

Qualitative RT-PCR of nkx2.5

Qualitative reverse-transcription polymerase chain reaction (RT-PCR) was used to quantify *nkx2.5* expression in morphant embryos. RT-PCR for *scn5Laa* and *scn5Lab* was used on wild-type embryos fixed at various stages to establish an expression time-course. A standard PCR protocol was used (94°C denaturing 30"; 60°C annealing 30", 72°C extension 30"), for 33 cycles (*βactin* control) or 38 cycles (*nkx2.5*). For oligonucleotide primer sequences, please refer to Appendix B.

In situ hybridization

In situ hybridizations were performed using a standard protocol [181] with digoxigenin-labeled probes. Embryos at appropriate stages were fixed in 4% PBST/formaldehyde, and incubated with previously-published antisense probes *nkx2.5* [61], or cloned using published gene sequences (*nkx2.7* , NM_131419). Probes were detected with mouse-anti-DIG antibody conjugated to alkaline phosphatase (Roche, 1:5000), and developed in BM Purple AP substrate (Roche). Except where otherwise noted, embryos were examined throughout development, and fixed at identical time points. 'Hours post-fertilization' refers to the developmental stage of the wildtype embryo. For embryos fixed during somitogenesis, individual somites were counted for each group to ensure identical developmental stages.

Injection of nkx2.5 mRNA

A cDNA library of zebrafish mRNA was obtained, and used to isolate cDNA for *nkx2.5*. The cDNA was cloned into pcGlobin2, which was prepped, digested with XmaI, and extracted using phenol-chloroform. *In vitro* transcription was performed using the mMessage, mMachine kit and a T7 RNA polymerase, followed by gel analysis and quantification. mRNA (75 pg or 150 pg) was microinjected into single cell embryos alone, or co-injected with AA-MO1 or AB-MO2 morpholino.

Exposure to Wnt and Bmp modulating agents

Dorsomorphin homologue 1 (DMH1 [182]) and 6-BromoIndirubin-3'-Oxime (BIO [183]) were diluted from stock solutions (10 mM in DMSO) into egg water at a final concentration of 50 nMol (DMH1) and 100 nMol (BIO). Embryos were exposed to drug treatment from 2 hpf to 5 hpf, followed by three serial washes. Both treated and untreated embryos were grown to 12 hpf, and formaldehyde fixed for *in situ* hybridization at the 6 somite stage. Staging was performed according to developmental stage rather than time.

Generation of pc-globin-HA, pcGlobin-scn5Lab constructs

The pcGlobin2 vector provides a modification of the pCS2 optimized for in vitro transcription and microinjection of zebrafish mRNA [184]. PCR primers (Appendix B) were used to isolate the triple hemagglutinin tag (3HA) from a donor plasmid, with a restriction site XhoI (CTCGAG) on each end. XhoI restriction and ligation was used to clone the 3HA segment into the multiple cloning site (MCS I) of pcGlobin2, followed by direct sequencing to verify direction of the insert. A site-directed mutatgenesis kit (QuikChange II) was used to eliminate the second XhoI site, allowing for complete use of the MCS in the new pcGlobin2-3HA plasmid. To generate the *pcGlobin2-scn5Lab-3HA* plasmid, SacII-XhoI restriction was used, with site-directed mutagenesis to eliminate the stop codon of the *scn5Lab* gene. To generate *pcGlobin-scn5Lab*, simple restriction (SacII, XhoI) and ligation was used from the plasmids previously described [61].

Generation of Tg(hsp70l:scn5Lab, cmlc2:gfp) zebrafish

A Tol2-based transposon system (Tol2Kit) (Figure 2.3) was used as previously described to generate a Tg(*hsp70l:scn5Lab, cmlc2:GFP*) line [185]. BssHII restriction was used to remove and replace the MCS of pME-MCS in the reverse orientation, creating pME-rMCS. Direct sequencing was used to verify direction, followed by SacII, XhoI cloning of *scn5Lab* from pcGlobin2-scn5Lab. p5E-Hsp70l, pME-rMCS-scn5Lab, and p5E-pA were recombined with the pDestTol2CG2 destination vector, using LR Clonase II plus (Invitrogen). Clones were identified through a combination of restriction of each component vector, followed by direct sequencing. Transgenic zebrafish were generated through microinjection of a positive clones with mRNA for transposase as described [185]. Transient transgenic zebrafish at 48 hpf with greater than 50% GFP-positive hearts were selected and grown to adulthood (F0) line. Adults were test-crossed to evaluate germline insertion of the transgene. GFP+ offspring of the testcrosses were cultivated as the F1 line, and used in subsequent experimentation. Heat shock

induction of the transgene was performed as previously described, for 1 hour at 38°C, followed by an immediate wash with 28°C egg water. For evaluation of induced expression, RNA was isolated using 1 mL Trizol, followed by 2x phenol, 2x chloroform extraction, and isopropanol precipitation. RT-PCR was performed using standard protocols; (94°C denaturing 30”; 59°C annealing 30”, 72°C extension 30”) for 38 cycles to identify expression of 5’ and 3’ ends of *scn5Lab*. See Appendix B for oligonucleotide primers used.

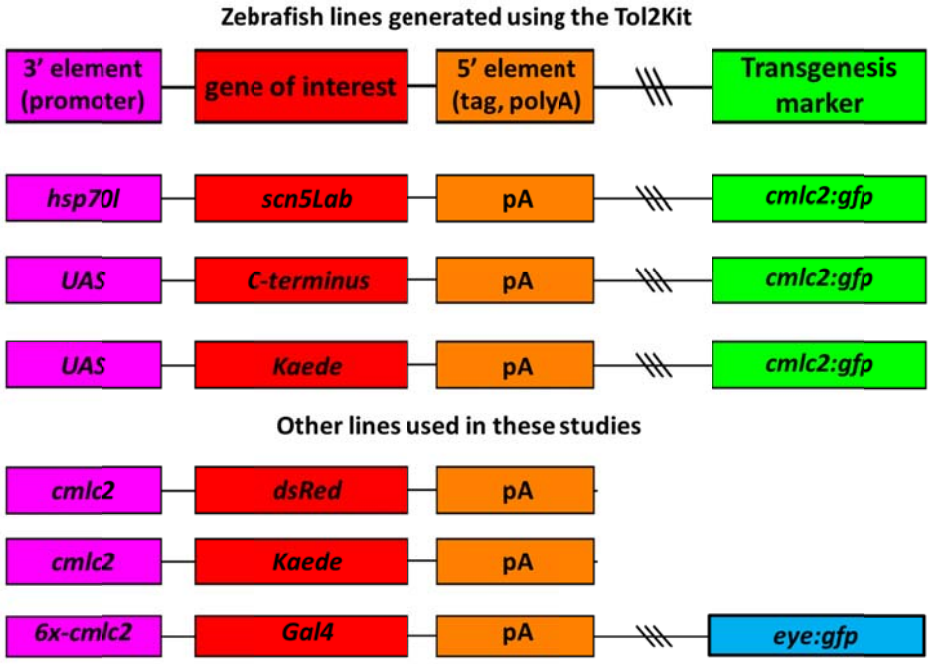

Figure 2.3: Tol2 transgenesis and transgenic lines used in these studies. Each Tol2Kit transgenesis construct consists of a 3’ promoter element (purple), a middle element (red) containing the coding sequence for a reporter gene or a gene of interest, and a 5’ tag or polyA element (orange). The constructs then are cloned into a destination vector with an optional heart-specific GFP transgenesis marker. Other lines used in this study are included above, obtained as gifts or as previously described above.

Results

Rescue efforts: scn5Lab mRNA injection, inducible scn5Lab transgenics

We have previously cloned the cDNA of *scn5Laa* and *scn5Lab* into expression vectors for heterologous expression and electrophysiology [61]. For rescue of the morphant phenotype, we cloned *scn5Lab* cDNA for the channel into a pc-Globin2 vector backbone containing the zebrafish β-globin untranslated regions (UTRs) [184]. This vector is optimized for mRNA stability following microinjection into the fertilized ovum. Additionally, we modified the vector to contain a triple hemagglutinin (3HA) tag from the influenza A virus. This new HA-pcGlobin2 vector modifies any protein cloned into the MCS with a C-terminal epitope tag. To verify expression of the channel, and the HA-tag, we transfected Chinese hamster ovary (CHO) cells with the plasmids, and performed electrophysiology studies on the cells. Each plasmid generated cells with a typical sodium current (Figure 2.4). The magnitude of the signal was decreased in the scn5Lab-3HA transfected cells versus scn5Lab transfected cells, but reflected a significant amount of mature channel in the plasma membrane. The HA tag was unable to be consistently detected using Western blotting of transfected CHO cells, or of zebrafish embryos injected with the construct. Further studies evaluating the protein expression and epitope tag placement are necessary to determine the reason.

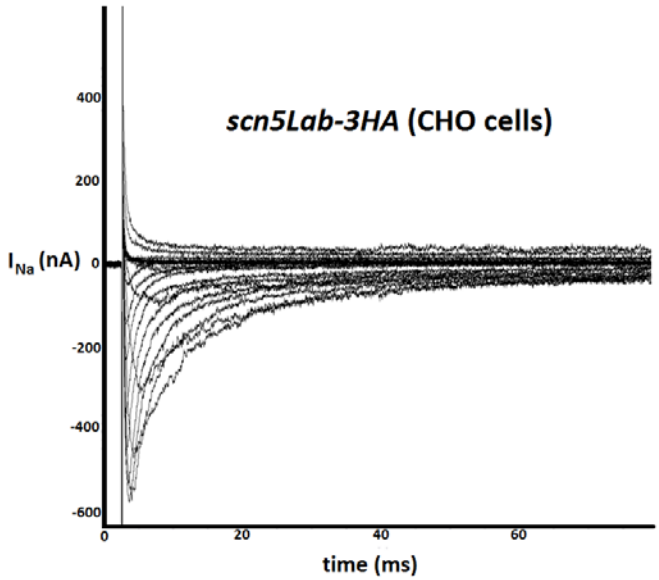

Figure 2.4: Heterologous expression of scn5Lab-3HA. Sodium current is detected after patch clamp of Chinese Hamster Ovary (CHO) cells transfected with *pcGlobin2-scn5Lab-3HA*.

Varying doses of mRNA were microinjected into one-cell embryos. A maximal tolerated dose of 400 ng was found, was co-injected with AB-MO2 morpholino. No significant rescue of cardiac morphology was found. As a complex membrane protein with multiple domains, it was possible the mRNA was not efficiently expressed to the plasma membrane. mRNA encoding scn5Lab-3HA was then injected into the embryos, and Western blotting was performed. No consistent detection of the 3HA signal was possible, suggesting the technical difficulty of translating a large membrane protein from in vitro synthesized mRNA was too much to overcome.

To avoid the pitfalls of in vitro transcription and subsequent cellular translation of large genes, we generated transgenic embryos expressing the full-length *scn5Lab* gene, under the inducible hsp70l promoter. Using the tol2kit, we generated *hsp70l:scn5Lab*, *cmlc2:gfp* transient transgenic animals, and selected them for germ-line insertion (Figure 2.5). Rescue of *nkx2.5* expression (evaluated via *in situ* hybridization) at 12 hpf was not observed following 38°C heat shock at either 90% epiboly, tail bud, or 1 somite stage. To verify inducible expression from the construct, embryos were exposed to heat shock for 1 hour, then RNA was collected, and reverse-transcription/PCR performed. An increase in *scn5Lab* mRNA was seen, along with amplification of both 5' and 3' transgenic-specific regions of transcript.

Phenotype from scn5La knockdown is likely not a result of non-specific effects of morpholino

To demonstrate specificity of the effect of anti-Scn5L morpholinos, we evaluated increasing doses of *scn5Laa* morpholino on the expression of *nkx2.5* through RT-PCR. Increasing doses of AA-MO1 resulted in decreased expression of *nkx2.5*, with a 6 ng dose nearly completely abolishing expression of the gene at 12 hpf (Figure 2.6 A) [61]. In situ hybridization with a morpholino to *scn5Lab* (AB-MO2) demonstrated a similar effect (Figure 2.6 B), with the maximum 2.5 ng dose resulting in nearly complete loss of *nkx2.5* from the ALPM.

Microinjection of morpholinos has been shown to result in an increase in P53-mediated cell death [180]. To ensure loss of *nkx2.5* was not an effect of off-target toxicity to the embryos, active

morpholinos were co-injected with 4.5 ng anti-P53 morpholino (Gene Tools Inc). Embryos injected with p53-MO alone showed no difference from uninjected embryos, either in *nkx2.5* expression at 6 somites (12 hpf), or in gross cardiac morphology at 48 hpf. Co-injection of p53-MO with AB-MO2 had no effect on the morphant phenotype (Figure 2.7). Embryos demonstrated nearly complete loss of *nkx2.5* expression, with cardiac dysmorphology at 48 hpf. A 5-base mismatch (MIS-MO2) morpholino was used to further demonstrate the specificity of the AB-MO2 morpholino. Wildtype and MIS-MO2 injected embryos displayed normal cardiac development through 48 hpf (Figure 2.8).

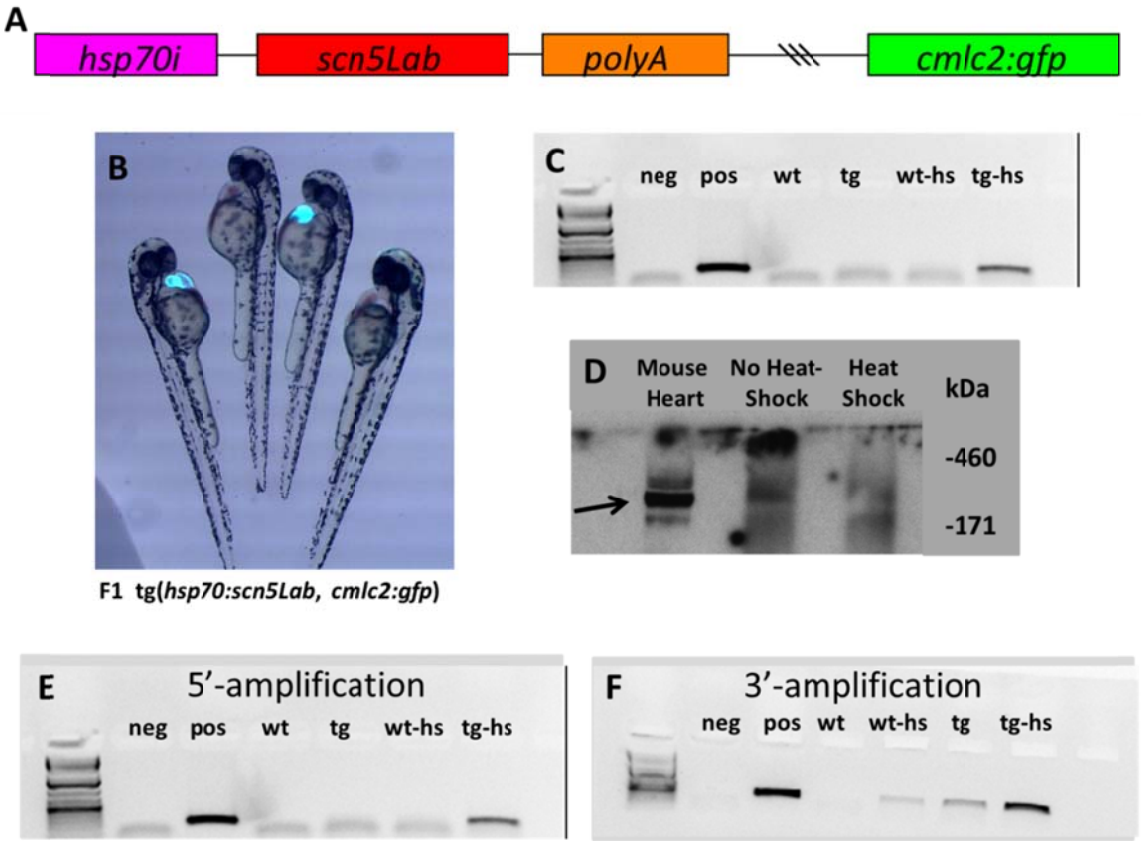

Figure 2.5: Inducible expression of scn5Lab. The tg(hsp70l:scn5Lab) line was evaluated for inducible scn5Lab expression. Embryos injected with the *hsp70l:scn5Lab* Tol2Kit construct (A) were selected for transient transgenesis, then crossed with wildtype and selected for germline transmission (GFP+ hearts, B). Adults from the F1 line were crossed with wildtype adults and embryos evaluated for *scn5Lab* expression. RT-PCR (C) detected *scn5Lab* transcripts in transgenic embryos (tg) after 1 hour exposure to heat shock (hs). Transcripts were not readily detected in wildtype (wt) embryos. Western blotting detected mouse SCN5A, but not zebrafish scn5Lab, with or without heat shock (D). Verification of transcript expression was performed by RT-PCR for primers specific to transgenic expression (E,F). Transgenic embryos exposed to heat shock had significantly increased expression of *scn5Lab* mRNA.

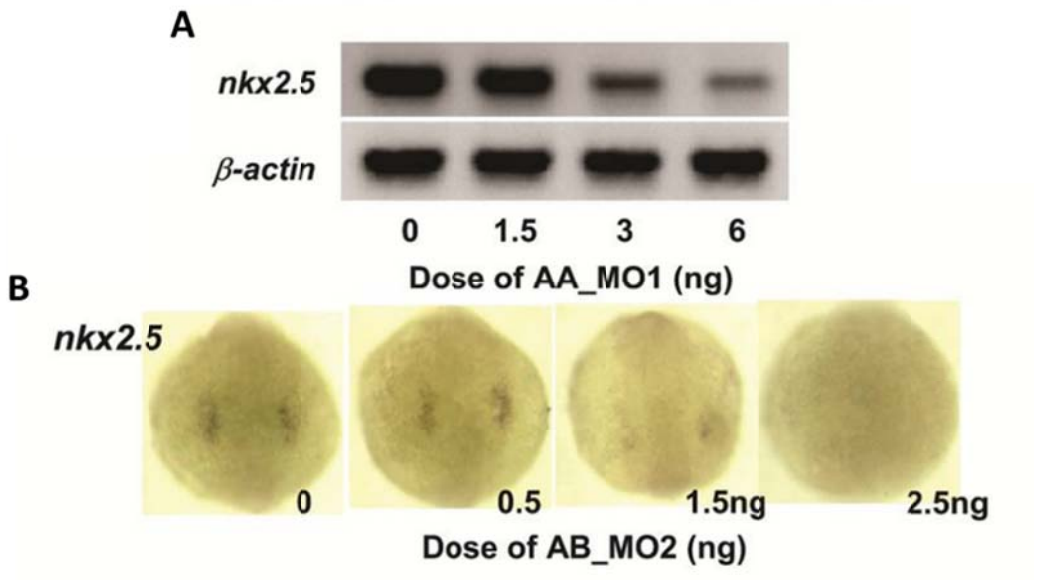

Figure 2.6: Dose response of nkx2.5 to *scn5La* knockdown. Increasing doses of anti-*scn5La* treatment result in decreased *nkx2.5* expression at 12 hpf. Injection of AA-MO1 (A) resulted in a dose-dependent decrease in *nkx2.5* evaluated with RT-PCR, with a dramatic reduction in whole-embryo *nkx2.5* after injection of 6 ng. Expression of β-actin appeared unchanged with any dose. *In situ* hybridization confirmed a similar effect with AB-MO2 injection (B). Embryos injected with 2.5ng AB MO2 had nearly completely abolished *nkx2.5* expression at 6 somites. (Modified from Chopra et al, 2010 [61].

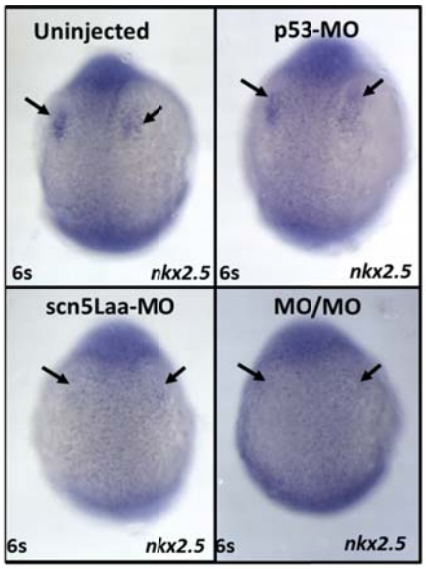

Figure 2.7: p53 morpholino does not rescue the morphant phenotype. Uninjected embryos and embryos injected with anti-p53 morpholino have normal expression of *nkx2.5* (arrows) in the ALPM at 12 hpf. Embryos injected with *scn5Laa*-MO (AA-MO1) have nearly completely abolished expression of *nkx2.5.* Co-injection of anti-p53 morpholino with scn5Laa-MO (MO/MO) has no effect on the morphant phenotype, and does not restore ALPM expression of *nkx2.5*.

Knockdown of scn5Lab inhibits expression of nkx2.5, but not nkx2.7

The phenotype observed in scn5Lab-depleted embryos is more similar to that of double *nkx2.5*/*nkx2.*7, with impaired cardiac looping, as well as a dramatically-reduced ventricle size; as opposed to single knockdown of nkx2.5, which has a minimal effect of cardiac development. Co-injection of *nkx2.5* alone failed to rescue the morphant phenotype. To further evaluate gene expression in the ALPM, *in situ* hybridization was performed on the related NK2 family gene *nkx2.7*. Embryos from a single AB-MO2 injection series were randomized and fixed at 12 hpf, then evaluated for *nkx2.5* or *nkx2.7* expression (Figure 2.9). As expected, expression of *nkx2.5* was nearly completely abolished. However, *nkx2.7* appeared to follow its normal expression pattern [144], with intensity and spread of the signal identical in both uninjected and morphant embryos (Figure 2.9 E-J). The data suggest the effect of *scn5La* on specification of pre-cardiac mesoderm is specific for *nkx2.5* and does not overlap with other genes in the NK2 family.

Nkx2.5 is known to function as both a specification factor in cardiac progenitors, as well as in differentiated myocardium, modulating growth of the early heart tube [151]. As *scn5La* appears to play a biphasic role in specification of myocardium, and later in growth of the heart, we evaluated the heart tube of uninjected and *scn5Lab*-morphant for expression of *nkx2.5* at 24 hpf. We found that while *scn5Lab* is required for early expression of *nkx2.5* in the ALPM, cardiomyocytes of the heart tube at 24 hpf appeared to have normal expression of the gene (Figure 2.9 C,D). The area of expression is reduced, consistent with decreased heart size; however the intensity of expression appears the same. The data suggest multiple temporal factors induce expression of cardiac-specific transcription factors, and *scn5La* may be important for nkx2.5 expression only during the early stages of cardiac development. Multiple signals are known to influence expression of *nkx2.5 [153, 165]* and it is likely that despite initial loss of *nkx2.5* resulting in a decrease in myocytes, other genes compensate for loss during differentiation.

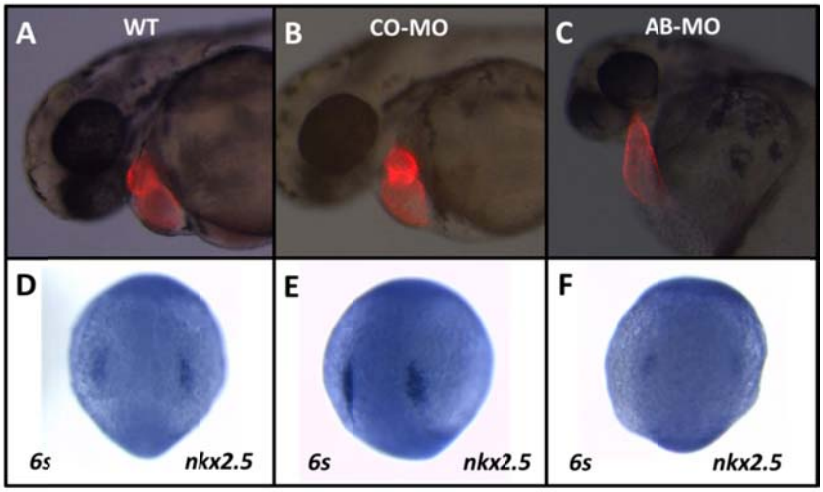

Figure 2.8: Mismatch morpholino-injected embryos have a wildtype cardiac phenotype. Embryos which are uninjected (A) or injected with 5 base mismatch morpholino (B) have normal cardiac development at 48 hpf. Embryos injected with active AB-MO2 morpholino (C) display cardiac malformations at 48 hpf, including un-looped hearts with small ventricles. Uninjected and mismatch-injected embryos also display normal expression of nkx2.5 by in situ hybridization (D,E) while morphant embryos (F) have impaired expression at 6 somites

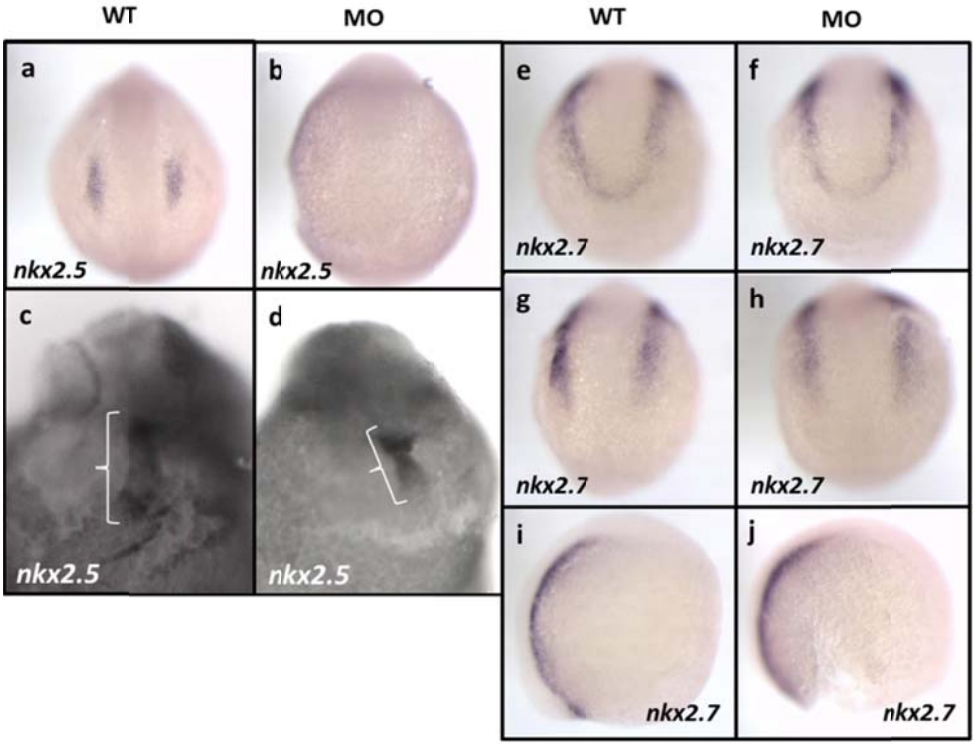

Figure 2.9: Embryos injected with active morpholino show impaired cardiac specification. In situ hybridization for the cardiac-specification transcription factor nkx2.5 (a-b) shows markedly reduced expression in the anterior lateral plate mesoderm. Expression of the related homeobox gene nkx2.7 (e-j) was unaffected in embryos from the same injection clutch. Cardiomyocytes at 26 hpf (c,d) have restored expression of nkx2.5, within the smaller heart tube. MO = morphants, WT = uninjected

Modulation of Wnt and BMP signaling in morphant embryos

External fertilization and development make the zebrafish a very accessible model in the study of pharmacologic modulation of gene expression. We examined two pathways important in cardiogenesis to attempt to 'rescue' the morphant loss of *nkx2.5* at 12 hpf. The Bmp and Wnt signaling pathways are both required to establish the expression of *nkx2.5* (and other markers of cardiac fate) in the ALPM [135, 137]. The AMP-Kinase inhibitor dorsomorphin has been shown to modulate BMP signaling, and increases adoption cardiac fate in embryonic stem cells [186]. A similar compound, DMH1, has been shown to modulate BMP signaling avoiding interfering with VEGF signaling [182]. Canonical Wnt signaling plays a biphasic role in specification of pre-cardiac mesoderm of zebrafish; expression before 5 hpf increases the size of the cardiac fields, while induction after 5 hpf resulted in a significantly smaller field [135]. Previous studies have identified the glycogen synthase kinase-3 (GSK-3) inhibitor Bio as a Wnt signaling agonist [183]. Wnt signaling is required for cardiogenesis, and inhibition of Wnt signaling (by induced expression of *dickkopf*) before 5 hpf results in dramatic decrease in *nkx2.5* expression [135]. Here we use activation of Wnt signaling through GSK-3 inhibition, to attempt to rescue expression of *nkx2.5* in morphant embryos.

We exposed developing uninjected and morphant embryos to 200 nM DMH1 and Bio from 2 hpf to 5 hpf, before allowing them to develop to the 6 somite stage. In situ hybridization for *nkx2.5* showed the uninjected and both drug-exposed groups had normal expression of *nkx2.5* in the ALPM (Figure 2.10 A-F). Morpholino-injected, and morphant embryos exposed to drug appeared to all have decreased expression of *nkx2.5*. To quantify the effect, we evaluated each treatment for robustness of expression, and compared the groups (Figure 2.10 G). Uninjected (WT) embryos had 97% of embryos with normal or robust expression of *nkx2.5*, while the morphant, and morphant exposed to Bio or DMH1 embryo each had approximately 25% of embryos with normal, and no robust expression of *nkx2.5*. Drug exposed embryos did have a decreased proportion of embryos with faint/absent *nkx2.5* (27% for morphants, 8%

for morphants + DMH1, 4% for morphants + Bio). The data indicate that the agents generate only a small effect on expression of *nkx2.5*, and that the role for *scn5Lab* in the expression of *nkx2.5* is not through modulation of BMP or Wnt signaling pathways.

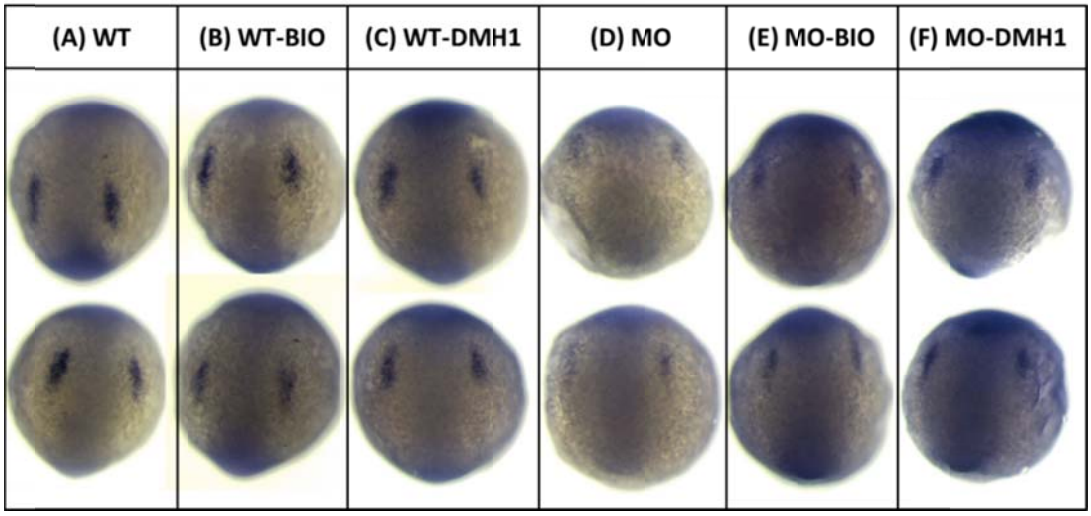

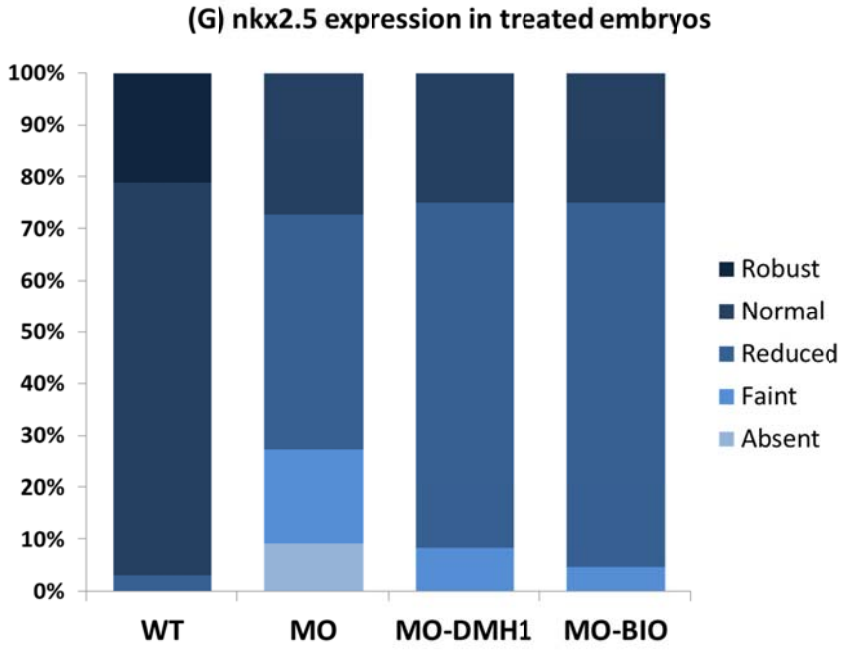

Figure 2.10: Modulation of Wnt and Bmp pathways fails to rescue the morphant phenotype. Wildtype embryos (A), embryos exposed to a Wnt activator (Bio, B), or a Bmp inhibitor (DMH1, C) all have normal or slightly increased expression of *nkx2.5* at 12 hpf. Loss of expression of *nkx2.5* in morphant embryos (D) is not rescued by exposure to Bio (E) or DMH1 (F). Quantification of *nkx2.5* expression in wildtype and treated morphant embryos (G) confirms failure of the drugs to rescue loss of *scn5Lab*, with no increase in the percentage (20-30%) of embryos expressing normal *nkx2.5*.

Given early loss of *nkx2.5* expression as the primary *scn5La* morphant phenotype, in the presence of a phenotype similar to that observed in combined *nkx2.5*/*nkx2.7* knockdown, we used an *in vitro* transcription kit to generate sense mRNA for microinjection into morphant embryos. As previously described by others, injection of 100 pg *nkx2.5* mRNA into wildtype Tg(*cmlc2:GFP*) embryos resulted in a larger heart with an intense GFP signal at 48 hpf. Co-injection of *nkx2.5* mRNA with AA-MO1 or AB-MO2 (Figure 2.11) had no rescue effect on the morphant phenotype. In many embryos, co-injection had a deleterious effect on the embryo, resulting in a more severe cardiac phenotype. As heart development was not rescued with addition of *nkx2.5*, there may still be yet undetermined genetic factors affected by loss of *scn5La* resulting in the morphant phenotype.

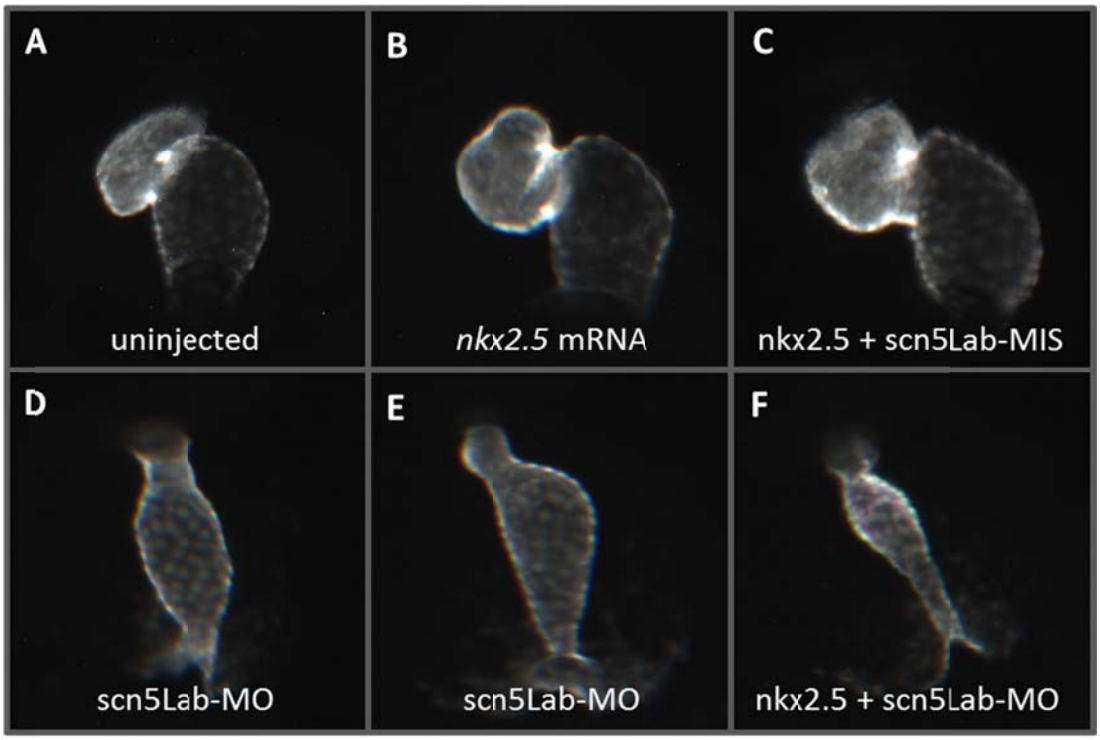

Figure 2.11: nkx2.5 mRNA is insufficient to rescue loss of scn5Lab. Wildtype embryos (a), or embryos injected with 150 pg nkx2.5 mRNA (b) or mRNA with scn5Lab-MIS morpholino (c) show no gross morphological phenotype. scn5Lab-MO injected embryos (d,e) are not rescued by co-injection of nkx2.5 (f).

Later gene expression unaffected in morphant embryos

Previous data have established loss of *scn5La* results in a smaller heart tube at 24 hpf. Despite early loss of *nkx2.5* expression, other genes, such as *vmhc* and *cmlc2* [61] are decreased in proportion to the smaller cardiac fields. In addition, we evaluated morphant embryos for expression of the t-box transcription factor *tbx5*. In morphant embryos, we observed decreased expression of *tbx5* with *in situ* hybridization at 10 somites. The bilateral pre-cardiac fields were present, however the signal was significantly reduced in AB-MO2 embryos and the fields appeared decreased in size (Figure 2.12 A-D). These data were consistent with loss of *scn5Lab* resulting in a smaller heart tube as a result of impaired initial specification of cardiac mesoderm.

Following initial expression of NK2 genes in the ALPM, specification and differentiation proceed as the bilateral stripes of cardiac precursors migrate dorsally to form the heart tube. We examined an additional marker of pre-cardiac and early differentiated mesoderm for expression in *scn5Lab* morphants. The *early cardiac connexin* (*cx36.7*/*ecx*) has been found to promote expression of *nkx2.5* in differentiating myocardium, and is critical in cardiac morphogenesis. We observed that morphant embryos were positive for *ecx* expression in the lateral plate mesoderm at 16 somites, and in the heart tube at 24 somites (Figure 2.12 E-H). Consistent with earlier loss of *nkx2.5*, the cardiac fields appeared decreased in size in morphant embryos. Both sets of data indicate expression of important cardiac specification genes is reduced following the loss of *nkx2.5* expression. Impaired differentiation of the primary heart tube may be a secondary result of decrease cardiac specification, and not a direct effect of loss of *scn5Lab*.

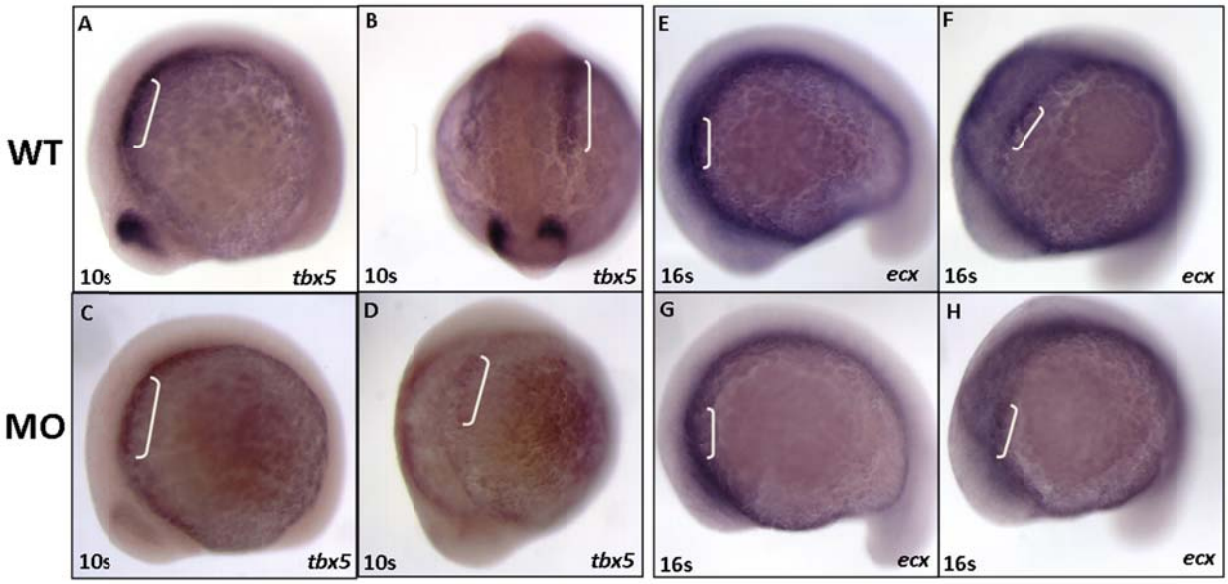

Figure 2.12: Pre-cardiac fields have reduced expression of *tbx5* and *ecx*. Wildtype embryos (A,B) express *tbx5* in bilateral stripes of cardiac precursors at 14 hpf (10 somites) detected by *in situ* hybridization. Embryos injected with AB-MO2 (C,D) have positive, but reduced expression of *tbx5*, consistent with decreased specification of pre-cardiac mesoderm observed earlier. Wildtype embryos express the early cardiac connexin (*ecx*) in bilateral stripes (E,F) during cardiac differentiation at 16 somites (16s). Morphant embryos (G,H) have reduced expression of the *ecx*.

Secondary heart field genes

Loss of *scn5La* disrupted the primary specification of myocardium through the loss of the transcription factor *nkx2.5*. Further *in situ* hybridizations were performed to evaluate expression of second heart field genes in morphant embryos at 24 hpf. Embryos were fixed at 24 hpf development, then stained for expression of *fgf8*. With robust neural expression of the gene immediately dorsal to the cardiac region, expression was not detected in the hearts of either the wildtype or morpholino-injected group. The feedback inhibitor of FGF signaling, *sprouty4* (*spry4*), has stronger relative expression in the heart and was used to subsequently evaluate the SHF. *In situ* hybridization on uninjected, mismatch-injected, and morpholino-injected (AB-MO2) embryos revealed expression of *spry4* in the region distal to the ventricle in all three groups (Figure 2.13). Additionally, another SHF gene, *ltbp3* was evaluated for expression in morphant embryos. Again, the gene was expressed in both wildtype and morphant

embryos. In the cases of *spry4* and *ltbp3*, comparative expression levels were difficult to assess among groups, with variable background, and a small region of expression. In particular, the prevalence of FGF signaling in many tissues, both obscured *in situ* comparisons, and made alternative gene expression assays such as quantitative PCR, impossible. To further evaluate the SHF and outflow tract myocardium in morphant embryos, we modified a method used previously by other groups to qualitatively and quantitatively assess SHF contribution to the outflow tract myocardium, which is discussed in Chapter IV.

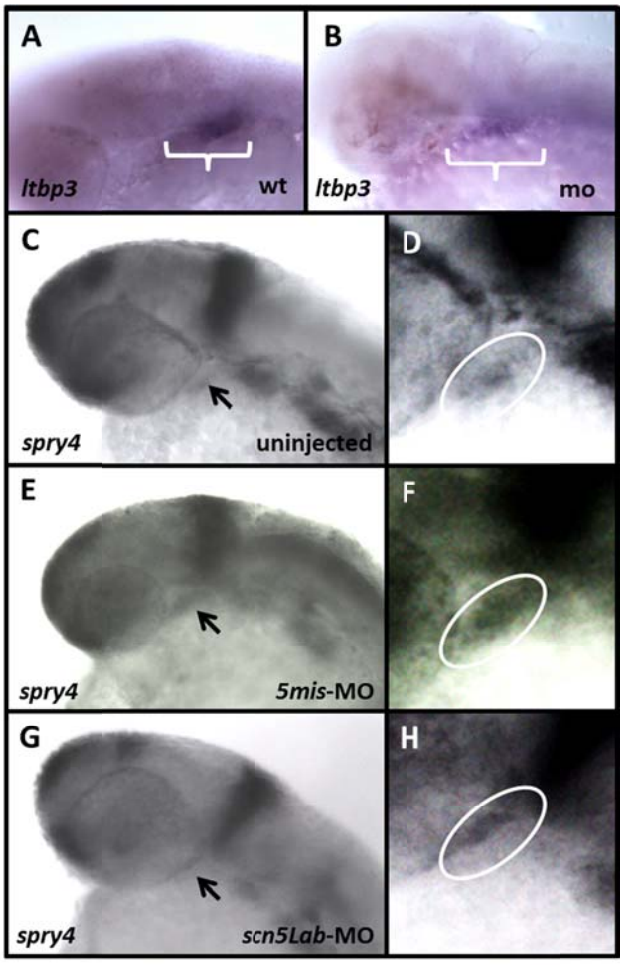

Figure 2.13: Morphant embryos express secondary heart field markers. Wildtype (A) and AB-MO2 (B) embryos both express *ltbp3* at 24 hpf, a marker of the secondary heart field (SHF). Uninjected (C, zoom D), mismatch (E, zoom F), and AB-MO2 (G, zoom H) embryos all express *spry4*, a marker of Fgf signaling in the SHF. Despite impaired primary specification, secondary differentiation appears intact in embryos without scn5Lab.

Discussion

Embryos deficient in scn5Lab exhibit preferential ALPM loss of nkx2.5

Embryos deficient in *scn5Laa* or *scn5Lab* showed dramatically decreased expression of *nkx2.5* in cardiac precursors at 12 hpf. Addition of *nkx2.5* mRNA to morphant embryos had no effect, or a deleterious effect on the knockdown phenotype. As the cardiac phenotype at 48 hpf is greater in severity than expected from isolated loss of *nkx2.5* expression it is likely additional genes are affected by loss of *scn5La*. As *nkx2.7* expression in the ALPM is unaffected in morphant embryos, we find here that loss of *scn5La* preferentially impairs expression of *nkx2.5* but not *nkx2.7*. In addition, failure of *nkx2.5* mRNA to rescue the morphant phenotype is suggestive that other upstream cardiac specification genes are involved, with *nkx2.5* serving as a read-out of impaired specification. Co-injection of mRNA may have a negative impact on the cardiac phenotype through feedback inhibition of those pathways.

While belonging to the same family and having somewhat redundant functions, *nkx2.5* and *nkx2.7* vary both in genes that activate their expression, and downstream transcriptional targets. Among other pathways, expression of *nkx2.5* is impaired in embryos deficient for *ecx* and *gata6*, or disrupted Bmp signaling [187], while there is no evidence of *nkx2.7* being affected in those mutations [156, 165]. While both genes promote transcription of genes required for cardiac function, the interactions and targets vary. Activation of *nkx2.7* is less well characterized, but as opposed to *nkx2.5*, *nkx2.7* modulates the expression of *tbx5* and *tbx20* during early cardiogenesis[150]. The data presented here suggest *scn5La* might affect Wnt or Bmp pathways, resulting in downregulation of *nkx2.5* and impaired cardiac specification. Whether reduced *tbx5* expression at 10 somites suggests its expression is affected by loss of *nkx2.5*, or if it is a result of normal *nkx2.7* expression in a smaller pre-cardiac field, is unknown.

Pharmacologic modulators of Bmp and Wnt signaling appeared to have no effect on *nkx2.5* expression in morphant embryos. The data provide an additional clue as to what pathways are not

affected by *scn5La*-downdown. The morphant phenotype with P53-MO co-injection appears restricted to the heart, and is not particularly suggestive of the dorsalized phenotypes typically observed in Bmp loss-of-function models [188] or the loss of dorsal features promoted by Wnt/β-catenin signals. Further pathway analysis should broadly assay gene expression at gastrulation stages, to identify differentially expressed genes in morphant embryos.

Evaluation of the secondary heart field is difficult in the context of the smaller heart tube found in morphant embryos. The overlap of genes such as *nkx2.5* and *vmhc* blur the distinction between the differentiated ventricle and the SHF. Expression of *ltbp3* and *spry4* is present in near the ventricles in morpholino-injected embryos. Morphological assessment of the late differentiation to the outflow tract would provide a more accurate assessment of the SHF in morphant embryos. Additionally, such a method allows for quantitative comparison of late differentiating cardiomyocytes between wildtype and morphant embryos.

Identification of genetic pathways involving scn5La

In *scn5La*-depleted embryos, we identify specific alteration of *nkx2.5* expression in morphant embryos, with a morphant phenotype more severe than seen in isolated loss of *nkx2.5*, and lack of rescue with *nkx2.5* mRNA. The perturbed expression appears to be a specific effect, as another NK2 family gene, *nkx2.7*, is unaffected at 12 hpf. Other genes (*gata4*, *hand2, tbx5, ecx*) appear to be decreased to a smaller degree, and may be more specific to the loss of *nkx2.5* expression than a direct transcriptional effect of *scn5La* knockdown. Differential gene expression analysis would provide a method to identify any misregulated genes in morphant embryos, particularly upstream of *nkx2.5*, before any identified morphant phenotype, determining if *scn5La* has a direct effect on *nkx2.5* transcription, or functions through a yet-unidentified intermediary pathway.

Further defects in signaling pathways required for specification of pre-cardiac mesoderm in the ALPM must exist. However, while genes required for differentiation and function of cardiomyocytes

have been well-characterized, evaluation of gene expression involved in cardiac specification is more difficult. There are many signaling pathways active during gastrulation, each of which affects the development of numerous tissues and organs beyond the heart. In addition, though there is an enriched region of cardiac precursors near the marginal zone at 40% epiboly [134], signals involved in cardiac specification are not necessarily localized to that region. It is necessary to quantitatively evaluate the whole embryo for perturbed gene expression, with a sensitive enough assay to detect small alterations in expression of pathways affected by loss of *scn5La*.

A hypothesis-free assay such as RNA-seq or microarrays would be a high-throughput means to detect significant changes in gene expression in morphant embryos. Technology has advanced such that the previous microarray standard has been replaced by RNA-seq, a more sensitive and accurate measure of differential gene expression. Thanks to advances in next-generation sequencing technology, and available chips, a multiplexed reaction can evaluate morphant and wildtype embryos at three different stages using a single reaction 'well'. An inherent advantage to using zebrafish is that within a single injection clutch is many biological replicates. A result suggesting differential expression between a treated and untreated embryo actually represents the averaged difference between hundreds of pooled embryos.

Other, directed expression assays are still a potential means to discover genes affected by *scn5La* knockdown. A method of high-throughput gene expression has been developed for whole mount *in situ* hybridization in zebrafish [189]. Adapting the methods to rapidly evaluate multiple known pathways involved in heart development would allow for rapid and accurate qualitative assessment of cardiac specification factors.

Limitations

The gold standard for validation of morpholino knockdown studies is phenotype rescue with mRNA replacement of the targeted gene. We have yet to consistently express and detect *scn5La* protein *in vivo*, which has made it impossible to demonstrate rescue of the morphant phenotype. The failure of full-length mRNA to rescue the phenotype, as well as the failure to detect increased scn5Lab expression in tg(*hsp70l:scn5Lab*) embryos, reflect the technical difficulties of heterologous expression of large, membrane-spanning proteins. Human diseases discussed above, such as cystic fibrosis, specifically arise from impaired folding and maturation of channel proteins. Chapter V discusses experiments designed at rescue of the morphant phenotype, and identification of functional domains of scn5Laa/scn5Lab important for cardiac specification.

Co-injection of anti-p53 morpholino mitigates cell death induced by antisense knockdown of gene expression [180]. However, off target effects of morpholinos do exist, and certain morphant phenotypes have not replicated when a germline knockout has become available. Identification of a zebrafish line possessing a loss of function mutation in *scn5Laa* or *scn5Lab* would eliminate any off-target effects and toxicity, while further establishing the morphant phenotype. It would also allow for less variation in morpholino amount injected, and provide a 'total' knockout. Such a reagent would facilitate the discovery of genes affected by loss of *scn5La*, and allow for more careful quantification of differential expression.

Conclusion

Here we demonstrate specificity of the phenotype observed after *scn5La* knockdown. The loss of *nkx2.5* expression at 12 hpf in the ALPM is both dose-dependent, and specific for *nkx2.5* (and not *nkx2.7*). Additionally, morpholino toxicity does not appear to cause the cardiac phenotype. Co-injection of *nkx2.5* mRNA does not restore normal cardiac development in the embryos, suggesting yet unknown

genetic pathways are affected. Pharmacologic modulation of Wnt and Bmp pathways failed to rescue *nkx2.5* expression, meaning disruption of either pathway is not likely to be directly responsible for loss for impaired specification of pre-cardiac mesoderm. Further assays are necessary to identify the pathways upstream and downstream of *nkx2.5* which are affected by loss of *scn5La*.

CHAPTER III

ELECTROPHYSIOLOGY OF VGSCs DURING CARDIAC DEVELOPMENT

Introduction: Electrophysiology and Development of the Zebrafish Heart

Zebrafish as a model in the study of cardiac electrophysiology

Zebrafish is a proven model studying cardiac development and electrophysiology, despite dramatically differing structural components from mammalian models. Where humans – and mice – have separate cardiac and pulmonary circulation in a four-chambered heart, zebrafish circulation combines systemic delivery and perfusion of blood into a single linear circuit. Mice have a dramatically different heart rate from humans (600 bpm vs. 100 bpm) and altered electrophysiology characteristics, including shorter action potential durations [190]. The embryonic zebrafish heart rate at 28°C is 120-130 bpm, much closer to that of humans [191], and many of the same currents contributing to human cardiac action potentials can be identified in the zebrafish heart [192]. In addition, easy manipulation through the aquatic environment, microinjection, or dissection and isolation of cardiomyocytes has facilitated electrophysiological studies in the developing hearts.

Electrophysiology of the zebrafish heart

Electrical activity of the zebrafish heart can be studied using *in vivo* electrocardiography [193]. Like humans, pacemaker activity of the heart begins at the sinoatrial (SA) node, located in the sinus venosus [194]. Action potentials are then propagated through the atrium, experiencing a 50ms delay through the AV canal, and into the ventricle. Like humans, zebrafish ECGs feature a P wave (representing atrial depolarization), a QRS complex (ventricle depolarization) and a T wave (ventricle repolarization)

[193, 195]. Action potentials recorded from isolated cardiomyocytes reveal further similarities between zebrafish and human cardiac electrophysiology. Resting membrane potential was found to be similar between the two species, and fish action potentials display a distinct plateau, as seen in humans but not mice; further, as in humans, atrial action potentials are shorter than those in ventricle [190].

Using a Tg(*cmlc2:gCaMP*)^{s878} transgenic zebrafish line, Chi *et al* developed a technique to optically map cardiac conduction in the developing heart [167]. At 24 hpf, the linear heart experiences peristaltic waves of contraction, and depolarization proceeds in a linear manner, originating from the SA node. From 36-48 hpf, a conduction delay develops at the AV canal, as each chamber develops and experiences its own synchronous beats. While an AV node has not been characterized in zebrafish, the conduction characteristics suggest myocytes at the atrio-ventricular canal possess electrophysiological profiles contributing to the delay. From 3-4 dpf, the ventricle develops a fast conduction network, which allows depolarization to proceed in an apex to base manner.

Generation and conduction of action potentials throughout the zebrafish heart is produced in much the same way as in mammals. A study published in 1997 of patch-clamped cultured embryonic cardiomyocytes identified multiple currents preserved across species, including sodium, potassium, and both L- and T-type calcium channels [192]. In studies summarized by Verkerke and Remme (2012), I_{Na} (voltage-gated sodium current), $I_{Ca,T}$ and $I_{Ca,L}$ (T-type and L-type calcium channels), and I_{Kr}, I_{Ks}, and I_{K1} (potassium currents) were identified in isolated freshly adult cardiomyocytes [61, 190]. Notably, I_{Kr} and I_{Ks} are critical potassium currents modulating repolarization in humans, but not in mice. Later studies further extended data that structure and electrical responses of adult cardiomyocytes was very similar to that observed in humans, furthering the concept of zebrafish as a model for human cardiac physiology [196].

The study by Chi *et al* also implicated mutations in multiple genes as producing cardiac rhythm abnormalities, including the homeobox transcription factor *tcf2*, which is critical for proper AV conduction. A later study by the same group found that cardiac conduction itself is required for normal cardiac development of zebrafish [197]. The *dco* mutation results in heart failure and uncoordinated ventricular contractions, as well as abnormal cardiomyocyte morphology. Positional cloning identified the affected locus as *gja3* (*cx46*), a gap junction protein forming electrical connections between cardiomyocytes. Studies of the *dco* mutation in a *silent heart* (*sih*) background revealed that electrical conduction of signals through the heart is required to produce normal cardiac morphology during development [197]. Cardiomyocytes at the outer curvature undergo a shape change from circular to elongated between 2 and 3 dpf, as the heart loops and [198]. While wildtype and *sih* embryos underwent normal shape changes at the outer curvature, both $dco^{-/-}$ and $dco^{-/-}$,$sih^{-/-}$ had decreased elongation, suggesting that electrical conduction through myocardium is required for development, regardless of the ability of the myocardium to contract in response to an electrical stimulus.

High-throughput forward genetic screens have identified large numbers of zebrafish mutations with abnormal cardiac rate and rhythm [130, 131]. Many mutations resulted in a silent heart, or were accompanied by gross defects in cardiac development, and others experienced ventricular dysfunction due to loss of structural proteins, rather than ion channels. The *tell tale heart* (*cardiac myosin light chain 2*) and *silent partner* (*troponin C*) are two structural mutations which prevent cardiac contractility in the presence of normal action potential conduction. Other mutations affecting rhythmicity, *breakdance*, *tremblor*, *island beat*, and *slow-mo*, among others, represent models in which to study human cardiac arrhythmias and the ion channels responsible for them, described further below.

Zebrafish mutations affecting cardiac rate and rhythm

In the past 20 years, the zebrafish has yielded important discoveries relating to cardiac electrophysiology. One study examined the *slow-mo* (*smo*) zebrafish mutation, identified as having a defective cardiac pacemaker and bradycardia. The group found normal currents in isolated embryonic cardiac myocytes, except for a defective I_h current [192]. I_h (also named I_f) is a non-selective Na^+/K^+ current, which had been hypothesized to control the baseline slow depolarization responsible for action potential generation [199]. A 2001 study by the same group further determined that I_h is required in adult zebrafish to maintain physiological heart rates, even in the presence of neural and hormonal modulation of heart rate [200].

Mutations in zebrafish ion channels can mimic human cardiac arrhythmias, particularly in the case of the zebrafish ether-a-go-go related gene (*zERG, kcnh2*). Mutations have been identified in the channel in the *reggae* (short QT) and *breakdance* (long QT) strains [201, 202]. Mutations within the voltage sensor of zERG results in increased potassium rapid delayed rectified current I_{Kr} and accelerated repolarization in the *reggae* line [201]. The mutation was the first animal model for human short QT syndrome, and accessibility of the cardiac space to pharmacological modulation represents an important tool to study the phenotype. Evaluation of the *breakdance* mutation revealed a persistent 2:1 heart block, in which the ventricle contracts with every second atrial contraction [202]. Further studies revealed an atrioventricular block caused by impaired repolarization of the ventricle and an increase in action potential duration. The phenotype largely mimics human LQTS (where 2:1 block is also seen in severe cases), and provides an additional model for the human phenotype. Later studies have focused on the use of both wildtype and mutant zebrafish lines to screen for drugs which modulate the QT interval [203, 204]. In 2011, the Rottbauer group identified disrupted zERG/I_{Kr} channel trafficking as the mechanism for diminished repolarization [205]. Administration of cisapride and dimethylsulfoxide was sufficient to increase cell surface channel density and rescue the long QT phenotype.

Zebrafish mutations affecting myocardial calcium handling in the heart

Excitation-contraction coupling in the heart is achieved through influx of Ca^{2+} through L-type calcium channels in response to membrane depolarization, and the calcium-induced release of calcium through ryanodine receptors (RyRs). During Phase 4 of the action potential, following repolarization, calcium ions are removed from the cytosol and returned to the intracellular and extracellular stores. The Na^{+}/Ca^{2+} exchanger (NCX) removes Ca^{2+} from the cytosol, in exchange for the entry of three Na^{+} ions into the cell [22]. The sarco/endoplasmic reticulum ATPase (SERCA) also removes Ca^{2+} from the cytosol, using ATP hydrolysis as an energy source [23]. *SERCA* handles approximately 70% of the intracellular calcium, recycling ions from the cytosol to the sarcoplasmic reticulum, a subcellular compartment responsible for Ca^{2+} storage [206]. Mutations affecting cardiac development in zebrafish have been identified in both of the major channels responsible for calcium handling within cardiomyocytes [207]. Morpholino knockdown has been used to study loss-of-function phenotypes of the zebrafish *SERCA* ortholog, *serca2* (*atp2a2a*) [208]. Inhibition of *atp2a2a* translation or pharmacologic inhibition of the serc2 channel in zebrafish embryos produced defects in cardiac contractility and morphology, without the arrhythmias identified in the *tremblor* mutants [208]. Both treatments produced intracellular overload of calcium, indicating an important role in calcium ion homeostasis for both cardiac function and development.

The *tremblor* locus in zebrafish encodes the cardiac sodium-calcium exchanger *ncx1h* (also known as *slc8a1a*) [209]. Depolarization of the myocardium in humans results in an influx of calcium to the extracellular space, and repolarization requires *NCX1*-mediated flux of calcium ions to the extracellular space, in exchange for sodium ions [206]. In zebrafish, loss of function of *ncx1h* results in cardiac fibrillation, uncoordinated contraction of the embryonic myocardium [209]. Expression of *ncx1h* is detected by 18 hpf during cardiac differentiation, though the first 24 hours of heart development appear normal. Homozygous mutant embryos die by 6 dpf, with small ventricles and cardiomyocytes with uncoordinated sarcomeres. The data suggest *ncxh1*, likely through regulation of intracellular calcium levels, is required for complete differentiation of myocardium and to establish structural

integrity of the sarcomere [208]. To date, there have been no human Mendelian phenotypes associated with variants in *NCX1*, however multiple non-synonymous single nucleotide polymorphisms (SNPs) in the gene have been reported, and at least one common variant has been associated with QT interval on electrocardiograms [210]. Because of this, the exchanger presents a potential therapeutic target in cardiac dysfunction phenotypes since pharmacologic inhibition of sodium-calcium exchange increases intracellular calcium, and appears to exert a positive inotropic (pro-contractility) effect on myocardium [211]. A 2008 study correlated inhibition of sodium-calcium exchanger function with improved repolarization and suppressed arrhythmias in a long QT syndrome rabbit model [23].

The sodium-potassium ATPase (Na,K-ATPase) functions to maintain high intracellular concentrations of potassium, and high extracellular concentrations of sodium in between action potentials [2]. Two Na,K ATPase isoforms in zebrafish (α1B1 and α2) have been shown to be critical in cardiac development in zebrafish as well [212]. The *heart and mind* zebrafish mutant features a loss of function of the α1B1 isoform, and as a result experiences defects in heart tube growth, cardiac differentiation, and bradycardia. Translation interference of the α2 isoform (*atp1a2a*) results in disrupted laterality of the embryo, including the heart [212, 213]. Though there is a high sequence identity between the two isoforms, it is thought the two phenotypes arise through different mechanisms; α1B1 through a structural and patterning role, and α2 through disrupted calcium handling within the embryo.

Both altered calcium handling and contractile dysfunction have been implicated in developmental cardiac phenotypes of cardiac ion channels. The *island beat* (*isl*) mutation disrupts the L-type calcium channel (LTCC) alpha subunit, and results in lethal perturbation of cardiac development in zebrafish [127]. In homozygous mutants, atrial myocytes contract chaotically, while the ventricle is silent. In addition, the ventricle fails to acquire physiologic numbers of myocytes, a phenomenon not entirely explained by loss of contraction [127, 133]. The role of Ca^{2+} as a second-messenger appears to

be as important for regulation of cardiac development, as it is in cardiac contraction. In addition, other studies in a rat model have found the C-terminus of the LTCC is cleaved and translocated to the nucleus, where it functions as a transcription factor in neurons and myocytes [76]. Gomez-Ospina *et al.* demonstrated the *calcium channel associated transcription* regulator (CCAT) associates with a nuclear protein in neurons to induce expression of genes required for neural differentiation and function [76]. Additional evidence for a non-electrical role in cardiac development for the LTCC has been provided by knockdown of *cacnb2*, the gene encoding a beta subunit (β2.1) for LTCCs [214]. Loss of β2.1 in zebrafish embryos results in heart failure, associated with decreased looping, reduced rate of proliferation, as well as disrupted integrity of the heart tube. Immunofluorescence demonstrated loss of the adherens junctions protein N-cadherin at the cell membrane, indicating the requirement for β2.1 in heart development is related to its function as a cell adhesion molecule, rather than electrophysiology of LTCCs.

Voltage-gated sodium channels in heart development

We have previously demonstrated *scn5Laa* and *scn5lab* are required for cardiac development in zebrafish [61]. As discussed above, expression of the cardiac specification factor *nkx2.5* is perturbed well before contractions of the heart tube are observed can be detected, suggesting there is a possibility of a non-electrogenic (signaling) role for the channel in the differentiation and growth of the heart. Expression of both *scn5La* isoforms can be detected in the fertilized ovum, and expression appears to increase during development [61]. Incubation of embryos with modulators of $Na_V1.5$ function (flecainide, veratridine), as well as channel-specific blockers (TTX) and openers (ATX II) had no effect on expression of nkx2.5 at 6 somites, or on cardiac morphology later in development. Chopra *et al.* further found that despite cardiac expression of *scn5La* being detected through cardiac development, injection into of TTX into the sinus venosus before 4 dpf had little to no effect on heart rate or rhythm, suggesting the channels are not required for cardiac depolarization at that stage [61]. Interestingly, injection of ATX

induced a 2:1 heart block in injected embryos as early as 2.5-3 dpf, demonstrating that while I_{Na} is not required for action potentials before 4 dpf, VGSCs are in the plasma membrane and at a high enough density to affect cardiac rhythm when pharmacologically opened. Injection of the LTCC blocker nisoldipine was sufficient to produce asystole at any stage during development, again pointing to the primacy of LTCCs in early electrical activity in heart. Interestingly, unlike LTCCs, the role for VGSCs in cardiac development appears to be limited to the alpha subunit. Though co-expression of beta subunits with scn5La in a heterologous system modulate the gating and activation of I_{Na}, knockdown of the beta subunits had no gross effect on cardiac development in the first 3 days of life [61, 92].

Question

Previous data suggest the effect of *scn5La* on cardiac development is likely independent of its functions in sodium permeation and cellular depolarization. Here we aim to characterize the developmental electrophysiology of voltage-gated sodium current in the heart, as well as to provide further evidence for the separation of electrical and non-electrogenic roles for voltage-gated sodium channels in heart development. We also aim to develop an assay for the expression of the C-termini of *scn5Laa* and *scn5Lab* and identify developmental properties of the *scn5La* C-terminus for possible rescue of the *scn5La* morphant phenotype.

Methods

Zebrafish lines

A zebrafish line expressing green fluorescent protein (GFP) under a *cardiac myosin light chain 2* (*cmlc2*) promoter was used as the source of cardiomyocytes for wildtype electrophysiology studies [215]. A wildtype (AB) zebrafish line was used in generation of transgenic lines. The Tol2Kit was used to generate germline transmission of *scn5La* transgenics [185]. Using constructs described below, the C-

terminus of *scn5Lab* was subcloned (SacII, XhoI) into the pME-MCS middle entry vector, followed by recombination with p5E-UAS (upstream activating sequence) and p3E-pA (poly A), with a cmlc2:GFP transgenesis marker. Germline transmission was identified and positive embryos were grown to adulthood.

Administration of VGSC-modulating toxins

Modulators of voltage-gated sodium channel function were delivered directly to the circulation of 48 hpf zebrafish. Anenome toxin (ATX II) is a peptide toxin which binds to open voltage-gated sodium channels and prevents inactivation [216, 217]. Tetrodotoxin (TTX) is a peptide toxin isolated from the puffer fish, which blocks the pore of voltage-gated sodium channels, and inhibits Na^+ flux [218, 219]. Embryos were lightly anesthetized with tricaine methanesulfonate to inhibit movement without affecting heart rate, and placed in 1.5% methyl cellulose in zebrafish egg water [181]. Borosilicate needles were used to deliver 2 nL (25ng/mL in H_2O) anemone toxin (Sigma) directly into the left common cardinal vein [220] to avoid volume-related disruption of cardiac function. Phenol red dye was used to evaluate for efficient delivery of the toxin. Embryos were then immediately transferred to egg water without anesthesia and evaluated for altered cardiac rhythm. The L-type calcium channel blocker nifedipine (2 nL, 15 mM) and H_2O (2 nL) were used as positive and negative controls, respectively.

Cardiomyocyte Isolation

Embryos at specific stages were anesthetized and transferred to Eppendorf tubes. Excess egg water was removed, and L15 media with 1% fetal bovine serum (FBS) was added. A 19 gauge needle on a 1 mL syringe was used to disrupt integrity of the embryos, and approximately 75-100 GFP-positive hearts were isolated under a fluorescent dissecting microscope. Hearts were then pelleted for 1 min at 3000 RPM, and washed twice with Hank's buffered saline solution (HBSS). Final volume was set to 0.1 mL, and 750 µL 0.5% trypsin was added. Low-retention micropipette tips were used to gently mix the

isolated hearts, which were then shaken for 5 minutes (5 dpf embryos) at room temperature. Cardiomyocytes were pelleted at 4000 RPM for 5 min in a micro-centrifuge, then washed twice with HBSS, and resuspended in 100 µL HBSS for electrophysiology.

Electrophysiology of cardiomyocytes, heterologous

Embryonic cardiomyocytes were obtained from wildtype zebrafish as described above. GFP-positive cells were identified and selected for studies. Internal INa pipette solution (10 mM NaF, 110 mM CsF, 20 mM CsCl, 10 mM EGTA, 10 mM HEPES) and external INa solution (20 mM NaCl, 110 mM CsCl, 1 mM $MgCl_2$, 0.1 mM $CaCl_2$, 5 mM TAA Cl, 10 mM HEPES, 0.2 mM $NiCl_2$, 10 mM Glucose, 2µM nisoldipine, 2 mM 4-aminopyridine) were used to isolate voltage-gated sodium current. Cells were voltage clamped using an Axopatch 200B amplifier, and voltage was held at -120mV. Cells were exposed to depolarizing pulses (50ms duration) from -80mV to +60mV in 10mV intervals, and current was measured.

Heterologous expression of scn5La

Transfection of *scn5La* constructs was performed on Chinese hamster ovary (CHO) cells. 6 µg plasmid (pcGlobin-scn5Lab, pcGlobin-scn5Lab-3HA) added to cell lines, with 1 µg pIRES-GFP vector as a transfection controls. Lipofectamine 2000 reagent (Invitrogen) and DNA were each added to Opti-Mem medium, followed by mixing and 5 minute incubation, then added to confluent CHO cell culture. Cells were manually harvested with a cell scraper and pelleted in a microcentrifuge. Electrophysiology was performed on GFP+ cells, and Western blotting was performed as described below.

Cloning and microinjection of C-terminal constructs

The C-termini described above (Figure 1.5) for *scn5Laa* (*scn5Laa-ct*), and *scn5Lab* (*scn5Lab-ct*) were isolated using PCR primers (Appendix B), with SacII/XhoI restriction enzymes sites. The segments were cloned into the pcGlobin2 or pcGlobin2-3HA described above, and sequenced to verify proper

insertion. For microinjection, 10 µg of plasmid was linearized with XbaI and gel purified, followed by *in vitro* transcription with the T7 mMessage, mMachine transcription kit (Ambion). mRNA was precipitated with LiCl, and quantified. 1 µL was analyzed on a gel to confirm transcription and exclude degradation (smearing). Doses of 100-400 ng were injected with anti-P53 morpholino, to limit non-specific toxicity to the embryo. For stable germline expression, *scn5Lab-ct* was cloned with pME-MCS (SacII, XhoI) followed by transgenesis as described above.

Western Blotting

Embryonic protein was acquired using a modified version of a previously-published protocol [221]. Embryos were dechorionated, and agitated in deyolking medium to disrupt yolk integrity. Tissue was then collected and pelleted in a 1.5 mL microcentrifuge tube. Protein was manually extracted with a pestle, in RIPA buffer (50 mM Tris, pH 7, 150 mM NaCl, 0.5% sodium deoxycholate, 1% NP-40) with 1 Complete Protease Inhibitor tablet (Roche) per 10mL buffer. Protein was quantified and electrophoresed on 7.5% tris-acetate polyacrylamide gel, followed by transfer to nitrocellulose membrane. Primary monoclonal antibody (mouse-anti-HA clone 12CA5, Roche) was added in blocking buffer, followed by horseradish peroxidase (HRP) conjugated goat-anti- mouse (Sigma) secondary antibody. Blots were washed 10 minutes in Western Blotting substrate (Pierce) and developed 30 seconds on Kodak Biomax film.

Results

Pharmacologic inhibition of embryonic heart rate

To evaluate currents responsible for action potential generation and propagation in the developing embryos, 48 hpf embryos were exposed to sodium channel blocking antiarrhythmic drugs. This class of drugs is effective at, though not specific for, inhibition of current through voltage-gated

sodium channels. Exposure to lidocaine, tetracaine, bupivacaine, mexiletine all decreased heart rate in 48 hpf embryos, with a dose-dependent effect (Figure 3.1). Exposure to tetracaine had the largest effect on heart rate, with a 31% decreased in heart rate (150.6 ± 2.5 vs. 104.1 ± 2.5 bpm) at a concentration of 150µM. Incubation in 300µM tetracaine, a dose producing mild to moderate bradycardia with the other drugs examined, resulted in nearly complete loss of cardiac contraction. A dose of 600 µM tetracaine resulted in complete loss of cardiac contractions.

Expression of VGSC in the early embryonic heart has already been demonstrated [56, 61], and it was initially considered that these drugs acted on embryonic $Na_V1.5$ to inhibit cardiac conduction and produce bradycardia; however multiple lines of evidence run counter to that hypothesis. Tetracaine (and other drugs of that class) has high affinity for the ryanodine receptor (RyR) as well as voltage-gated sodium channels [222]. RyR is largely responsible for intracellular calcium release within a depolarized myocyte, coupling the depolarizing action potential to contraction of the sarcomere. As tetracaine had the strongest ability to slow the heart rate, it was possible the effect of sodium channel blockers on heart rate was a result of inhibition of uncoupling of the excitation and contraction, or direct inhibition of calcium handling in pacemaker cell responsible for maintaining heart rate. Based on data presented here, tetracaine would appear to have the strongest affinity for binding to RyR, followed by bupivacaine, lidocaine, and mexiletine. Additionally, evidence suggests embryonic action potentials are initially driven by depolarization through L-type calcium channels [223]. In mice, robust sodium current is not detected before E14.5, well after cardiac contractility is required for perfusion of the embryo [126]. The effect seen of these drugs on 48 hpf embryos could have been a result of promiscuity of the drug class, affecting Ca^{2+} handling in the heart and producing decreasing the heart rate. To further determine if voltage-gated sodium current is responsible for cardiac conduction at 48 hpf, it was necessary to administer specific VGSC-blocking peptide toxins.

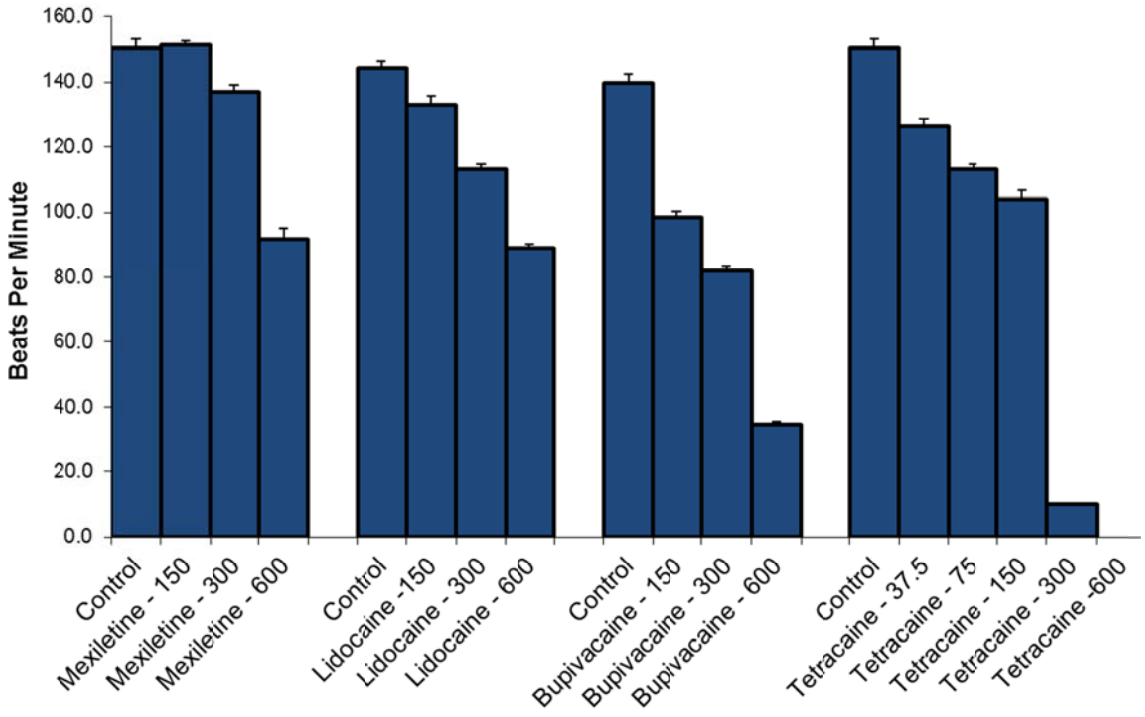

Figure 3.1: Sodium channel blockers dramatically affect embryonic heart rate. Exposure of 48 hpf embryos to lidocaine, tetracaine, mexiletine, and bupivacaine inhibits heart rate in a dose-dependent manner. Exposure to 300µM mexiletine resulted in a 9% reduction in heart rate (150.6 vs.137.0 bpm). The same dose of lidocaine (22%, 144.3 vs. 113.1) and bupivacaine (41%, 139.8 vs. 82.1 bpm) each produced significant bradycardia. Acute tetracaine exposure resulted in nearly complete bradycardia (10 bpm) at 300µM.

Voltage-gated sodium channels are not required for cardiac rhythm at 48 hpf

Previous studies had shown that exposing the developing heart to the sodium channel blocking toxin tetrodotoxin by pressure injection to the sinus venosus demonstrated no effect on cardiac rhythm before 4 dpf [61], thus indicating that permeation through sodium channels does not contribute to cardiac electrical activity at these early stages. To further evaluate sodium currents in the developing heart, we exposed embryos at varying stages to specific modulators of voltage-gated sodium channels, tetrodotoxin (TTX) and anemone toxin (ATX II). Exposure of 24-96 hpf embryos to the L-type calcium channel-blocker nifedipine (100 µM in E3 medium) resulted in complete arrest of cardiac output. Incubation of embryos in medium containing ATXII and TTX had no effect on heart rate or rhythm. To

ensure adequate delivery of the drugs, embryos were microinjected with the drugs at 24 and 48 hpf into the pericardial region. Delivery of 2 nL water resulted in immediate arrest due to volume disruption of the pericardium, with the heart returning to normal activity within a minute. Injection of ATX II and TTX had no effect on cardiac rate and rhythm at 24 hpf or 36 hpf. In addition, embryos injected with TTX experienced complete paralysis, while ATX II injections yielded periods of spastic tonicity, evidence of adequate systemic delivery of the drug.

To avoid volume disruption of the pericardium, and to allow for immediate delivery of the drugs to systemic circulation, further studies were performed using microinjection and delivery of toxins to the common cardinal vein. Control injections of 2 nL water into the common cardinal vein at 48 hpf had no effect on heart rate (n=8). Control injections of nifedipine at 48 hpf resulted in complete cardiac arrest at 36 hpf and 48 hpf in 100% (9/9) of embryos, which persisted for over two hours in 56% (5/9) of embryos at 48 hpf. As previous studies suggested an increased concentration of VGSCs at 2.5-3 dpf, we injected 2 nL (25 ng/mL) anemone toxin (ATX II) [216], a specific inhibitor of voltage-gated sodium channel inactivation, directly into the zebrafish circulation at 48 hpf through the common cardinal vein [220]. An effect from ATX II injection would indicate that channels – not necessarily yet contributing to cardiac electrical activity – were present in the cell membrane at 2 dpf. All treated embryos (n=29) displayed hyperactivity and tonic spasms followed by periods of paralysis, consistent with systemic distribution of the drug. Cardiac arrhythmias in the form of 2:1 heart block were observed in 24% (7/29) of embryos (Figure 3.2). This response was only seen in 9% (1/11) of embryos exposed at 36 hpf. Arrhythmias appeared within 30 minutes of drug injection, and persisted for at least 4 hours. Injection of TTX at 48 hpf resulted in complete paralysis of all (13/13) embryos, but had no effect on heart rate. Our group has previously demonstrated an effect after TTX injection in 4.5 dpf embryos. Here I have shown a small I_{Na} current in isolated 3 dpf cardiomyocytes, and an effect of TTX to produce arrhythmias at 48 hpf. These data demonstrate that latent VGSCs are present in the cell membrane by 48 hpf, though they may

only begin to contribute importantly to cardiac electrogenesis by 3.5-4 dpf, and thus a developmental effect from loss of $Na_V1.5$ may represent a non-electrogenic action of channel expression.

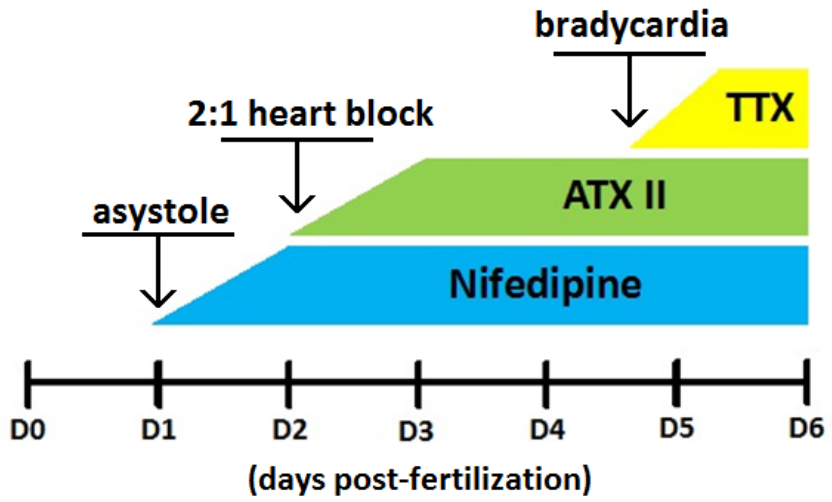

Figure 3.2 Timeline of pharmacologic effects on cardiac rhythm during development. Blockers of L-type calcium channel function (nifedipine) results in asystole as early as 24 hpf (D1), when cardiac contractility is first observed. A 2:1 heart block is produced by injection of the voltage-gated sodium channel (VGSC) activator ATX II in 25% of embryos at 48 hpf (D2), suggesting voltage-gated sodium channels are present in the cell membranes of cardiomyocytes. Bradycardia and heart block are not observed in embryos injected with the VGSC inhibitor TTX before 4.5 dpf (D4-D5)

Voltage-gated sodium currents in isolated cardiomyocytes

To electrophysiologically demonstrate the continual increase in voltage-gated sodium current in the heart during the first week of development, we prepared dissociated cardiomyocytes for electrophysiology studies. Electrophysiology was performed jointly with Hiroshi Watanabe, and images are adapted from those studies. Cardiomyocytes positive for expression of GFP were selected, and patch-clamped using a standard protocol in solution containing blockers of Ca^{2+} (nifedipine) and K^{+} (4-aminopyridine) currents.

Consistent with toxin studies described above, cardiomyocytes from 3 dpf embryos had a small but detectable Na^{+} current during the studies (Figure 3.3 A). Immature cardiomyocytes are difficult to isolate at early stages, and the trypsin preparation often damages the cell membranes. We evaluated inward current through L-type calcium channels, and detected approximately 100 nA current, suggesting the low amplitude of I_{Na} is a trait specific to the age of the cells, rather than the methods of dissociation. Later in development, voltage-gated sodium currents from isolated cardiomyocytes had larger amplitudes. Consistent with the development of the fast cardiac conduction system at 4 dpf, cells from 4 dpf embryos (~450 nA) and 5 dpf (~600 nA) possessed much larger voltage-gates sodium current (Figure 3.3 B-D). In addition, the data reflect an increase in Na^{+} current expected from increased dependence on sodium permeation for depolarization and propagation of action potentials, observed in our toxin studies. By day 7, robust (600+ nA) Na^{+} currents were consistently detected. Electrophysiologic characteristics of the sodium channels at 5 dpf were similar to those observed in studies of human *SCN5A* [21]. The maximal I_{Na} density was observed at a -20 mV test potential. Normalization to determine a voltage-activation relationship found that 50% of the current was achieved at a -28.4±1.4 mV (n=10) test potential (Figure 3.3 E), a slightly more positive voltage than observed in human cardiomyocytes.

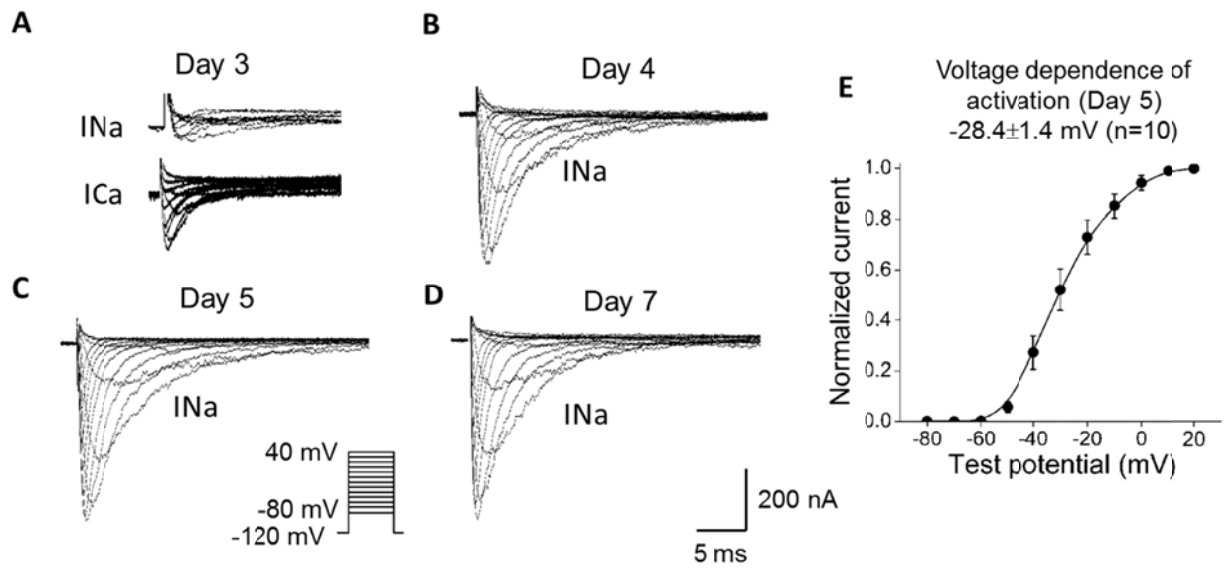

Figure 3.3: Voltage-gated sodium current in Embryonic Cardiomyocytes. At 3 dpf (A), small sodium (INa) currents are detected in isolated cardiomyocytes. Inward calcium (ICa) current is significantly larger than sodium current at this stage. INa increases during cardiac development, from ~450 nA at 4 dpf (B), to over 600 nA in 5 and 7 dpf (C,D) cardiomyocytes. In 5 dpf cardiomyocytes, INa is nearly completely inactive at -60 mV, with 50% activation at -28.4±1.4 mV (n=10) mV (E).

Developmental bioactivity of the C-terminus of scn5Laa and scn5Lab

Morpholino-knockdown and pharmacologic data have established a role for *scn5La* in heart development of zebrafish, likely independent of the channel's function in sodium permeation. To establish a rescue model of the morphant phenotype, and to evaluate functional domains of *scn5La* for bioactivity during development, we generated multiple plasmid constructs of both full and partial *scn5Laa* and *scn5Lab* genes. Full C-terminal domains were cloned into the pcGlobin2 vector from both *scn5Laa* and *scn5Lab*, beginning at the C-terminal 1693E residue of *scn5Laa*, and the 1714E residue of *scn5Lab*. A triple-hemagglutinin tag was added to the C-terminus residues of each, to verify expression. mRNA was transcribed *in vitro*, and injected into early-stage embryos. The 3-HA epitope was detected easily by Western blotting for 10 hpf post-injection, but the signal disappeared by 24 hpf (Figure 3.4 A).

Interestingly, many wildtype embryos injected with C-terminus mRNA demonstrated developmental defects. The phenotypes consisted of midline defects ranging from varying degrees of cyclopia and a phenotype resembling the *one-eyed pinhead* (*oep*) mutant phenotype were observed in embryos injected with *scn5Laa-c* or *scn5Lab-c* mRNA (Figure 3.4 B,C). The most severe phenotypes were seen in embryos injected with *scn5Lab-c* mRNA, with nearly half the embryos having a midline-related defect visible at 48 hpf (Figure 3.4 D). Despite the unexpected phenotypes, no significant cardiac effects were evident at 48 hpf, and no difference in *nkx2.5* expression was observed at 12 hpf.

To determine if altered Wnt signaling was responsible for the mid-line developmental defects, we partnered with the Charles Hong laboratory. An *in vitro* Wnt-luciferase assay was used to evaluate activation of the Wnt pathway following treatment of cells. Exposure to Wnt conditioned medium resulted in a dramatic increase in reporter (luciferase) expression. Transfection of control plasmids, or *scn5Laa* or *scn5Lab* C-terminus had no effect on luciferase, suggesting whatever effect ectopic expression of *scn5La* C-termini has on development is likely not a result of Wnt activation (Figure 3.5).

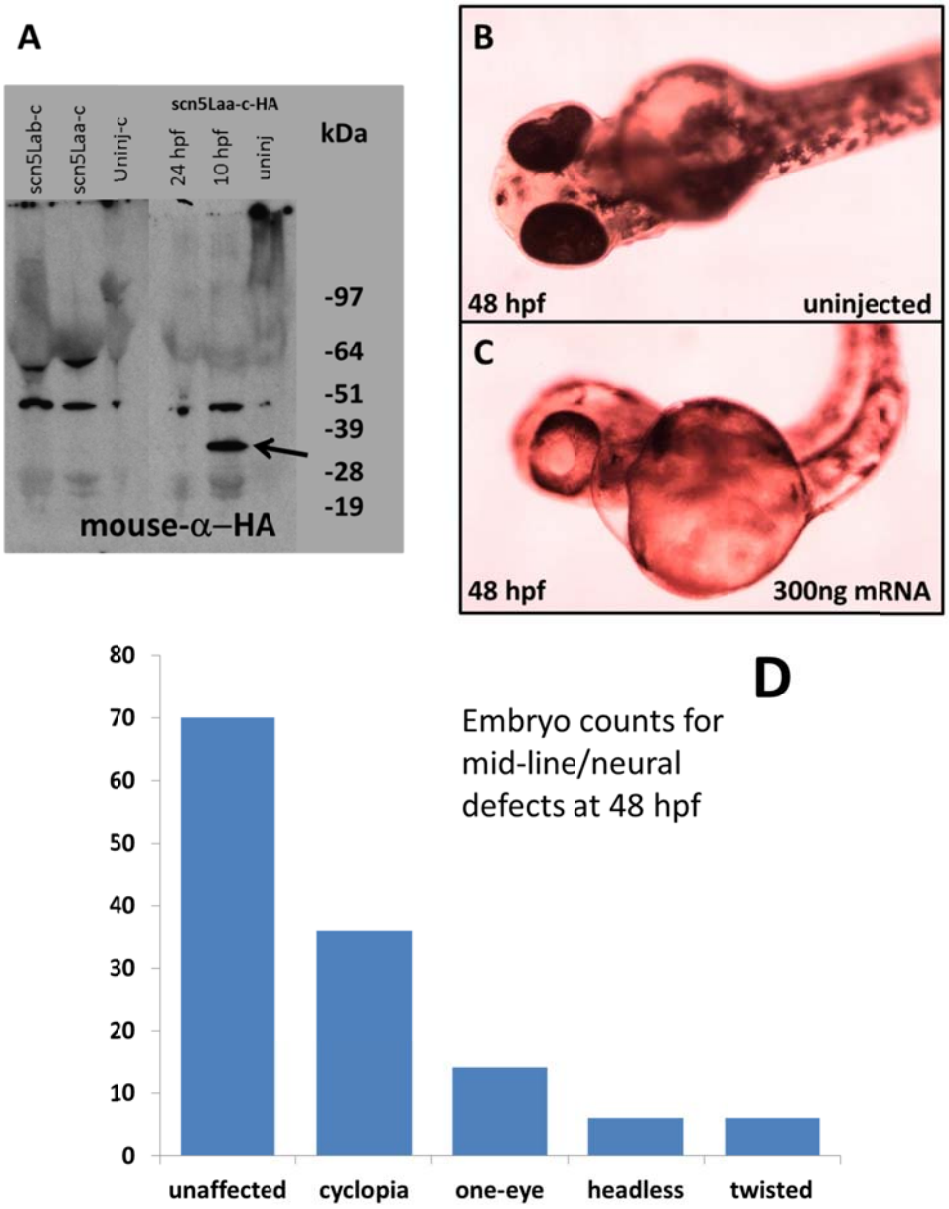

Figure 3.4: Expression of *scn5Lab*-cterminus mRNA results in midline developmental defects. Western blotting detected the HA tag after scn5Laa-C-terminus-3HA, but neither untagged scn5Laa nor scn5Lab. Robust detection was present at 10 hpf, but was negative at 24 hpf, suggesting protein is only evident in the first day post-injection. Uninjected (B) embryos developed normally, while embryos injected with 300ng *scn5lab-cterm* mRNA developed midline defects such as cyclopia (C), as well as one-eyed pinhead, headless, and twisted anterior-posterior body axis phenotypes. Counts of injected embryos (D) suggested 50% developed abnormally, approximately 25% with some degree of cyclopia.

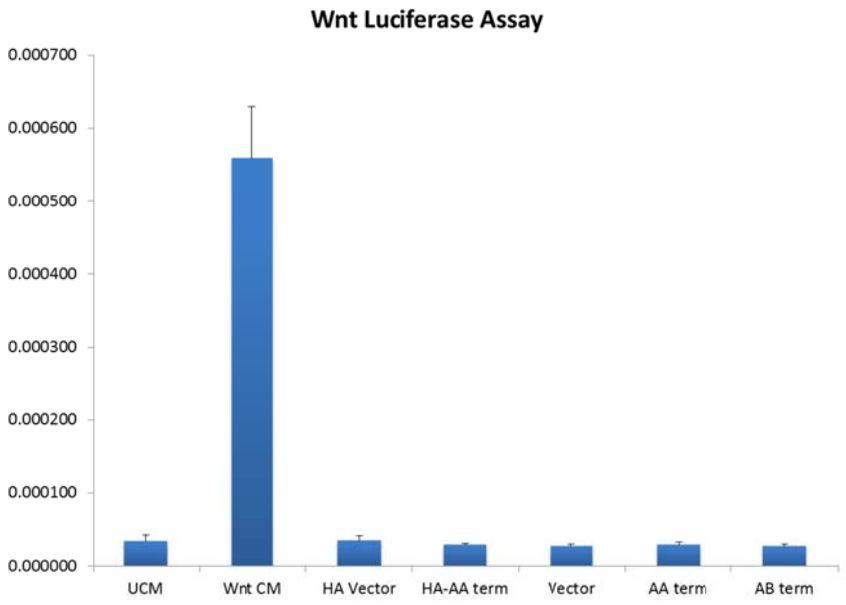

Figure 3.5: scn5Lab C-terminus does not activate Wnt signaling. A Wnt luciferase assay detecting activation of Wnt signaling was performed following transfection of *scn5La* C-terminal constructs. In unconditioned media (UCM), a baseline signal was detected, with robust luciferase activation when grown in Wnt conditioned media (Wnt CM). Transfection of control vector and HA vector resulted in no activation of Wnt signaling. Transfection of C-terminal constructs for scn5laa (AA term), scn5Lab (AB term) and scn5Laa-HA (HA-AA term) resulted in no Wnt activation either.

Multiple methods exist to determine the specificity of this observation, including injection of control mRNA, or mutated versions of *scn5La-ct* mRNA. We generated a line of stable transgenic embryos, expressing the C-terminus under a UAS promoter (Figure 3.6). The tg(*UAS:scn5Laa-c*), tg(*UAS:scn5Laa-c-HA*), and tg(*UAS:scn5Lab-c*) lines each contains a *cmlc2:gfp* transgene for identification of transgenic embryos. The resulting embryos, when crossed to a *cmlc2:Gal4* driver line with CFP expressed in the eye, would express the C-terminus of *scn5Lab* in differentiating cardiomyocytes as early at 18 hpf. A cross of *UAS:scn5Lab-c* X *cmlc2:Gal4* would yield:

25% embryos with no transgene

25% embryos expressing the Gal4 driver in cardiac tissue, with CFP+ eyes

25% embryos with the unexpressed C-terminal transgene , with GFP+ hearts

25% embryos expressing the Gal4 driver, the C-terminus transgene, with GFP+ hearts, CFP+ eyes

Injection of morpholino into embryos from the cross, followed by selection of GFP+ hearts selects for embryos possessing the C-terminal transgene. Rescue could be evaluated by comparison of *nkx2.5* expression and ventricular morphology in GFP+/CFP+ vs. GFP+/CFP- embryos (embryos expressing the Gal4 driver, as well). To this point, detection of CFP+ eyes by immunofluorescence has provided insurmountable technical obstacles.

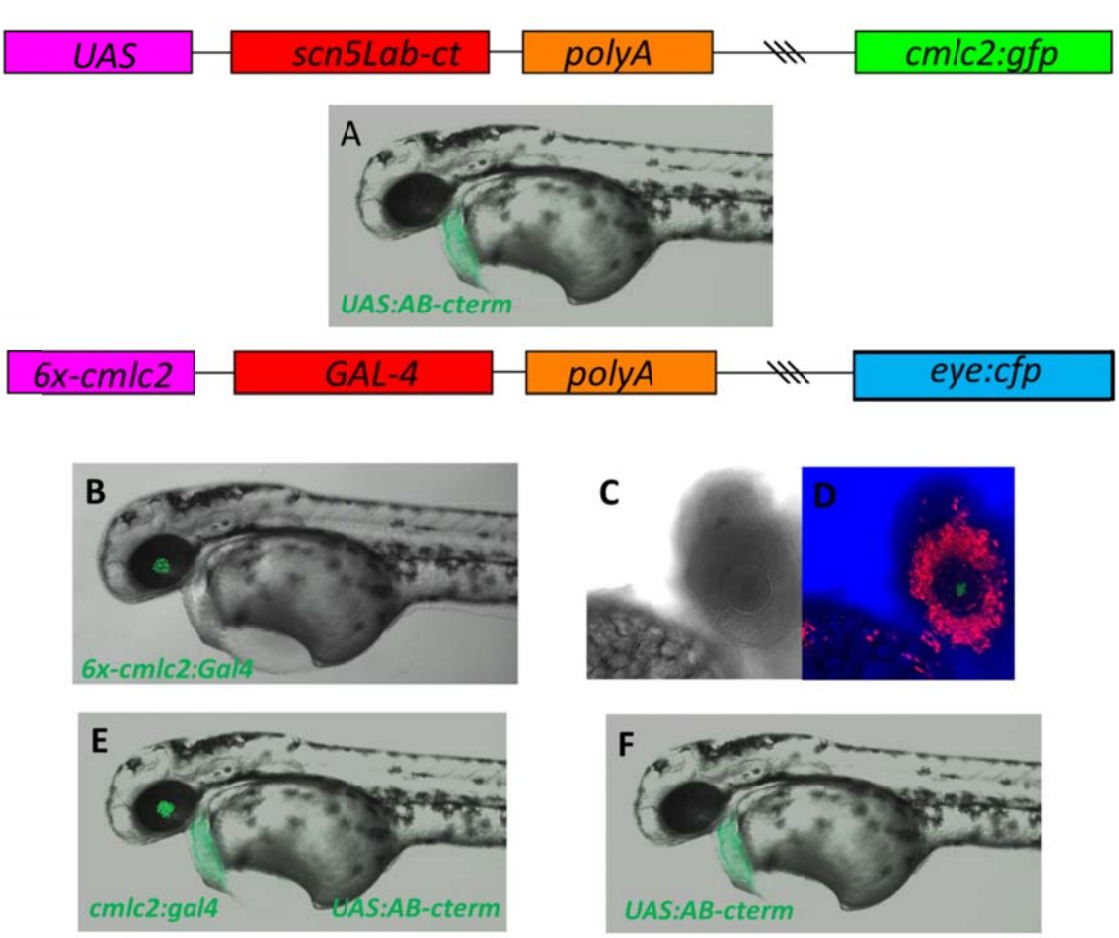

Figure 3.6: Experimental schematic of scn5Lab-cterm expression. A tg(UAS:scn5Lab-ct) with a GFP+ transgenesis marker (A) is crossed to a Tg(6x-cmlc2:Gal4) driver line, with a CFP+ eye transgenesis marker (enhanced in B). Confocal microscopy (C,D) can be used to identify embryos containing the driver. The result of a cross between the two lines are treated embryos which can be selected for C-terminus expression driven by Gal4 (E), and control embryos (F) containing the unexpressed C-terminal transgene. To evaluate rescue of the morphant phenotype, crosses contain internal morphant controls, rather than uninjected controls with confounding variables such as morpholino toxicity.

Discussion

Sodium channels are present but latent during early cardiac development

The requirement for *scn5Lab* in cardiac development of zebrafish appears to be independent of its functions in sodium permeation and action potential generation in mature cardiac tissue. Previous studies have shown early expression of the voltage-gated sodium channels *scn5Laa* and *scn5Lab* [32, 61], during cardiac differentiation and the early stages of heart tube formation. We have shown here that incubation of 48 hpf embryos in media containing non-specific blockers of sodium channels results in bradycardia, with the sodium channel blocker tetracaine having the strongest effect. Interestingly, tetracaine has an affinity for RyR, suggesting the drugs may be modulating intracellular calcium, rather than sodium. Despite that others have demonstrated expression of *scn5La* in the heart before 4 dpf [56, 61], electrophysiology of isolated cardiomyocytes detect minimal I_{Na} before 4 dpf. We did however detect L-type calcium channel activity ($I_{Ca,L}$), suggesting VGSCs, while expressed before 4 dpf, are present in the plasma membrane at low density. After 4 dpf, robust sodium current is detected, and is required for normal cardiac rhythm.

Further studies demonstrate the non-specific effect of tetracaine and heart rate, and suggest an effect on current through voltage gated sodium channels is not responsible for bradycardia at 48 hpf. Administration of tetrodotoxin has little effect before 4 dpf, the timepoint at which the ventricle develops a fast conduction network [167]. Conversely, ATX II incudes 2:1 arrhythmias in embryos as early as 48 hpf, demonstrating the presence of mature sodium channels on the plasma membrane of cardiomyocytes. The channels are expressed well before they are needed for action potential generation and propagation in wildtype embryos. That may be indicative of alternative function in cardiac development, necessitating expression of the channel earlier than necessary for normal cardiac rhythm.

Alternatively, differentiation of cardiomyocytes may result in expression of sodium channels, which remain relatively latent during the early stages of development.

The effect of ATX II indicates the channels do transiently open during normal cardiac function at this stage, allowing the toxin to bind to an open channel and prevent preventing inactivation. Only a small fraction of the potential sodium current is active during this stage. One possibility is the membrane potential in early heart development does not become sufficiently hyperpolarized to allow transition of the channel from the inactive state to the closed state, lowering the fraction of available channels to produce inward current. Electrophysiology on isolated cells demonstrated only a low amplitude sodium current at 3 dpf, suggesting the channels are expressed, but either inhibited from producing depolarizing current, or expressed at a low density before 4 dpf. The effect of ATX II in producing 2:1 heart block indicates the cumulative effect of alterations of intracellular sodium, but not necessarily robustness of I_{Na} current at that stage.

scn5Lab likely influences cardiac development independently of sodium ion permeation

Ion flux-dependent and independent functions of ion channels in zebrafish have been previously described [207]. Calcium ion signaling through the L -type calcium channel is critical for cardiac development in zebrafish independent of cardiac function [127]. Mutations in potassium channels on the other hand, present with an electrophysiology phenotype with no morphologic abnormalities [207]. Here, we have demonstrated a requirement for the voltage-gated sodium channel *scn5Lab* in both specification of pre-cardiac mesoderm, and growth of the developing heart. Both developmental processes occur well before we observe sodium ion influx to be required for action potential generation and propagation *in vivo*, at 4-5 dpf, suggesting an unexpected role for *scn5La* in cardiac development. *In vitro* electrophysiology confirms robust sodium currents are not present in zebrafish cardiomyocytes during the first three days of life.

Other studies have implicated unexpected roles for the sodium channel in human pathophysiology. In some human cancers, *SCN5A* expression has been associated with increased severity and metastasis [224, 225]. In the ovarian cancer line cell line SKOV, VGSC expression was associated with increased invasiveness of the tumor cells *in vitro*, and administration of TTX had an inhibitory effect on migration [225]. A similar effect using the anticonvulsant drug phenytoin has been observed in human breast cancer cell lines, and presents a potential therapeutic target [226]. Neither study observed an effect of $Na_V1.5$ inhibition on tumor cell proliferation.

Voltage-gated sodium channels have little contribution to cardiac action potential in zebrafish before 4 dpf, but are present and mature well before then. One possible function for the channels in cardiac development and other non-canonical roles is in establishing a gradient of membrane potential in the tissue. Transmembrane voltage gradients have already been shown to be required for left-right patterning and anatomic polarity [227]. Additional studies have identified bioelectric signals influencing cell cycle regulation and cellular proliferation [228, 229]. It is possible that voltage-gated sodium channels in the plasma membrane control intracellular ion concentrations, and as a result have an impact on cardiac specification and growth. Effects of altered membrane potential on cardiac development could easily be tested in morphant embryos, using injection of mRNA encoding an alternative depolarizing channel, like the glycine receptor (GlyR) chloride channel [230]. The channel can be artificially opened using the drug ivermectin [231], depolarizing the target cells in absence of voltage-gated sodium current. The lack of disrupted cardiac contraction and rhythm observed in embryos incubated or injected with the sodium channel blocker TTX suggests that is unlikely to be the case, and VGSCs have a more direct effect on cardiac development.

Future Directions

As described in Chapter V, rescue of the morphant phenotype with full-length mRNA is the gold standard to demonstrate the specificity of a phenotype observed with morpholino-knockdown. Rescue

of the morphant phenotype using a non-permeant version of a voltage-gated sodium channel would further demonstrate the non-electrogenic functions of *scn5La* in cardiac development, as well as provide insight into the functional domains and protein binding partners of the channel. The development bioactivity of *scn5La* C-termini is an interesting finding which must be followed-up by additional controls and experimentation. Injection of an identical amount of 'control' mRNA should be performed to determine non-specific effects of the channel. Developmental defects of the midline were observed more often after *scn5Lab-ct* injection, suggesting the effects observed after mRNA injection are related to the protein encoded, and not simply non-specific. Additionally, mutagenesis of the domain(s) responsible for the effect would correlate well with studies proposed in Chapter II to identify pathways interacting with *scn5La* during development.

Isolation of cardiomyocytes for electrophysiological studies is difficult before 3 dpf. Studies on cardiomyocytes of the heart tube and early heart would require flow cytometry of cardiomyocytes expressing a fluorescent transgene. An additional advantage would be the ability to select chamber-specific cells for electrophysiology studies, with new transgenic zebrafish lines available [232]. Additional studies on cardiomyocytes between 24 hpf and 7 dpf could identify the dynamic currents involved in action potential generation and propagation during development, as well as better assess the flux as a ratio of current/surface area of the myocyte. Further characterization of voltage-gated sodium channels during development would require *in vivo* studies examining the resting membrane potential and conduction velocity of action potentials on live hearts. The optical transparency of zebrafish lends itself to such a study, and multiple studies have demonstrated the ability to optically map and measure depolarization in the developing heart. Cardiac-specific expression of gCaMP, a fluorescent calcium indicator, provides an important tool in these studies [167, 233]. Modulation of voltage-gated sodium current with toxins or morpholino injection would further demonstrate the role (or lack of role) for I_{Na} in early cardiac conduction.

CHAPTER IV

SCN5LAB IS REQUIRED FOR CARDIAC GROWTH AND PROLIFERATION

Introduction

Control of cardiomyocyte number in the developing heart

Regulation of cardiomyocyte number in the developing heart occurs through multiple mechanisms. Differentiation from the first and second heart field each is important in providing the heart with physiological numbers of cardiomyocytes. Following differentiation, proliferation and hypertrophy of the myocardium is tasked with providing growth of the heart. Differentiation of the FHF can be visualized as early as 16 hpf, well before the formation of the heart tube or myocyte contraction can be observed. Chamber-specific heavy chain myosin can be identified by *in situ* hybridization in the differentiating myocardium of the ALPM, as well as upregulation of other sarcomeric genes [160]. Alteration in the number of differentiating cardiomyocytes in the FHF is often a result of defects in specification, well before differentiation. Perturbed gene expression can increase or decrease cardiomyocyte number, as well as shift the fraction of atrial versus ventricular myocytes. Discussed in Chapter II, fate mapping studies have identified the region 60-120 degrees of dorsal, at the marginal zone during mid-epiboly that is enriched for cardiac precursors. Expression of Wnt signals before this stage has a time-sensitive effect on cardiomyocyte specification. Ectopic expression of *wnt8* results in an enlarged pre-cardiac field (*nkx2.5*+) in the ALPM at 12 hpf, as well as an increased number of cardiomyocytes in the heart tube at 24 hpf [135]. Inhibition of Wnt signals through ectopic expression of *dickkopf* (*dkk1*), or activation of Wnt signaling after 50% epiboly, has the opposite effect.

Following primary differentiation of the heart tube, cardiomyocyte number is primarily increased through differentiation of the second heart field (SHF). The SHF, an extracardiac population of cardiac progenitors, has been extensively characterized in mammalian and chick models. The genetics of SHF specification and differentiation are discussed above. Primarily in zebrafish, cardiomyocytes derived from the second heart field contribute to the poles of the heart; the venous pole of the atrium, and the outflow tract at the arterial pole of the ventricle. Following differentiation of the heart tube by 24 hpf, circulation becomes established and the heart beats in peristaltic waves. A study by de Pater *et al*. in 2010 identified the distinct phases of cardiac differentiation and their contribution to the maturing heart [175]. In another study aimed to quantify the contribution of the SHF to the ventricle found approximately 25% of ventricle myocardium (30 vs. 90 cells) is differentiated from the SHF between 30 hpf and 48 hpf.

Proliferation of myocardium during development

The zebrafish is largely unique from mammalian models of cardiac growth in that it can repair and regenerate damaged heart tissue [234]. Cardiomyocytes in a damaged heart undergo a process of de-differentiation, followed to a proliferative phase to regenerate myocardium [235]. Through this process, up to 20% of the ventricle can be ablated and replaced in an adult zebrafish. Further analysis of the gene expression in regenerating heart has implicated growth factors (*pdgf-a*, *pdgf-b*), and cardiac transcription factors (*tbx2a*, *tbx3b*) in this process [236, 237].

A requirement for proliferation during cardiac development of zebrafish is less well-characterized. First heart field (FHF) and second heart field (SHF) differentiation is largely responsible for physiologic numbers of cardiomyocytes in the early heart at 36 hpf [171, 175, 238]. By 48 hpf, differentiation of myocardium is largely complete, and further increases in cardiomyocyte number appear to largely be a result of cellular proliferation and division [214]. Studies have suggested multiple factors control cardiomyocyte proliferation in the developing heart, yet the specific factors and

requirements have not been identified. In one study, loss of *nkx2.7*, particularly in the absence of *nkx2.5*, resulted in impaired myocardial proliferation [150]. It was suggested *nkx2.7* modulates the expression of *tbx5*, *tbx20,* and BMP signaling in proliferation of differentiated cardiomyocytes. Cardiomyocytes derived from both FHF and SHF undergo proliferation, as shown by the requirement for *ltbp3* (discussed above) in proliferation of SHF-derived myocardial cells.

In 2008, *ndrg4*, a member of the N-myc downstream regulated gene (NDRG) family was shown to be required for proliferation of myocardium in the developing zebrafish [239]. The phenotype observed after morpholino knockdown of *ndrg4* phenocopies the *heartstrings* (*tbx5*) mutant, with impaired looping, bradycardia, and decreased cardiac function [166]. Expression of *ndrg* was detected following specification during differentiation in the ALPM, and increased as development proceeded, particularly in the ventricle. Markers of cardiac differentiation appeared normal, however proliferation at 48 hpf was significantly reduced in morphant hearts. In hearts lacking *ndrg4*, *bmp4* and *versican* retained dispersed expression throughout the ventricle, rather than restriction to the AV junction at 48 hpf, as seen in wildtype embryos. Injection of *tbx5* 'rescued' the expression of *ndrg4*, providing evidence that *tbx5* is required in the heart for normal levels of *ndrg4* expression, and *ndrg4* functions downstream of *tbx5* to promote myocardial proliferation, as well as AV junction restriction of *bmp4* and *versican*.

Another study has identified *nerve growth factor* (*ngf*) as an inducer of proliferation in the embryonic heart [240]. At 72 hpf, zebrafish larvae were exposed to aristocholic acid, inducing cardiac injury and mimicking a heart failure phenotype. Damaged hearts were found to have reduced (42% decrease) expression of *ngf*. Even more significantly, exposure of the embryos to exogenous *ngf* reduced the heart failure phenotype, and promoted proliferation of the myocardium. Further studies are necessary to determine if *ngf* is required for proliferation of myocardium in undamaged hearts, and exactly what role it plays in regeneration of a damaged fully-developed adult zebrafish heart.

A requirement for ion channels and their binding partners has also been demonstrated in zebrafish heart development. Loss of L-type calcium channel alpha subunit (*island beat*) results in cardiac malformations and a nearly silent ventricle [127]. More recent studies identified the LTCC beta subunit *cacnb2* as being required for proliferation in the zebrafish ventricle [214]. Morpholino knockdown of *cacnb2* resulted in decreased proliferation both during SHF differentiation (24-36 hpf) and after differentiation is complete, during the looping phase of the heart (42-48 hpf). Heart tube integrity, and outer curvature shape change required for cardiac looping were also affected. The relationship between impaired cardiac function and morphology, and the observed loss of proliferation is unknown.

Cardiac morphology during development

Not all cardiac mutations resulting in a dysmorphic heart arise from decreased cardiomyocyte number as a primary cause. During cardiac growth, the heart tube undergoes elongation, followed by morphologic distinction of the chambers, and cardiac looping (Figure 4.1) [241]. As the embryo continues to grow, the walls of ventricle undergo compaction and concentric thickening to accommodate the increasing arterial pressures necessary for perfusion. In addition to genes described above which are required for proliferation of the heart, cardiac function and contractility has been suggested as a requirement for normal morphology. Multiple mutant strains possessing altered cardiac morphology have been identified through forward genetic screens [17, 130, 131].

The *heart and soul* (*has*) and *nagie oko* (*nok*) mutations result in small dense hearts with impaired heart tube extension. Positional cloning identified *has* as encoding *protein kinase C iota* (PKCi) and *nok* as *MAGUK p55 subfamily member 5* (*mpp5*), a gene encoding a protein required to establish polarity in epithelial cells and coherence of myocardial cells [242]. Expression of each is required in myocardium to induce shape change and cell size of cardiomyocytes required in heart tube extension and growth. In *has* and *nok* mutants, organization and polarity of cardiomyocytes, rather than altered cell number or proliferation, is responsible for the phenotype.

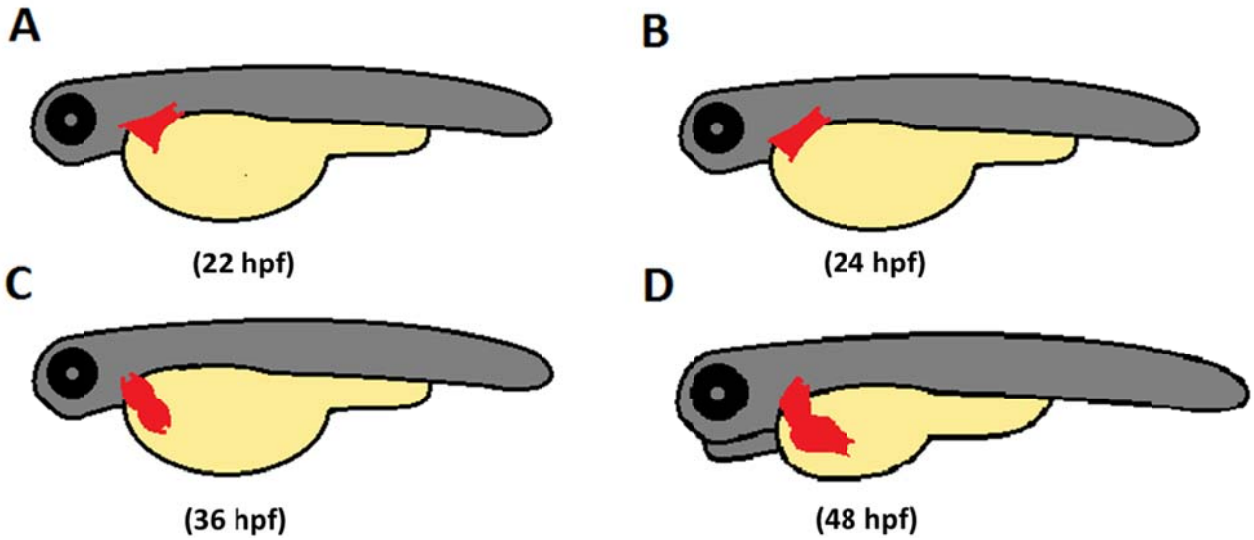

Figure 4.1: Cardiac morphology in zebrafish development. At 22 hours, a beating heart cone can be observed (A) in zebrafish embryos. The cone elongates into the heart tube (B) by 24 hpf, and represents differentiation of the primary heart field. Between 24 and 36 hpf (C), chambers become visibly apparent, and cells are added to both poles of the heart through differentiation of the second heart field. After 36 hpf, the heart continues to undergo growth (D) through proliferation, as well as looping of the atrium and ventricle. After 48 hpf, the ventricle continues to thicken and trabeculate, as pressures required to maintain systemic perfusion increase.

Three mutants, *heart of glass*, *santa* and *valentine* each develops with a large, distended heart [243, 244]. Interestingly, the number of cardiomyocytes at 48 hpf was determined to be unaffected in *santa* and *valentine* hearts, and the 'large heart' phenotype appears to be a result solely of impaired cardiac function and chamber dilatation. Positional cloning identified *santa* as the *ccm1* gene and *valentine* as *ccm2*. The two genes interact with each other and with integrins of the extracellular matrix to modulate cell-cell integrity of the myocardium [243]. Studies in mouse models as well as zebrafish suggest the two genes are in a genetic pathway with the endothelial-expressed gene *heart of glass* (*heg1*), and together regulate concentric growth of the myocardium independently of proliferation [245, 246].

A combination of genetics and cardiac function is required for proper morphology of the developing heart. A 2011 study implicated neuregulin signaling as being required for the initiation of myocardial protrusion into the ventricular lumen, a process resulting in trabeculation [247]. The group

also found normal cardiac function and blood flow to be required to complete the process. The *silent heart* (*sih*) zebrafish line possesses a mutation in cardiac troponin, rendering homozygote hearts unable to undergo contractions in response to action potential propagation throughout the heart [133]. While *sih* hearts appear to develop normally throughout the first few days of life, it is unknown if proliferation is truly unaffected in these hearts, and if cardiac contractility is fully required for cardiac development.

Question

The voltage-gated sodium channel *scn5Lab* is required for early specification of pre-cardiac mesoderm, as well as growth of the heart following differentiation of the heart tube [61]. Morphant hearts have a cell number deficit following FHF differentiation, and at 4 dpf, but it is not known precisely when, or by what mechanism, the deficit arises. The ventricles of these embryos are small and fail to undergo concentric thickening, but it is not known if the outflow tract is intact, or if altered SHF differentiation is partially responsible for the phenotype. Additionally, it is unknown if cardiomyocyte proliferation is present in morphant embryos. Here we aim to identify the perturbed developmental processes resulting in the small, dysmorphic ventricles observed in morphant embryos.

Methods

Zebrafish Lines

For counting and proliferation studies, we used zebrafish with a transgene for the red-fluorescent protein dsRed localized to the nucleus and driven by the cardiac myosin light chain promoter (*cmlc2:dsRed2-nuc*) [244]**.** For qualitative secondary differentiation studies, we generated a line of zebrafish expressing Kaede under control of the cardiac-specific *cmlc2* promoter. The *Kaede* gene from *Trachyphyllia geoffroyi* is a photo-convertible fluorescent protein, which upon exposure to ultraviolet (420nm) light permanently converts from green (native) to red fluorescence [176, 248]. The previously

identified [249] promoter region for cardiac myosin light chain (*cmlc2*/*myl7*) was first isolated using standard PCR protocols (see Appendix B for primers). The region was then subcloned using HindIII and KpnI restriction enzymes into the 5E-MCS element of the Tol2Kit [185], and combined with a middle element containing the sequence for the photo-convertible Kaede to generate an insertion vector. Single-cell embryos were injected with the vector, selected for transient Kaede expression. Adult zebrafish were then test-crossed to verify germline insertion, and bred to homozygosity, and multiple lines were crossed to maximize fluorescence.

In addition, we utilized the Gal4-UAS transactivator system to increase the cardiac expression of Kaede so that a more accurate quantitative evaluation of secondary differentiation could be performed. The cardiac myosin light chain (*cmlc2*) promoter [249] was cloned upstream of *Gal4* transactivator sequence in a Tol2 based vector (kind gift from M.Nonet, Wash U St. Louis). This construct was then utilized to create a stable transgenic line that had cardiac restricted expression of the Gal4 protein. This line (cmlc2:Gal4) was then crossed with the previously described tg(*UAS:Kaede*)^{s1999t} line [250]. Resulting double transgenic embryos had robust cardiac restricted expression of Kaede, which maintained red (CY3+) and green (FITC+) fluorescence after formaldehyde fixation and processing.

Cardiomyocyte counting

To count cardiomyocytes in wildtype and morphant embryos, zebrafish with nuclear cardiomyocyte fluorescence *cmlc2:dsRed2-nuc* were grown to specific time-points during development, and fixed for 1 hour in 4% formaldehyde/PBST, followed by dechorionation and 10 minute fixation in acetone. Fixed embryos were then permeabilized with Triton X (0.5% in PBS) and washed in blocking buffer (2mg/ml BSA, 2% normal goat serum, 1% DMSO). Sequential primary (anti-dsRed antibody, 1:300, Rockland) and secondary (goat-anti-Rabbit Alexa Fluor 568, 1:200, Invitrogen) antibody incubation was followed by washes in PBST (0.05% Tween20). Embryos were partially dissected to remove the head, and oriented on bridge slides in mounting medium (Vectashield H-1000) on bridge slides. Hearts were

imaged with an Olympus FluoView 1000 confocal microscope, and nuclei of differentiated cardiomyocytes were counted using ImageJ software (Figure 4.2) [251] (http://rsbweb.nih.gov/ij/).

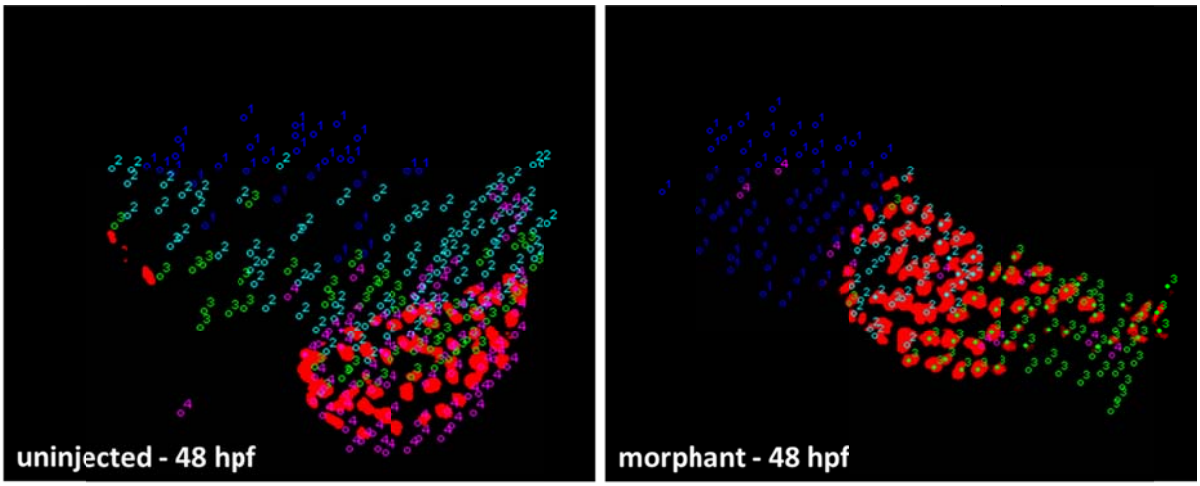

Figure 4.2: Counting of cardiomyocytes. Tg(cmlc2:dsRed) wildtype (left) and morphant (right) embryos are grown to 48 hpf, then fixed and immunofluorescence used to detect nuclear-localized dsRed. Confocal sections are scanned, and marked to avoid double counting. In these examples, the wildtype heart has 220 dsRed+ cardiomyocytes, while the morphant heart has 160.

Contribution of secondary differentiation to myocardium and outflow trace

Qualitative evaluation of secondary differentiation of cardiomyocytes was performed on embryos with FITC+ hearts from the tg(*cmlc2:Kaede*) zebrafish described above. As previously described by others [175], wildtype and morpholino-injected embryos were exposed to UV laser irradiation at 30 hpf, to allow cardiomyocytes of the heart tube (primary cardiac differentiation) to produce sufficient Kaede protein. Embryos were visualized as UV laser irradiation (330-385 nm) photo-converted cardiomyocytes from green (FITC+ fluorescence, Figure 4.3 A,D) to red (CY3-positive fluorescence, Figure 4.3 B,E), and focused along the z axis until complete throughout the entire heart (approximately 30 seconds per embryo). Embryos then were allowed to develop to 48 hpf, anesthetized and mounted in 1% methyl cellulose. Hearts were imaged in live anesthetized embryos on an Olympus FluoView 1000 confocal microscope, using FITC (488nm, green) and CY3 (568nm, red) lasers to detect primary (red, green) and secondary (green only) cardiomyocytes (Figure 4.4)

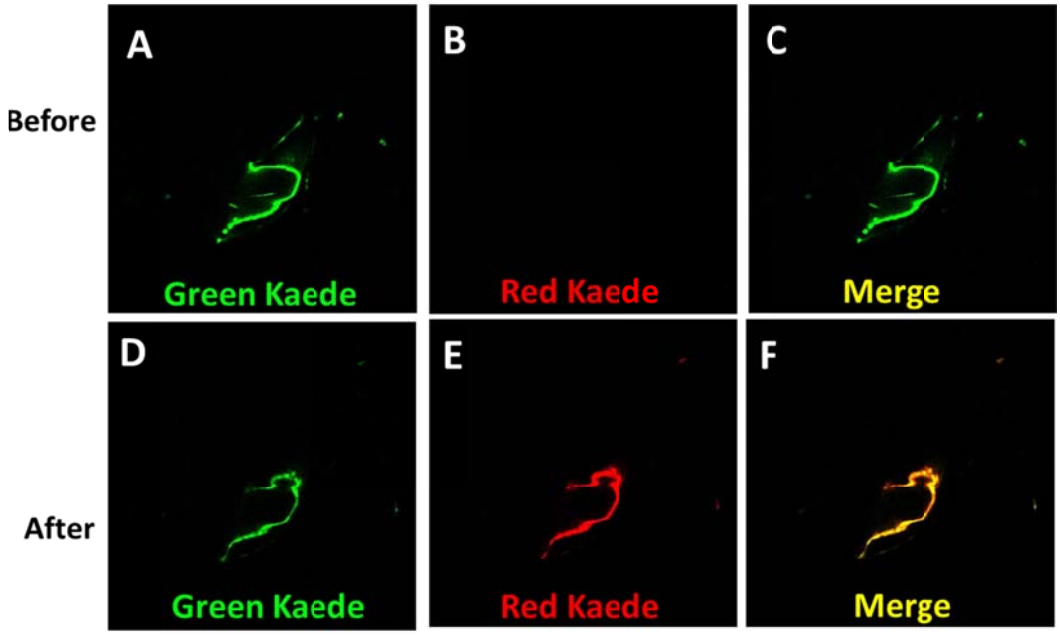

Figure 4.3: Kaede photo-conversion. Embryos from a cross of tg(cmlc2:Gal4) x tg(10x-UAS:Kaede) stable transgenic lines strongly express green (FITC+) Kaede in the 30 hpf heart (A-C). A confocal microscope equipped with a UV laser (280 nm) is used to immediately and permanently photoconvert Kaede from green to red (CY3+) fluorescence (D-E). Native green fluorescence is markedly reduced, and photoconverted cardiomyocytes show colocalization of red and green Kaede (F), mark early-differentiated cardiomyocytes.

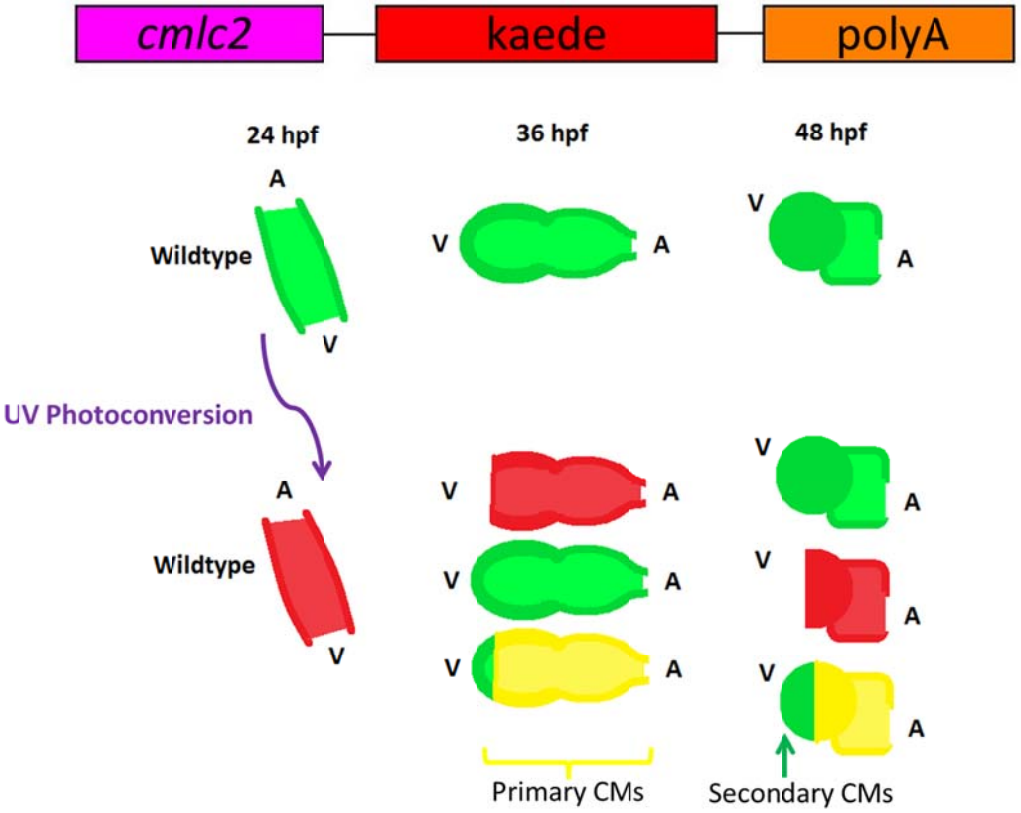

Figure 4.4: Photoconversion to evaluate second heart field contribution to the heart. At 24 hpf, tg(cmlc2:Kaede) have a green fluorescent heart tube, which will continue to grow and express native (green) Kaede during development to 48 hpf. When the heart tube is exposed to an ultraviolet laser, the green Kaede is permanently photo-converted, marking all heart tube (primary differentiation) cardiomyocytes as red. As the heart continues to grow, both original heart tube myocytes, as well as secondary differentiated cardiomyocytes continue to express new native (green) Kaede. Primary cardiomyocytes fluoresce both green and red (yellow), while newly-added (secondary heart field) cardiomyocytes fluoresce green only.

Quantification of SHF differentiation

The reporter line described above tg(UAS:Kaede)^{s1999t} [250] was crossed to the tg(*cmlc2*:Gal4) driver line to increase expression of Kaede protein in cmlc2-expressing cardiomyocytes. Wildtype and morpholino-injected embryos were exposed to UV irradiation at 30 hpf, then grown to 48 hpf and fixed in 4% paraformaldehyde. Embryos were then permeabilized using 0.5% Triton-X in PBS, and washed in blocking buffer containing 1µM TO-PRO-3-Iodide (Invitrogen). Samples were partially dissected to

expose the heart, and placed in mounting medium on bridge slides and imaged on an Olympus FluoView 1000 confocal microscope. Nuclei of secondary-differentiated cardiomyocytes were identified as FITC+ (expressing Kaede) and CY3- (not expressing Kaede before 30 hpf) and were counted using the ImageJ software [251].

Assessment of myocardial proliferation

BrdU injection to 48 hpf embryos was performed as previously described [237, 239]. Briefly, morphant or wildtype tg(*cmlc2:*mCherry) embryos were injected with 2 nL (1mg/mL) BrdU into the pericardiac region, then placed on ice for 20 minutes, and incubated in E3 egg water for five hours. Embryos were then fixed in 4% paraformaldehyde (1 hour, room temperate) and acetone (10 minutes). Embryos were then bleached 10 minutes in a 3% hydrogen peroxide/1% KOH solution. Embryos were permeabilized in PBS + TritonX-100 (0.5%) for 1 hour, followed by a denaturizing wash in 2N HCl. Immunofluorescence was performed with mouse-anti-BrdU (G3G4, Developmental Studies Hybridoma, 1:300) and rabbit-anti-RFP (polyclonal, Rockland, 1:300). Embryos were washed in PBS + Tween20 (0.05%) then stripped of their heads and mounted on bridge slides in Vectashield H-1000 mounting medium. Samples were imaged on an Olympus FluoView 1000 confocal microscope. Images were analyzed with ImageJ software package [251], using the cell counting feature to identify and mark proliferating cardiomyocytes.

Statistical Methods Used

Except where noted, data are presented as mean ± SEM. Pair-wise comparisons of normally-distributed data were performed using Student's *t*-test. The Kruskal-Wallis test was used for comparisons of non-parametric data.

Results

Morphant hearts have fewer cardiomyocytes throughout development

Zebrafish deficient in *scn5Lab* develop with visibly smaller, un-looped hearts, slow heart rates, and pericardial edema. To determine if reduced heart size resulted from fewer cells, we counted cardiomyocytes at each stage of early heart development. Beginning with initial peristaltic contractions of the wildtype heart tube at 24 hpf, uninjected and morpholino-injected embryos were formaldehyde-fixed at 12 hour-increments and immunofluorescence was performed to identify dsRed+ cardiomyocytes. Compared to uninjected wildtype embryos, zebrafish deficient in *scn5Lab* (morphants) had significantly reduced numbers of cardiomyocytes at 24 hpf (Figure 4.5 A,E, I). Following initial differentiation and establishment of the heart tube, wildtype zebrafish embryos continued to add cardiomyocytes throughout the second day (24-48 hpf) of development (Figure 4.5 B-C, F-G, I). During this same period, however, morphant hearts also continued to grow, with a similar increase in cardiomyocyte number as the uninjected embryos. After 48 hpf, uninjected and morphant hearts again diverged in cardiomyocyte number, as wildtype hearts continued to acquire dsRed+ cells, while morphant hearts failed to sufficiently add cardiomyocytes, accompanied by impaired cardiac function and embryonic death (Figure 4.5 D,H, I). Additionally, wildtype hearts underwent normal cardiac looping, while adding myocytes, whereas morphant hearts remained un-looped or partially looped.

Secondary cardiomyocyte differentiation is normal in scn5Lab morphant embryos

In situ hybridization data suggest that while primary specification of pre-cardiac mesoderm is impaired, specification and differentiation from the second heart field-like population may be unaffected. To determine if scn5Lab is required for late differentiation of myocardium, we used the Tg(cmlc2:kaede) line described above as previously reported [175]. Cmlc2+ myocytes expressing the green fluorescent Kaede at 30 hpf were permanently photo-converted to red fluorescence, marking the

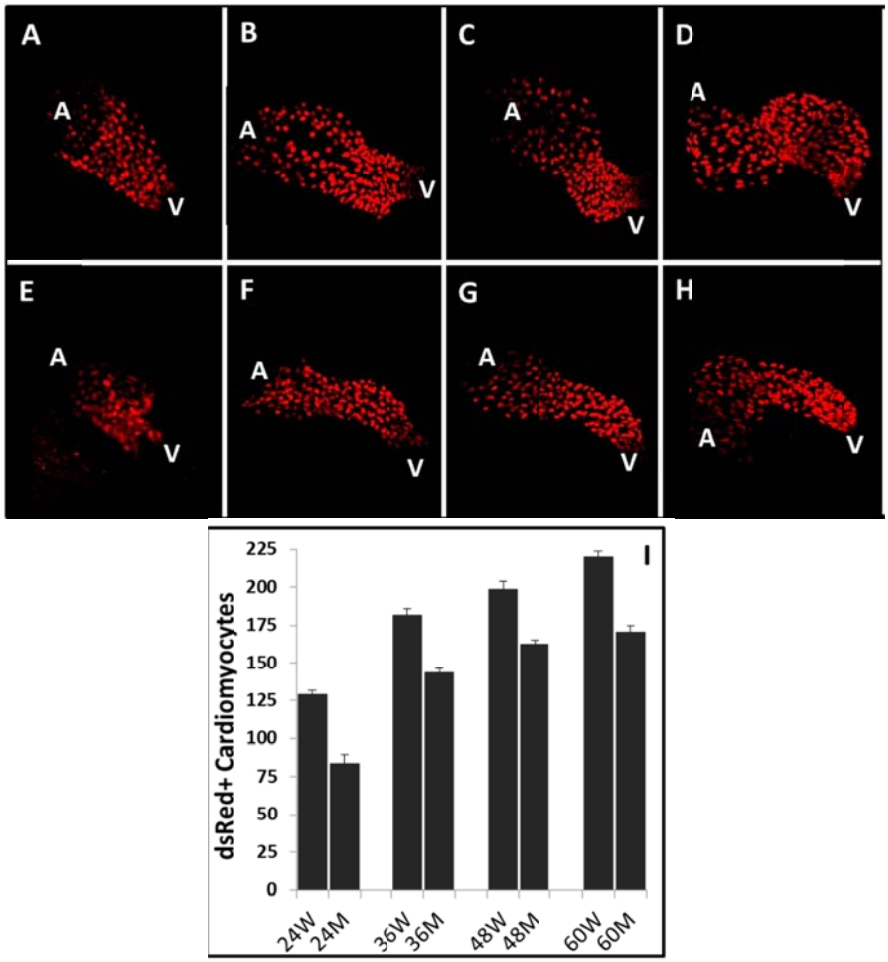

Figure 4.5: scn5Lab is required to maintain adequate cardiomyocyte numbers throughout development. Throughout development, morpholino-injected embryos have fewer cmlc2+-cardiomyocytes than uninjected embryos. At 24hpf (A,E,I), the number of cells in the initial heart tube is dramatically decreased in morphant embryos (129.2±5.8 vs. 83.6±16.1, n=6,7, p<.001). As development progresses, both morphant and wildtype embryos continue to add cardiomyocytes. At 36 hpf (B,F,I), uninjected embryos continue to have a significantly greater number of cardiomyocytes (182±10.4 vs. 143.5±7.2, n=6, p<.001). Between 48 hpf(C,G,I; 198.5±12.8 vs. 162.5±5.9, n=6, p<.001) and 60 hpf (D,H,I; 219.8±10.1 vs. 170.5±10.2, n=7,6, p<.001) wildtype embryos continue to add cardiomyocytes to the hearts, while morphant embryos have slowed in growth. A = atrium, V = ventricle, W = wildtype, M = morphant.

initial phase of cardiac differentiation. As embryos continued to develop, both primary and secondary cardiomyocytes expressed green (new) Kaede, marking primary cardiomyocytes as both red and green fluorescent, while secondary myocytes expressed green Kaede only. Using this approach, we found that the extent of secondary differentiation at the arterial pole between 30 and 48 hpf was similar in uninjected wildtype and scn5Lab (AB-MO2) morphant embryos. Photo-conversion at 30 hpf followed

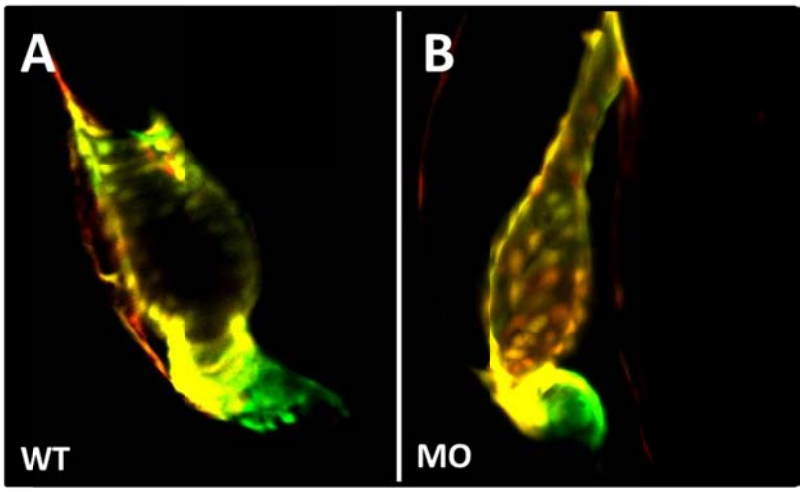

Figure 4.6 : Secondary phase of differentiation is normal in morphant embryos before 48 hpf. Wildtype (WT, A) and morpholino-injected embryos (MO, B) were exposed to UV irradiation at 30 hpf and allowed to develop until 48 hpf. Stacked confocal imaging shows photoconverted primary (yellow) cardiomyocytes, and new (green) cardiomyocytes. Between 30 and 48 hpf, secondary differentiation of cardiomyocytes occurred exclusively at the arterial pole of the ventricle in wildtype and morphant embryos. Both groups appeared to efficiently add cells between 30 and 48 hpf.

by imaging at 48 hpf displayed in clustering of FITC+, CY3- myocytes at the ventricular outflow tract in wildtype, as expected based on previous studies of secondary differentiation [175, 178, 179] and this was unchanged in morphants (Figure 4.6).

Morphant embryos add normal number of cells to the arterial pole

To test the hypothesis that differentiation of outflow tract myocardium proceeds normally in embryos deficient in scn5Lab, we quantitated secondary differentiation in wildtype and morphant ventricles. Stable transgenic zebrafish tg(UAS:Kaede) were crossed with a cardiac-specific driver line tg(cmlc2:Gal4) to generate robust expression of Kaede protein. Embryos were photo-converted as above at 30 hpf and then allowed to grow to 48 hpf and fixed. Embryos stained with the nuclear marker TO-PRO-3-Iodide to identify individual cells, and quantitatively assay secondary cardiac differentiation at the arterial pole (Figure 4.7 A-E). There was no difference in the number of arterial pole myocytes differentiating between 30 and 48 hpf in wildtype versus morphant embryos (34.8±4.3 vs. 33.1±4.4,

n≥8, p>0.2, Figure 4.7 F). The overall average number of new myocytes (34.1±4.3, n=18) observed at this stage was consistent with previously published counts [178]. Despite impaired early specification and differentiation of pre-cardiac mesoderm, scn5Lab-morphant embryos exhibited a normal secondary phase of cardiac differentiation. This result indicates perturbation of the second heart field is not responsible for sub-physiological number of ventricular myocytes in the embryos.

Ventricular cardiomyocyte proliferation is impaired in morphant embryos at 48 hpf.

After 48 hpf, cardiac differentiation in the zebrafish is largely complete [139, 175], and ventricle size and cell number increases predominantly through growth and proliferation of myocardium [214, 239, 243]. One potential contributor to the continued cardiomyocyte deficit in morphant embryos after initial heart tube formation is the loss of ability of differentiated cardiomyocytes to divide. To examine proliferation in the embryonic heart, we examined embryos exposed to BrdU for a five-hour window at 48 hpf, a time point reflecting completed secondary differentiation of myocardium. Embryos were formaldehyde-fixed, and immunofluorescence was performed, to evaluate mismatch and active morpholino-injected embryos for altered cellular proliferation (Figure 4.8). While both wildtype (5.8±2.1, n=14) and mismatch (4.0±3.0, n=11) hearts showed double positive (BrdU+, dsRed+) cardiomyocytes, there were no proliferating cardiomyocytes (n= 12, Kruskal-Wallis test p<10-5) from 48-53 hpf in morphant embryos (Figure 4.9). The results indicate that proliferation of post-differentiation myocardium requires the voltage-gated sodium channel scn5Lab.

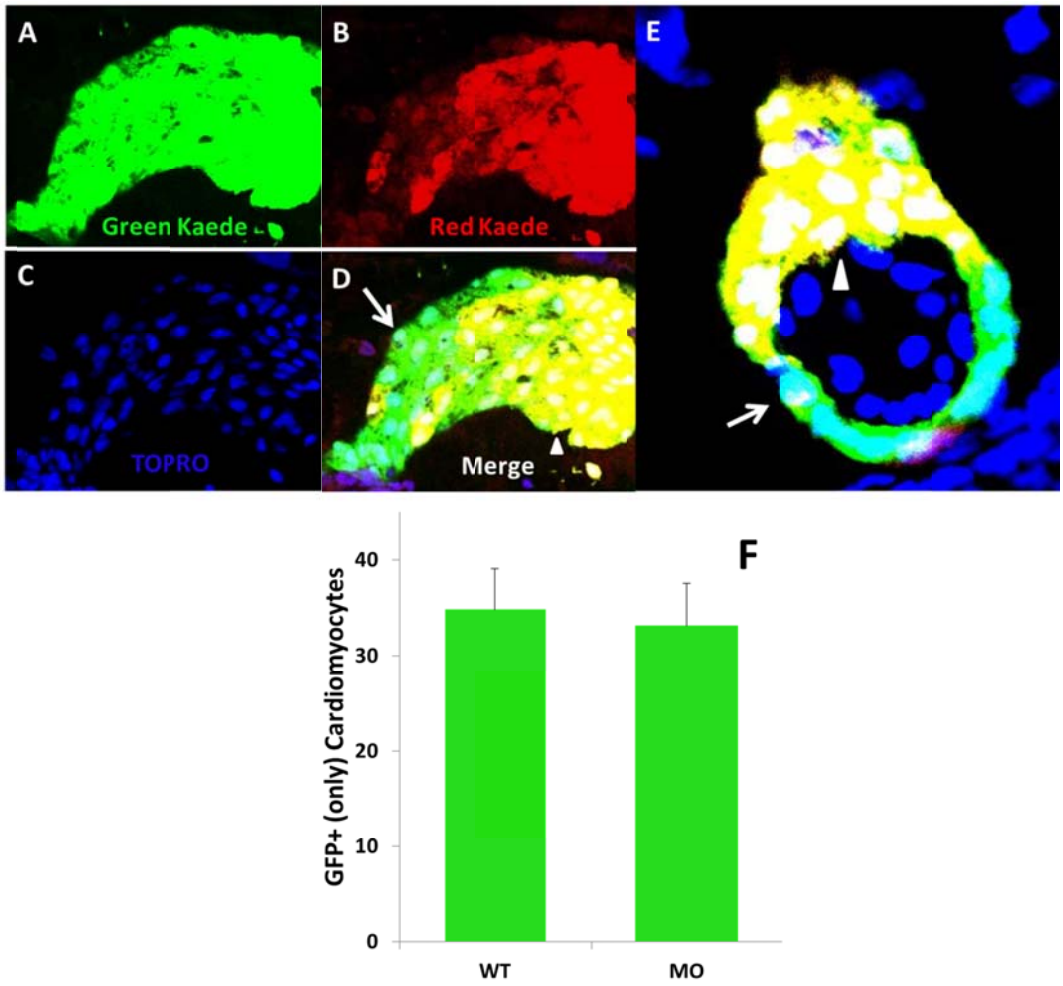

Figure 4.7: Quantification of secondary differentiation. Formaldehyde-fixed tg(cmlc2:gal4, UAS:kaede) embryos maintain green (A) and red (B) fluorescence after processing. Topro3-I (C) marks nuclei without affecting identification of secondary cardiomyocytes (D). Secondary cardiomyocytes form the arterial pole of the ventricle, forming the outflow tract and appear green with blue nuclei, while older, primary cardiomyocytes appear as yellow with white nuclei. At 100x magnification (E), primary (arrowhead) and secondary (arrow) cardiomyocytes can be identified and counted (F). Wildtype (34.8±4.3, n=10) and morpholino-injected (33.1±4.4, n=8) embryos add equal numbers of cells to the arterial pole between 30 and 48 ($p>0.2$).

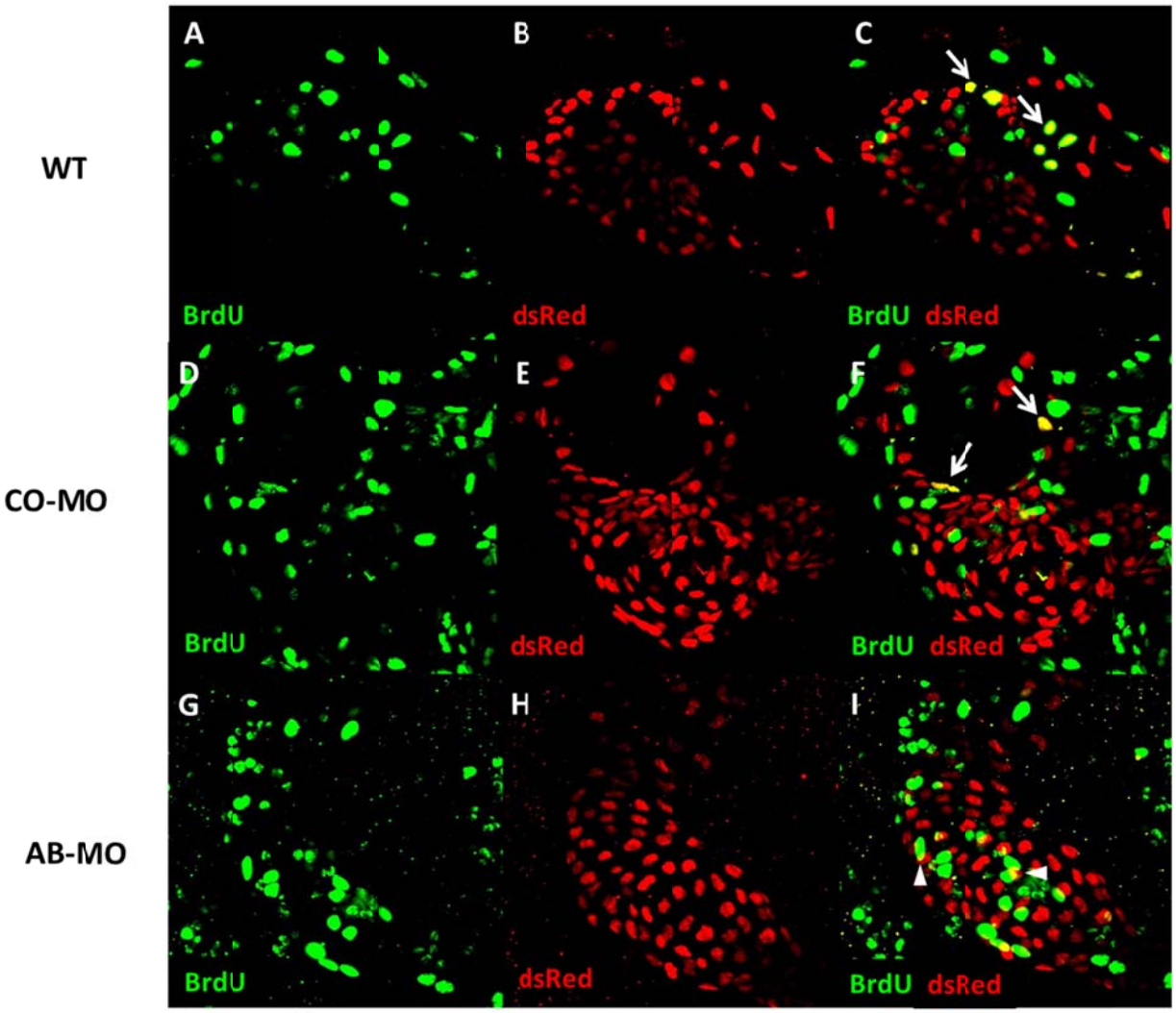

Figure 4.8: scn5Lab is required for proliferation of differentiated myocardium. BrdU-injected tg(cmlc2:dsRed) embryos identify proliferating cardiomyocytes in wildtype (A-C), 5 base mismatch morpholino-injected (D-F), and morphant (G-I) embryos. Embryos injected with BrdU at 48 hpf, and incubated for 5 hours, show colocalization (arrows: C,F) of the BrdU (green) and dsRed (red)signals. Embryos injected with active morpholino do not show any colocalization of the two signals (I). Despite having no proliferation in the myocardium, morphant embryos do appear to have normal proliferation in other tissues (arrowheads).

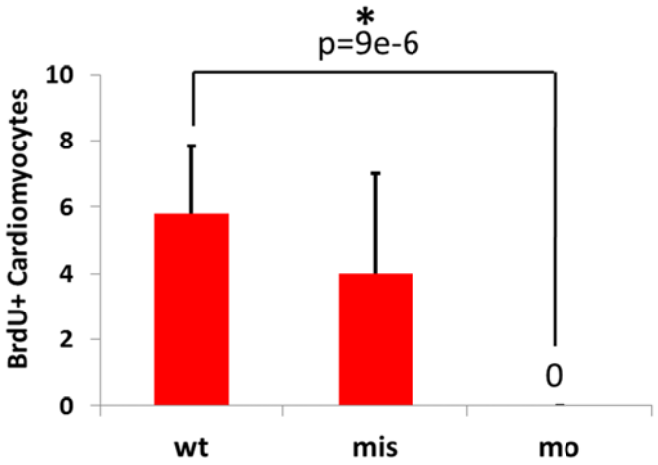

Figure 4.9: Quantification of proliferation defect. Quantification of BrdU-positive cardiomyocytes (J) suggest embryos deficient in Scn5Lab have a proliferation defect. Embryos were imaged and sections hyperstacked in ImageJ. Cells positive for both BrdU and dsRed were counted. Embryos injected with active morpholino (mo) had no evidence of myocardial proliferation (0 double-positive cells, n=12) compared to uninjected (wt, 5.8±2.1, n=14) and mismatch-injected (mis, 4±3.0, n=11) hearts.

Circulation is not required for cardiomyocyte proliferation

To evaluate the importance of cardiac contractility in myocardial growth and proliferation, we exposed developing embryos to multiple doses of the L-type calcium channel blocker nifedipine. Growth in 10µM nifedipine resulted in bradycardia similar to that observed in *scn5La* morphant embryos, while hearts appeared to develop normally through 48 hpf (Figure 4.10). Embryos exposed to 50µM nifedipine experienced complete cardiac arrest; however the hearts largely appeared normal, with a ventricle appearing smaller and more densely fluorescent. To further demonstrate this effect, we phenocopied the silent heart mutant zebrafish line using previously described morpholino against cardiac troponin (tnnt2-MO) [252]. Despite complete loss of cardiac contraction, the hearts appeared to develop normally through 60 hpf development. Using morpholinos in the Tg(*cmlc2:dsRed-nuc*) line, we injected BrdU into the pericardium of the *tnnt2-MO, tnnt2*-MO + *scn5Lab*-mismatch (MIS), and *tnnt2*-MO + *scn5Lab*-morpholino (MO) embryos, and counted proliferating cardiomyocytes (Figure 4.11). Proliferation appeared slightly reduced in *tnnt2*-MO compared to wildtype embryos (2.1±0.5 vs. 1.1±0.3,

n= 24,22, p=0.08, Figure 4.12). Co-injection of *scn5Lab*-MIS with *tnnt2*-MO appeared to have no effect on proliferation vs. *tnnt2*-MO alone (p=0.69); however, the effect of co-injection of active *scn5Lab* morpholino was identical to that observed in the non-silent heart fish: there was nearly complete absence of proliferation (1.2±0.3 vs. 0.1±0.1, n=12,10, p=0.007).

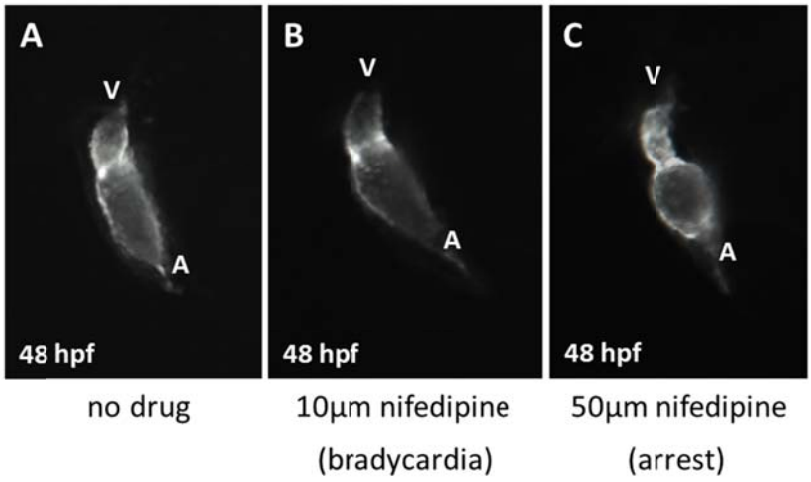

Figure 4.10: Cardiac development proceeds in absence of contraction and perfusion. Exposure to nifedipine from 24-48 hpf at concentrations high enough to slow (B) or arrest (C) the heart has little effect on development. Embryos exposed to 10µM nifedipine have identical cardiac development at 48 hpf. Embryos in complete asystole (C) continue to develop with apparently normal sized hearts, with contracted ventricles.

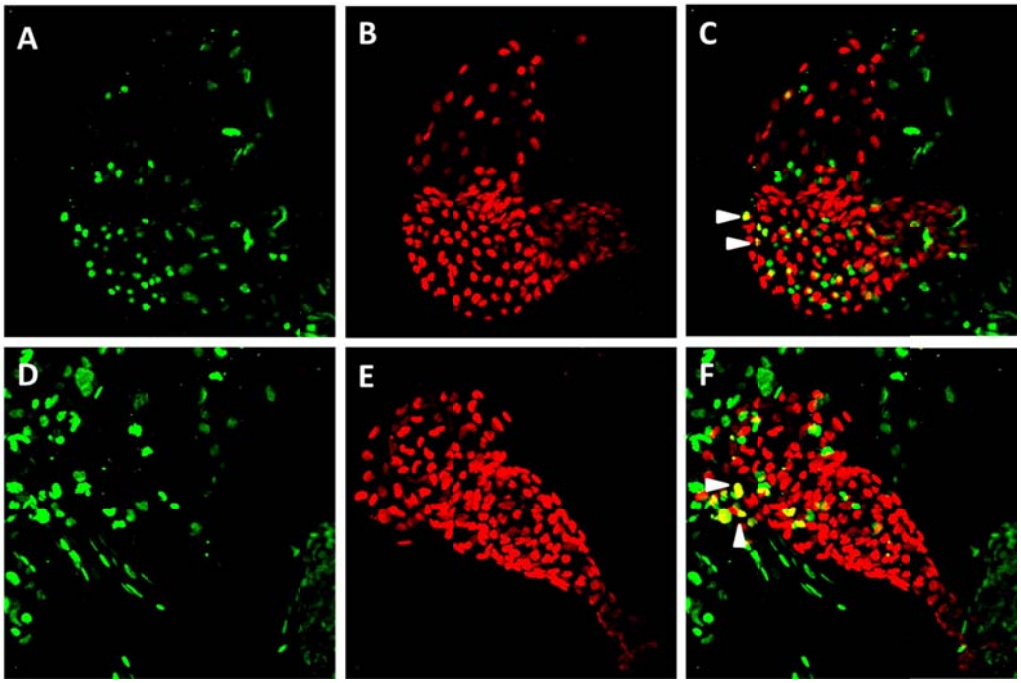

Figure 4.11: Cardiomyocyte proliferation is detected in silent heart phenocopy embryos. Wildtype and silent heart phenocopy tg(cmlc2:dsRed) embryos are stained for dsRed+ cardiomyocytes (red) and BrdU+ nuclei (green). Wildtype embryos (A-C) have BrdU-positive (yellow) cardiomyocytes (C, arrowheads) from 48-53 hpf. Embryos injected with tnnt2-MO (D-F) also have BrdU-positive cardiomyocytes (F, arrowheads).

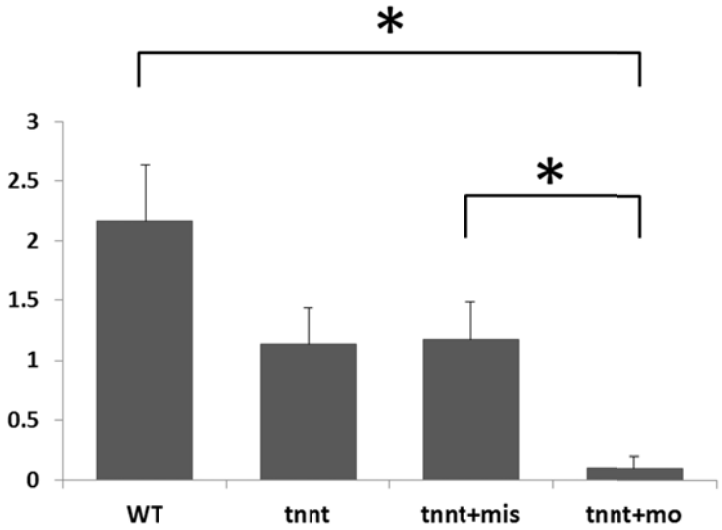

Figure 4.12: Impaired cardiac function is not responsible for loss of proliferation in scn5Lab-MO injected embryos. WT, tnnt2-MO, tnnt2-MO+scn5Lab-MIS embryos all have detectable proliferation at 48 hpf, while scn5Lab-MO embryos had none (Kruskal Wallis test p=0.004). Mann-Whitney U test identified proliferation as significantly decreased in tnnt2-MO/scn5Lab-MO co-injected embryos vs. tnnt2-MO/scn5Lab-MIS (0.1±0.1 vs. 1.1±0.3, n=12,10; p=0.007) and wildtype (2.2±0.5, n=10,24; p=0.001) hearts. Silent heart phenocopy embryos injected with tnnt2-MO were suggestive of impaired proliferation (1.1±0.3 vs. 2.2±0.5, n=22,24; p=0.08).

SCN5A may promote proliferation in neonatal rat ventricular myocytes

To evaluate the role for *Scn5a* in proliferation of cardiomyocytes in other animal models, we collaborated with the Becker laboratory to use siRNA transfection to knock down expression of *Scn5a* in neonatal rat ventricular myocytes. Compared to control siRNA-transfected group, NRVMs transfected with 10 nM siRNA targeting *Scn5a* (siRNA #s130413, Invitrogen) had a 12% reduction in proliferation. RNA was collected from each group, and RT-PCR performed to verify loss of *Scn5a* mRNA. 10 nM siRNA was insufficient to inhibit detection of *Scn5a* mRNA, and a higher dose may produce a more significant decrease in proliferation (Figure 4.13). In addition, pharmacologic agents inhibiting $Na_V1.5$ function (veratridine, flecainide) or toxins specific to VGSCs (tetrodotoxin) could be used to verify if the effect is independent of the channels' functions in sodium ion permeation.

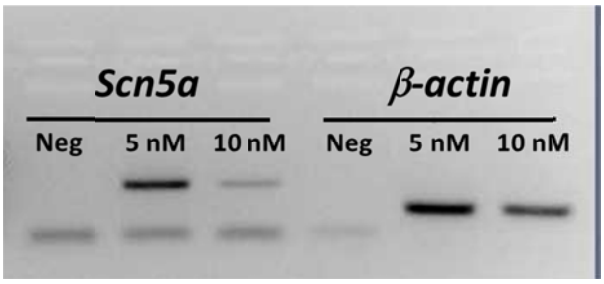

Figure 4.13: siRNA knockdown of Scn5a *in vitro.* A 12% reduction in proliferation was observed in neonatal rat ventricular myocytes (NRVMs) following transfection of 10 nM siRNA targeting *Scn5a*. RT-PCR of cultured myocytes suggests knockdown of Scn5a was incomplete, with detection of a strong Scn5a band at 5 nM and a weaker but positive band at 10 nM (upper bands). The β-actin control was strongly positive in both samples. 15 nM or 20 nM siRNA is required for complete knockdown and observation of the effect of Scn5A on *in vitro* proliferation of NRVMs.

Discussion

scn5Lab-depleted embryos have a cardiomyocyte deficit

Cardiomyocyte counting revealed a cell number deficit within the developing myocardium of zebrafish deficient in *scn5Lab*. In addition, the deficit does not appear to be consistent throughout development; morphant embryos at 24 hpf have a heart tube with significantly fewer cardiomyocytes, but are able to add myocardium in the subsequent 24 hpf, before ceasing to acquire cardiomyocytes, while wildtype embryos continue to gain new cells. Previous genetic studies have indicated a significant defect in cardiac specification, with loss of *nkx2.5* expression in the ALPM. While *scn5Lab* is required for early specification of pre-cardiac mesoderm, the integrity of gene expression in the SHF, and *nkx2.5* expression in the heart at 24 hpf, appeared intact.

Qualitative and quantitative studies here suggest the ventricular outflow tract is preserved despite dramatic perturbation of FHF specification. Our morphologic studies demonstrate that morphant embryos have smaller initial heart tubes, but add physiologic numbers of cardiomyocytes to the heart tube between 24 and 48 hpf. We demonstrate using photoconversion of Kaede that SHF differentiation occurs at the distal portion of the ventricle and forms the OT. Quantification found no difference in SHF cardiomyocytes between wildtype and morphant embryos, and observed similar numbers in the outflow tract to previous studies by others [178]. Despite impaired primary specification and differentiation of the heart tube, and a later growth defect in morphant embryos, differentiation of the secondary heart field appears intact. Distinct pathways controlling the differentiation of the two fields [160, 175] have been identified in prior studies, and here we show *scn5Lab* is required for differentiation of the FHF and the heart tube, but not for differentiation between 24 and 36 hpf.

Evaluation using BrdU injection into the myocardium suggests impaired myocardial proliferation, and not secondary differentiation, is responsible for the increasing cardiomyocyte deficit

after 24 hpf. While wildtype myocardium continues to grow and undergo concentric thickening, morphant embryos arrest in cardiac growth, an inevitably lethal phenotype. The question remains whether the proliferation defect in morphant embryos is unique to cardiomyocytes differentiating in the primary heart tube, or if seemingly 'unaffected' outflow tract myocardium fails to proliferate as well following differentiation. Further studies would be needed to determine if proliferation in the developing heart is typically stereotyped both in location and direction, or if all cardiomyocytes divide at similar rates. It is possible polarized proliferation is partly responsible for the looping of the heart tube, as well cardiomyocyte shape change between 36 and 60 hpf. Genes involved in cardiac proliferation, *tbx5* and *ndrg4*, have already been shown to be required in localized expression of AV-junction genes, and cardiac looping. In that case, the proliferation defect in morphant embryos would exist primarily in early differentiated myocardium forming the tissue around the AV junction, and largely not have an effect on SHF-derived tissue at the outflow tract.

Cardiac function and proliferation

Multiple mutant zebrafish lines have demonstrated a requirement for blood flow and cardiac function in promoting the proper morphology of the developing heart [247, 253]. Data here suggest the proliferation defect in *scn5La*-deficient embryos is independent of impaired cardiac function observed in the morphants. Uninjected embryos grown in both sodium channel blockers and L-type calcium channel blockers have generally normal cardiac development through 2.5 dpf. Studies in the *silent heart* (*tnnt2*) mutant line of zebrafish have shown the hearts appear to develop normally through 48-60 hpf, a time during which proliferation is observed in the embryonic heart [133]. Our studies here show that physiologically silent hearts in tnnt2-MO injected embryos continue to grow, and while they experience reduced proliferation, it is significantly greater than seen in *scn5La*-morphant embryos. While optimal blood flow through the ventricle is required for trabeculation, we observe a phenotype which begins before that process, and is clouded by the perturbed morphology. It is also important to remember that

morphant embryos are able to maintain circulation of blood, and do experience cardiac function. Any effect on proliferation due to impaired cardiac function of *scn5La*-depleted hearts would presumably be smaller than that observed in *tnnt2*-MO injected embryos. Further genetic analysis of morphant embryos should evaluate the differential expression of genes required for proliferation and morphologic growth of the heart such as *ndrg* and *neuregulin.* Moreover, we know *tbx5* is required for AV canal expression of *bmp4* and *versican*, as well as *ndrg4*-induced proliferation. These genes all represent possible targets in evaluation of the mechanism through which *scn5La* affects cardiac proliferation. Importantly, morphant embryos display a heart failure-like phenotype, which progresses during development, resulting in embryonic lethality. Evaluation of factors requiring *scn5Lab* expression for proliferation and growth is best performed on embryos before pericardial edema and cardiac failure become severe, and impaired function results in a secondary phenotype such as down-regulation of *ngf*.

$Na_V1.5$ in cellular proliferation

While the mechanism of the requirement for *scn5Lab* in proliferation of embryonic myocardium is unknown, evidence cited above indicates that this function is likely independent of the channel's contribution to the cardiac action potential [133, 254]. Promoting cellular proliferation is not without precedent for voltage-gated sodium channels. Ion channels are increasingly becoming implicated in tumor initiation and progression [224]. mRNA for $Na_V1.5$ was recently shown to be significantly increased in some human ovarian cancer, with protein expression possibly correlated to grade and metastasis status of the tumor [225]. Additionally, a protein shown to bind to $Na_V1.5$ in some cell lines, the sigma-1 receptor, has been shown to promote cancer proliferation and invasiveness [255]. While the effect was inhibited by administration of sodium channel blockers, the exact mechanism for *SCN5A* in tumor growth is unknown [52, 226]. Voltage-gated sodium channels are an integral component of the mature cardiomyocyte and as such may be part of a critical checkpoint for myocardial division, as well as promoting proliferation of tumor cells when expressed inappropriately. Unlike the *in vitro* phenotypes

observed in human tumor lines, growth of the heart appears unaffected by exposure to positive and negative modulators of sodium current, further suggesting the mechanism for *scn5Lab* in promoting proliferation of myocardium is unrelated to sodium ion flux.

CHAPTER V

DISCUSSION AND FUTURE DIRECTIONS

Discussion

Summary of findings

Here we demonstrate a biphasic role for the voltage-gated sodium channel scn5Lab in cardiac development. Early in development, before differentiated cardiomyocytes begin to beat and establish circulation, *scn5Lab* is required for expression of *nkx2.5* but not *nkx2.7* in the anterior lateral plate mesoderm. The specificity of this finding suggests *scn5Lab* participates in a genetic pathway of which *nkx2.5* is a downstream target. The result is impaired differentiation and a smaller heart tube. We have further identified expression of genes in the heart and pericardiac which are required for differentiation of the second heart field. A developmental timecourse evaluating cardiomyocyte numbers every 12 hours is reflective of both an early and late defect. Consistent with the expression of SHF factors, photoconversion and tracking of cardiomyocytes expressing Kaede suggest the outflow tract of morphant ventricles is intact. We find that reduced proliferation, rather than differentiation, is responsible for the progressive deficit in cardiomyocytes number in *scn5La*-depleted embryos after 24 hpf (Figure 5.1). Additional data we present here qualify this finding as likely being independent of electrophysiologic and functional alterations in the affected hearts. Firstly, we find that while voltage-gated sodium current is present at the 48-54 hpf timepoint where proliferation is studied, it is not required for maintenance of cardiac conduction or heart rate. Depolarizing inward current through L-type calcium channels is the primary driver of rate and rhythm at this stage, though pharmacologic

modulation of sodium current can induce a 2:1 heart block. Secondly, we find that cardiac contractility is important to cardiac growth, and proliferation is significantly decreased, though present, in *silent heart* embryos. Morpholino-injected embryos at 48 hpf do have impaired cardiac function; however the heart still does contract and establish circulation. Injection of morpholino in *silent heart* phenocopy embryos still results in nearly absent proliferation, suggesting that while cardiac contractility is important for proliferation, loss of function is unable to explain the observed phenotype in *scn5Lab*-depleted embryos.

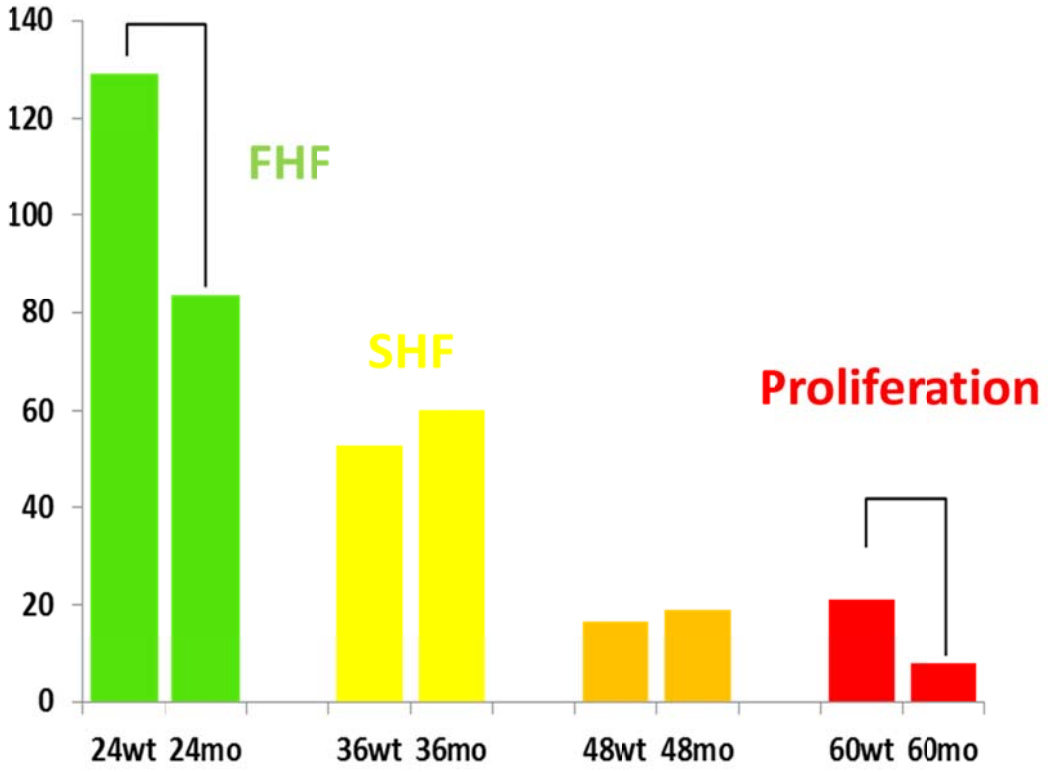

Figure 5.1: A biphasic requirement for scn5Lab in cardiac development. At 24 hpf, the differentiation of the heart tube from the first heart field (FHF) is impaired in scn5Lab-morphant (24mo) embryos. Between 24 and 36 hpf, second heart field (SHF) contribution to the heart is adequate in both wildtype (36wt) and morphant (36mo) embryos. Between 48 and 60 hpf, a second significant deficit in cardiomyocyte number is observed in morphant (60mo) embryos, which fail to undergo myocardial proliferation and growth. The data suggest *scn5Lab* is required in multiple phases of cardiac development, in which an early defect in differentiation or specification of the heart tube is followed by a late defect in proliferation. (Stage-specific cardiomyocyte numbers are inferred from averaged data in Figure 4.5)

Two genes… one phenotype

One of the pervasive questions from these studies is what mechanism is responsible for the same observed phenotype from knockdown of two distinct genes, *scn5Laa* and *scn5Lab*. Moreover, the phenotype resulting from double knockdown of both *scn5La* genes is suggestive of the most severe phenotype from single knockdown of either gene. The two genes do have a high degree of conservation at the amino acid level, as they arose from genomic duplication, suggesting the regulatory elements around the gene may be similar. One possible explanation is that there is some amount of genetic co-regulation of *scn5Laa* and *scn5Lab*, where knockdown of one gene results in decreased expression of the other. Unpublished observations from our lab suggest this may be the case, and further studies would be necessary to show that knockdown of one homolog results in altered expression of the other. Use of translation-blocking morpholinos have the added benefit of determining if loss of protein, or properly spliced mRNA, is responsible for any effect on expression. Regulatory elements can exist within immature mRNA. For example, genes for micro RNAs (miRNAs) have been identified in introns of unspliced mRNA [256]. The first intron of many human voltage-gated sodium channels is not translated, yet still contains highly conserved regions. One element, *CNS28*, of the human cardiac sodium channel mRNA (*SCN5A*) has been found to modulate expression and translation of the channel at the mRNA level [54]. However, identical phenotypes between ATG morpholinos and splice site morpholinos make it improbable that loss of RNA elements within the gene produces the observed phenotypes.

The simplest explanation is that there are off-target morpholino effects, and intended knockdown of one gene results in knockdown of both. Mismatch evidence refutes this point, in that each morpholino designed in the original study by Chopra *et al.* has eight or more mismatched bases to the opposite isoform, while mismatch morpholinos had no apparent off-target phenotype, with five bases mismatched [61]. PCR of transcripts appeared to confirm the specificity of the morpholinos, with intron inclusion not identified in mRNA of the non-targeted isoform. Morpholinos were specifically

designed to inhibit translation of splicing of one isoform independently of the other. One interesting experiment could be done to evaluate double knockdown using morpholinos designed against the highly homologous exon boundaries, rather than the divergent regions. A single morpholino could be used to knock down both genes, and the results verified on RT-PCR to show intron inclusion in transcripts of both isoforms.

Another possible explanation is that the two channels function as obligate heterodimers during cardiac development, and that loss of one channel results in a loss-of function phenotype for both. If the two channels function synergistically in mediating a developmental process or signal, loss of either would have resulted in a phenotype similar to that of dual knockdown. A dominant-negative effect has already been observed with $Na_V1.5$ mutations [65, 257]. In one study, the R1432G mutation in *SCN5A* was shown to significantly inhibit sodium current when co-transfected with the wildtype channel. Interestingly, the β1 subunit was required for the effect to occur *in vitro*, demonstrating that while there is interaction between VGSC alpha subunits, subunit proteins mediate the contact. In the second study, two N-terminal mutations in the channel led to misfolding and endoplasmic reticulum (ER) retention of the protein [65]. The authors demonstrate interaction between wildtype and mutated channels in the ER, resulting in retention of both wildtype and mutant proteins. The two studies demonstrate multiple mechanisms for a dominant negative effect in VGSCs with two different alleles of a single gene. The latter mechanism is unlikely responsible for the *scn5La*-morphant phenotype in zebrafish, as channel expression is altered, rather than protein function. Interaction between *scn5Laa* and *scn5Lab* is possible, though difficult to examine with the reagents available.

To date, we have described much of the genetic and morphologic phenotype observed after knockdown of *scn5La*. While *nkx2.5* expression and lack of ventricle growth is observed in both, the two phenotypes may be more divergent than at first appears. *Nkx2.5* is useful as a readout of cardiac specification at 12 hpf, however expression of the gene at 24 hpf, and failure of *nkx2.5* mRNA to rescue

the phenotype indicate an earlier genetic lesion exists prior to 12 hpf. The upstream genes resulting in loss of pre-cardiac mesoderm may be different for *scn5Laa* and *scn5Lab*. A high-throughput expression assay that can identify genes altered in embryos would allow us to further refine the genetic phenotypes observed, and determine if the two genes function in a single mechanism, or have evolved to modulate cardiac development through divergent pathways.

Possible mechanisms for scn5Lab in cardiac development of zebrafish

Here we have demonstrated a biphasic requirement for *scn5Lab* development, in which loss of *scn5Lab* affects multiple phases of cardiac growth. Identification of the potential mechanisms for that role will require further evaluation of and refinement of the phenotype. Based on data presented here, it is unlikely that sodium ion flux through VGSCs is required for either the specification or proliferation phenotypes observed. Moreover, the phenotypes observed with morpholinos targeting splice junctions and translation initiation suggest miRNA or other RNA regulatory elements are also likely not responsible. A means of identifying the functional domains of the channel is discussed below. Selective mutation of domains of the sodium channel could identify the functional elements involved in the mechanism, and binding partners or downstream proteins which interact with the channel. Additionally, conservation of those regions between *scn5Laa* and *scn5Lab* could determine if divergent mechanisms or pathways, or convergent regulation of expression, is responsible for the apparent identical phenotypes from knockdown of each gene.

Within the C-terminus of $Na_V1.5$ are multiple conserved strings of amino acids which may play an important role in the subcellular localization and activity of the channel. The C-terminus of one L-type calcium channel has been shown in some cell populations to be cleaved and function as a transcription factor [76]. Such a process has not been suggested with a VGSC, but could be evaluated. Chromatin immunoprecipitation (ChIP) is a commonly used method to demonstrate the DNA-binding ability and targets of proteins.. Chromatin-protein complexes are fixed *in situ* using formaldehyde, followed by

sonication to shear the DNA into 300-100 base pair segments. An antibody versus the targeted protein (for example, the C-terminus of *scn5Lab*) is then used to isolate the protein-DNA complex. The DNA can then be isolated, and identified by sequencing or PCR. Transcription factor function could be determined if the C-terminus of scn5Lab is found to associate with known regulators of transcription, and is able to induce or enhance expression of a reporter gene with a promoter containing those elements.

Little evidence suggests *scn5Lab* functions as a direct transcription factor during development, or that the C-terminus has DNA-binding affinity. It much more likely that protein-protein interactions are responsible for whatever transcriptional or structural defect results in the morphant phenotype. For example, the sigma-1 receptor binds to *SCN5A* in some human cancer lines and controls proliferation and invasiveness [255]. Identification of binding partners for VGSCs can be achieved using immunoprecipitation. A cell population (e.g. the heart) can be identified and isolated using manual excision, followed by extraction and isolation of the protein. An antibody targeting the gene of interest (anti-scn5Lab) is then used to 'pull down' the gene of interest, along with interacting proteins. These partners can be identified using Western blotting with antibodies which recognize suspected targets, or a high-throughput method using mass-spectrometry. This method has already been used to identify a complex containing syntrophin and dystrophin as regulating $Na_V1.5$ function and expression [75]. Additionally, mutation of the PDZ domain in the C-terminus was used to abolish the interaction, and identify the mechanism by which regulation occurred. Another method to evaluate interaction is the yeast two-hybrid assay. Each protein in question is cloned to create a fusion protein with part of the Gal4 transcription factor. One protein is cloned to the DNA binding domain, which will bind to the upstream activating sequence (UAS) of a reporter gene (for example luciferase or lacZ). The other protein is fused to the transcription activating domain of Gal4. Interaction between the two proteins in question will be required to bring both Gal4 domains and initiate transcription of the reporter gene.

Some domains in the C-terminus are less likely to reveal a developmental role than others. Multiple mutation models have identified calcium homeostasis as critical for both signaling and depolarization in developing myocardium [127, 214]. The C-terminus of *scn5Lab* contains two EF-hand-like motifs which bind to Ca^{2+}. The domains are largely uncharacterized, but have been speculated to modulate gating and function of the channel, rather than a developmental pathway [258]. Another unlikely target is the Nedd4-like ubiquitin ligase interacting domain. *In vitro* studies suggest Nedd4-2 interacts with $Na_V1.5$ at the PY-motif (xPPxY), resulting in ubiquitination and control of the membrane half-life and channel density [82, 259]. In zebrafish, the observed phenotype from *scn5La* knockdown results from a loss of expression of the channel, therefore eliminating the interactions with Nedd4 completely. It is unlikely a defect in recycling of a channel which is not expressed is responsible for impaired cardiac specification.

The fibroblast growth factor homologous factor (fhf1b) binding site in the C-terminus presents a more interesting possible target. Studies in human *SCN5A* have found FHF1B binds to the C-terminus of $Na_V1.5$, modulating channel function, hyperpolarizing the voltage dependence of inactivation [80]. Interestingly, a LQTS mutation in C-terminus has been shown to disrupt binding of FHF1B. To date, possible functions of FHFs in development have not been identified. Despite high homology between FGF and FHF, the roles of the two families of proteins appear to be divergent, and FHFs do not activate FGF receptors [260]. Other signaling pathways might also be affected by loss of *scn5Lab*. Multiple elements of the sarcomere have been found to associate with $Na_V1.5$ [75]. Each one represents an interaction between two proteins, which in turn have their own protein interactions. It is possible that rather than playing a direct role in signaling cardiac development, *scn5La* functions within the scaffolding of the cardiomyocyte to bring together multiple proteins which are required either for signaling, or as to serve as a checkpoint in differentiation. Failure of the cardiomyocyte to assemble protein complexes required for cardiac function may result in loss of signals for growth and

proliferation. This presents a mechanism which would be unique to the latter (proliferation, rather than specification) phenotype observed in morphant embryos, resulting in a biphasic role with two distinct mechanisms.

Though cardiac function is required for growth and proliferation in the ventricle, data presented here suggest the requirement for *scn5Lab* in proliferation of myocardium is not explained fully by impaired cardiac function. Other studies have observed loss of ion channels or their associated proteins results in developmental cardiac defects, a result of defective cell-cell interactions and an inability to remodel and undergo shape change to respond to increasing blood pressures. Multiple studies in other models have identified a function in cell adhesion for β-subunits of VGSCs, though a comprehensive study examining loss of function of β-subunits in the zebrafish has not been performed. Unpublished data from our laboratory suggests that morpholino knockdown of any of the five zebrafish VGSC β-subunits does not phenocopy *scn5La* morphants. Either through subunit redundancy, or yet-undefined protein partners, affected interactions between cardiomyocytes – or with the endocardium or epicardium – could be responsible for impaired proliferation. The combination of impaired function, and impaired intercellular adhesions might explain the morphant phenotype.

While many possible mechanisms described would explain just one aspect of the roles observed for *scn5La* in cardiac development, a requirement in cell shape and adhesion could explain both. Phalloidin, which binds to f-actin, along with anti-cardiac or anti-GFP/dsRed antibodies has been used to observe the shape changes required for cardiac growth [198]. The bilateral stripes of cardiac precursors in the ALPM must migrate dorsomedially to fuse and form the heart tube. A hypothetical disruption of cellular adhesions affecting migration and cell-cell communication would suggest that impaired specification of pre-cardiac mesoderm is actually a result of impaired migration of specified cells to the ALPM (Figure 5.2). As outlined above, such a mechanism could affect the integrity of the cell-cell contacts required for growth and proliferation in the ventricle. Generation of a 40% epiboly fate-map of

future myocardium (as performed by Keegan et al) [134], would identify a decreased population of cardiac progenitors at 40% epiboly, or normally distributed cardiac progenitors that fail to migrate properly to the ALPM. Such an experiment would also serve to further identify the developmental stages impacted by loss of *scn5La* and provide more specific targets in refining the genetic phenotype of knockdown of the channels.

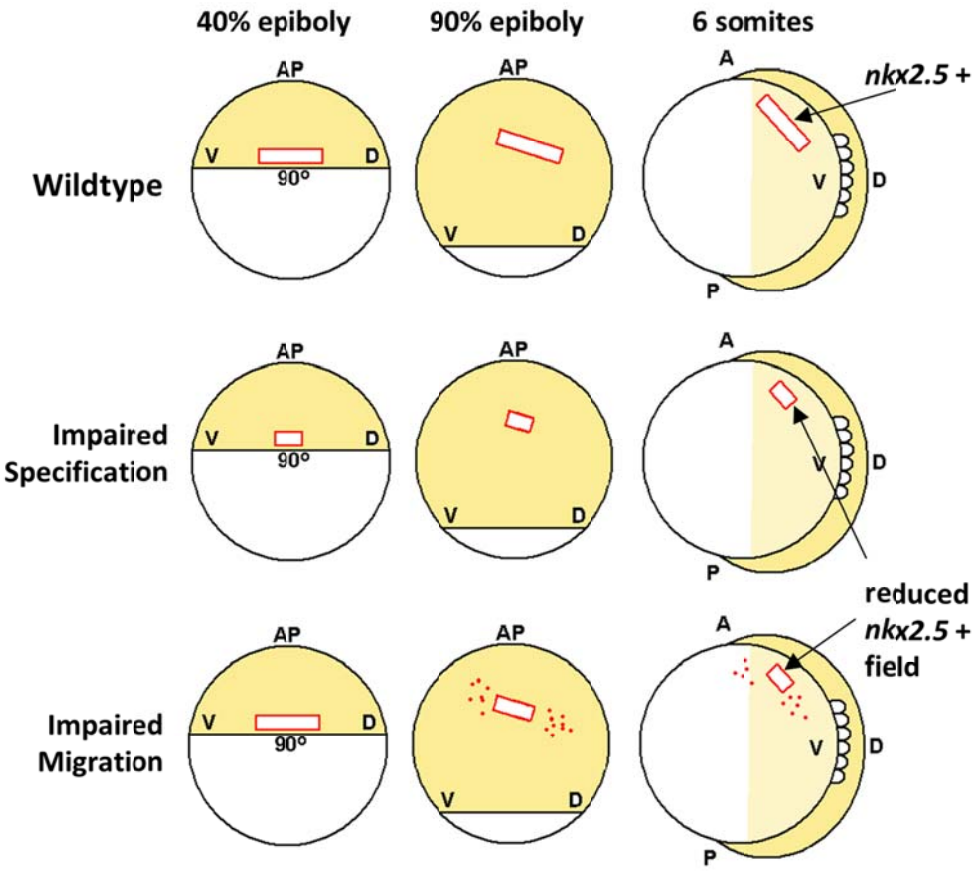

Figure 5.2 Migration and specification in cardiac development. Two possibilities for impaired expression of *nkx2.5* in the lateral plate mesoderm at 12 hpf include defects in specification, and migration. Cardiac progenitors can be identified through fate-mapping between 60-120 degrees of dorsal in the first four tiers of blastomeres at 40% epiboly (top left). Cardiac precursors migrate dorsally (top middle) and express *nkx2.5* by 12 hpf (top right). If loss of *nkx2.5* at 12 hpf is a result of impaired specification, a decreased field of cardiac progenitors would be observed at 40% epiboly (middle left), which despite adequate migration (middle), would result in decreased ALPM expression of *nkx2.5* (middle right). In the case of impaired migration, a normal field of cardiac progenitors would be specified at 40% epiboly (bottom left), but as migration of cardiac precursors proceeds during gastrulation (bottom middle), cardiac progenitors are lost, and are unable to express *nkx2.5* (bottom right).

Future Directions

Identification of an scn5La knockout model

Ideally, loss-of-function genotype-phenotype studies include germ-line disruption of a gene. Despite an abundance of control experiments, phenotypes identified through morpholino knockdown have not always recapitulated in knockout models. Production of gene-specific germ-line knockout zebrafish models has proven difficult. Whereas the mouse genome can be manipulated through homologous recombination, the technology has not transferred to the zebrafish [261]. Early forward genetic screens identified the potential of the zebrafish in functional genetic studies [262]. Random chemically-induced point mutations were induced using N-ethyl-N-nitrosourea (ENU), followed by phenotype screens and positional cloning. The methods proved exceedingly useful in discovery of genes important in embryonic development [263]. In particular, many genes involved in development of the cardiovascular system of zebrafish were identified [130, 131]. Later on, after sequencing and annotation of the *Danio rerio* genome was completed, retroviral insertional mutagenesis was used to induce mutations, which were easily more easily localized in the genome, though still random in nature [264, 265]. Recent efforts by the Sanger Institute have set out to identify mutations in each protein-encoding sequence in the zebrafish genome [266]. Using an efficient chemical mutagenesis and high-throughput sequencing, they have identified mutations in 38% of *Danio* genes, including three pairs of voltage-gated sodium channels. To date, mutations found in genes annotated as *scn5Laa* and *scn5Lab* map to putatively non-functional partial duplications of the genes, rather than the full-length channel sequences obtained from cDNA libraries.

Recent progress in the *Danio* model system has advanced our ability to produce targeted disruption of the genome. Zinc finger nucleases were initially engineered as a chimera of the DNA-binding zinc-finger domain and the fok1 nuclease to induce gene-targeted double stranded breaks in cell

lines [267]. The technology was later adapted to use the nucleases to target the zebrafish genome, resulting in the first ZFN-targeted knockout zebrafish line, a *vascular endothelial growth factor*, (*vegf*) knockout [268]. Despite the advancement, the ZFN method remained expensive and labor-intensive, requiring multiple ZFN clones and specificity selection to generate a transgenic line. Newer technology has produced more widespread success. Transcription activator-like effector nucleases (TALENs) have multiple advantages over ZFNs. For one, TAL effectors have specific recognition of DNA sequences, and require less selection and optimization of nuclease clones [269]. Because of this, TALENs can better target longer specific DNA sequences than ZFNs, and require less intensive design and processing. Recent methods have optimized the TALEN process, allowing for high throughput and low cost generation of sequence-specific genome targeting [270].

An even newer genome editing technology has been recently described [271]. Bacteria naturally use the CRISPR (clustered regularly interspaced short palindromic repeats)-Cas system as an immune system, to identify and silence foreign (e.g. viral) DNA. Transcripts (RNA) of foreign DNA are inserted into the CRISPR locus, and CRISPR RNA (crRNA) is made, targeting the invading DNA. Cas proteins identify trans-activating crRNA (tracrRNA), and silence the gene [269, 272]. The system has been adapted to *in vitro* and zebrafish model systems. A synthetic single guide RNA (sgRNA) is used to direct the Cas9 endonuclease to induce a double-stranded break in the genome. Evidence suggests CRISPR can be used to induce site-specific germline knockouts in both alleles of a gene, and the technology represents an important advance in generating zebrafish gene knockout models.

With the availability of efficient sequence-specific genome editing, an *scn5La* knockout model would be ideal to further explore the phenotype observed through morpholino knockdown. The elimination of off-target effects would allow for specific phenotype analysis, though germline knockout models do have drawbacks. Any *scn5La* knockout model would be expected to have homozygous lethality, and the line would have to be maintained as a heterozygous line. Data from *Scn5a*$^{+/-}$ mouse

line suggest a *scn5Laa*$^{+/-}$ or *scn5Lab*$^{+/-}$ phenotype would be viable, however only 1/4 of embryos from a mating cross would have the desired mutant (-/-) genotype, and the corresponding phenotype. A double *scn5La* knockout model would require a cross of a Tg(*scn5Laa*$^{+/-}$/*scn5Lab*$^{+/-}$) line, where just 1/16 embryos would have the double knockout genotype. Morpholino and targeted-nuclease transgenesis each have their benefits, and would be best used in concert to study the role for *scn5La* in development.

Identification of a structure function relationship for scn5La in development

As detailed above, rescue of the morphant phenotype using full-length *scn5Laa*/*scn5Lab* mRNA has proven to have technical obstacles. Rescue using co-injection of affected genes has shown to be incomplete, as the exact mechanisms and pathways by which *scn5La* modulates cardiac development are unknown. Ideal demonstration of the requirement for *scn5La* in cardiac development would include mRNA rescue of the morphant phenotype, but the technique could be further used to explore the mechanisms involved in the role. An elegant identification of channel domains involved in the phenotype would require rescue using mRNA expressing a full-length mature functional channel.

Electrophysiological data presented here suggest current through voltage-gated sodium channels is not critical for either action potential generation or propagation during primary and secondary differentiation of myocardium, or proliferation which occurs at 48 hpf. To demonstrate the independence of the role for *scn5La* in development from its function in sodium permeation, rescue using a non-permeant mutated channel would be an ideal experiment. The intracellular aspect of the channel pore is predominantly blocked during fast inactivation by the linker connecting domains III and IV. This region is a possible target for mutagenesis resulting in a non-permeant channel. Additionally, each domain possesses a voltage-sensing membrane-spanning helix which responds to a hyperpolarized membrane, altering channel conformation and opening the pore [1]. Selected mutation of arginine and lysine residues in those helices provided they (1) had no effect on protein expression or stability and (2)

completely occluded sodium current through the channel, would be another target to demonstrate a non-electrogenic mechanism.

Selectively-mutated mRNA rescue would be a useful tool to further explore a non-electrogenic role for *scn5La* in development. The C-terminal, as well as multiple other regions of voltage-gated sodium channels, possesses multiple known and yet-uncharacterized protein interacting domains [68, 79, 273]. Rescue of the morphant phenotype with an impermeant channel, followed by failure to rescue with an impermeant channel with mutations in these critical residues would further demonstrate a non-electrogenic role for *scn5La* in cardiac development. Additionally, mutations which phenocopy the morphant phenotype could potentially identify the binding partners and pathways involved. We have demonstrated here a biphasic requirement for *scn5Lab* in cardiac specification and myocardial proliferation. It is possible that mutational analysis might identify a single interacting domain responsible for the effect of *scn5Lab* during both phases of cardiac development, or multiple domains through which the channel modulates cardiac differentiation pathways, as well as checkpoints involved in terminal myocardial differentiation and proliferation.

Differential gene expression in scn5La-deficient embryos

In situ hybridization (ISH) has revealed multiple gene expression defects in the ALPM in *scn5La*-morphant zebrafish at 12 hpf, as well as genes which are unaffected by loss of *scn5La*. While ideal for the study of spatial and temporal expression of specific genes, ISH is unable to function in either a high-throughput or hypothesis-free manner. For some time, microarrays were the standard of identifying differentially-expressed genes between two cohorts [274]. mRNA from a specific tissue or whole-embryo sample was isolated and reverse-transcribed into a cDNA library. The samples were then hybridized to the microarray chip, binding to short DNA sequences antisense to the mRNA sequence and quantified with DNA-binding dyes. Even with recent advances in technology, microarrays are prohibitively expensive for many labs, and require large (500 ng) amounts of sample mRNA for maximal

efficiency and quality testing. The assay also lacks the ability to detect smaller variations in mRNA expression, and is subject to dye bias, a false-positive result [275]. An amplification step necessary for smaller sample amounts significantly reduces the ability to detect smaller variations in gene expression [276].

With the advent of next-generation sequencing, transcriptome analysis has become far more sensitive. RNA-seq poses certain advantages over standard microarray analysis. Next-generation sequencing technology is quantitative, based on direct counts of read sequences, rather than relying on hybridization, and does not require genomic input or for probe sequences for the experimental design. Rather, RNA-seq uses an Illumina platform to read the total RNA (including miRNA) in the sample, followed by a computationally intensive process of analysis to apply the latest genomic annotations to the reads. The process allows for more quantitative comparison of gene expression between two groups, while avoiding the pitfalls of cross-hybridization and inefficient binding common with microarrays. Advancements in multiplexing using up to six unique sample-identifying adapters has allowed RNA-seq to rapidly evolve into the cost-efficient technology of choice for differential gene expression analysis.

With the availability of new technology, it is possible to identify genes affected by loss of *scn5La* in a hypothesis-free manner. Data here suggests that *nkx2.5* is lost in morphant embryos at 12 hpf, while other genes in the ALPM are minimally affected or unaffected. It is known that cardiac specification begins as early as 40% epiboly, based on fate-mapping experiments [134]. RNA-seq provides a technologically advanced method of transcriptome analysis, in which any stage of development can easily be assayed for differential expression in morphant embryos. Evaluation of embryos at 40% epiboly would provide an early insight not only into the regulation of *scn5La* expression, but into the pathways critical to early heart development, before any known markers of cardiac fate are expressed. Unlike microarrays, differentially expressed genes would not have to be known in advance,

nor would a chip have to be specifically designed for genes enriched during development. Additionally, pooling embryos provides natural biological replicates, eliminating a potential source of variability. Just as importantly, RNA-seq can be used to probe gene expression within differentiating myocardium. Heart tissue could be manually excised, or with the availability of cardiac-specific fluorescent lines, cardiomyocytes could be isolated using flow-sorting. RNA-seq could then be performed on even a small amount of mRNA; generally samples are under 100ng, and obtaining gene expression data on the mRNA of a single cell is possible [274, 277, 278]. Factors involved in terminal differentiation and proliferation of myocardium, upstream and downstream of *scn5La* would be identified through this manner. With the availability of ventricle-specific fluorescent lines [232], very specific aspects of cardiac development, including chamber-localized control of proliferation, could be probed.

Conclusion

Here we present data demonstrating a biphasic role for the cardiac voltage-gated sodium channels *scn5Laa* and *scn5Lab* in heart development of zebrafish. The channels are required for expression of *nkx2.5* in the pre-cardiac population in the ALPM, as well as for proliferation and growth in the ventricle at 48 hpf. Further studies are necessary to determine the mechanism(s) by which scn5Laa and scn5Lab influence cardiac development, and what relationship the two genes have to each other. The zebrafish has already proven itself an invaluable tool in the study of cardiac development and physiology, and in identification of mutations which affects them. This study provides further depth to the study of the genes and processes important for cardiac development in zebrafish, as well as data which can be extrapolated in studies in other organisms. The high level of conservation in voltage-gated sodium channel genes suggests ion flux-independent functions of *scn5La* orthologs may be present in other organisms as well.

Appendix

Appendix A: Morpholinos used in these studies

Morpholino	Gene	Type	Sequence (5'-3')	Dose (ng)
AA-MO1	*scn5Laa*	ATG	CCGCTGGTAAGAGCATGGTCGCCAT	6
AB-MO1	*scn5Lab*	E6-splice	AGCGGCCTCTCACCTGGGATGACTG	4
AB-MO2	*scn5Lab*	E25-splice	AGTTTGTGCTGACCGGTGGTCTGGG	1.5
AB-MIS2	*scn5Lab*	E25-splice	ACTTTCTGCTGAGCGGTGCTCTGCG	1.5
P53-MO	*tp53*	ATG	GCGCCATTGCTTTGCAAGAATTG	4.5
TNNT2-MO	*tnnt2*	ATG	CATGTTTGCTCTGATCTGACACGCA	4

Appendix B: Oligonucleotide primers used in these studies

Gene/Primer	Species	Sequence	Usage
nkx2.5-F	zebrafish	5′-GCGAAGACCTTCAGGAGGACAAAGGCAAC-3′	dose effect RT-PCR
nkx2.5-R	zebrafish	5′-CGAGGCTTCCTCCTCTTCCTCTGCTTGGG-3′	dose effect RT-PCR
βActin-F	zebrafish	5′-CAGCTAGTGCGAATATCATCT-3′	dose effect RT-PCR
βActin-R	zebrafish	5′-TTTCTGTCCCATACCAACC-3′	dose effect RT-PCR
XhoI-HA tag-F	viral	5'-CATCTCGAGCGCATCTTTTACCCATACGA-'3	XhoI subcloning
XhoI-HA tag-R	viral	5'-GTACTCGAGCTACTGAGCAGCGTAATCTG-'3	XhoI subcloning
cmlc2-F	zebrafish	5'-ATAGGTACCCTCTTCACGTCCCCCTC-'3	promoter subcloning
cmlc2-R	zebrafish	5'-ATAAAGCTTGTTCCTGTCTGCTTTGC-'3	promoter subcloning
pcGlobin-SDM-F	vector	5'-TACGCTGCTCAGTAGTTCGAGTCTCATCGCG-'3	pcGlobin2-XhoI removal
pcGlobin-SDM-R	vector	5'-GGCGATGAGACTCGAACTACTGAGCAGCGTA-'3	pcGlobin2-XhoI removal
hsp70l-F	zebrafish	5'-CAACAACCTGCTGGGCAAA-'3	qualitative PCR
hsp70l-R	zebrafish	5'-GCGTCGATGTCGAAGGTCA-'3	qualitative PCR
scn5Lab-F	zebrafish	5'-GTGAACCGGACGGGTTTCATCTATAATTCC-'3	qualitative PCR
scn5Lab-R	zebrafish	5'-AACAGGAGCGTCCGGATGCCTTTA-'3	qualitative PCR
scn5Lab-3'F	zebrafish	5'-TTCGTAGACAGTTAAAACAAGCGTCG-3'	qualitative PCR
scn5Lab-3'R	zebrafish	5'-TGTACAAGAAAGCTGGGTGCTATGAC-'3	qualitative PCR
aa-cterm-F	zebrafish	5′-AGACCGCGGATGGAGAACTTCAGCGTGGCCACT-3′	subcloning
aa-cterm-R	zebrafish	5′-TCTCTCGAGCTAAAGAAAGGTCTCTTCGTATGTCTC-3′	subcloning
ab-cterm-F	zebrafish	5′-AGAGGATCCATGGAGAACTTCAGTGTGGCGACG-3′	subcloning
ab-cterm-R	zebrafish	5′-TCTCTCGAGTCACAGAAAAGTTTCGCTCTCTTTTTCTGC-3′	subcloning
ab-cterm-R	zebrafish	5′-TCTCTCGAGTCCCAGAAAAGTTTCGCTCTCTTTTTCTGC-3′	subcloning (no stop)
aa-cterm-R	zebrafish	5′-TCTCTCGAGCAAAAGAAAGGTCTCTTCGTATGTCTC-3′	subcloning (no stop)
ab-cterm-Fseq	zebrafish	5′-GCGGATGGAGAACTTCAGTG-3′	qualitative PCR
ab-cterm-Rseq	zebrafish	5′-GCTGAGGATTTCATTCGTCTC-3′	qualitative PCR
kaede-Fseq	coral	5'-TAAACGGGCACCAGTTTGTT-3′	sequencing
kaede-Rseq	coral	5'-ACTTGACACCCTCCTGCCTA-3′	sequencing
Scn5a-F	rat	5′-GGCACAGAGGAAGAGTCCAG-3′	qualitative PCR
Scn5a-R	rat	5′-GAGCAGCATCTCCAACACAA-3′	qualitative PCR

References

1. Catterall, W.A., *Ion channel voltage sensors: structure, function, and pathophysiology.* Neuron, 2010. **67**(6): p. 915-28.
2. Alberts, B., *Molecular biology of the cell*. 4th ed. 2002, New York: Garland Science. xxxiv, 1548 p.
3. Kleven, D.T., C.R. McCudden, and M.S. Willis, *Cystic fibrosis: newborn screening in America.* MLO Med Lab Obs, 2008. **40**(7): p. 16-8, 22, 24-7.
4. Lukacs, G.L. and A.S. Verkman, *CFTR: folding, misfolding and correcting the DeltaF508 conformational defect.* Trends Mol Med, 2012. **18**(2): p. 81-91.
5. Kim Chiaw, P., P.D. Eckford, and C.E. Bear, *Insights into the mechanisms underlying CFTR channel activity, the molecular basis for cystic fibrosis and strategies for therapy.* Essays Biochem, 2011. **50**(1): p. 233-48.
6. Kumar, V., et al., *Robbins and Cotran pathologic basis of disease*. 7th ed. 2005, Philadelphia: Elsevier Saunders. xv, 1525 p.
7. Wang, T., *Renal outer medullary potassium channel knockout models reveal thick ascending limb function and dysfunction.* Clin Exp Nephrol, 2012. **16**(1): p. 49-54.
8. Sun, Y., et al., *Role of the epithelial sodium channel in salt-sensitive hypertension.* Acta Pharmacol Sin, 2011. **32**(6): p. 789-97.
9. Thakker, R.V., *The role of renal chloride channel mutations in kidney stone disease and nephrocalcinosis.* Curr Opin Nephrol Hypertens, 1998. **7**(4): p. 385-8.
10. Belmont, J.W., et al., *Genetic disorders with both hearing loss and cardiovascular abnormalities.* Adv Otorhinolaryngol, 2011. **70**: p. 66-74.
11. Nie, L., *KCNQ4 mutations associated with nonsyndromic progressive sensorineural hearing loss.* Curr Opin Otolaryngol Head Neck Surg, 2008. **16**(5): p. 441-4.
12. Oliva, M., S.F. Berkovic, and S. Petrou, *Sodium channels and the neurobiology of epilepsy.* Epilepsia, 2012. **53**(11): p. 1849-59.
13. Koopmann, T.T., C.R. Bezzina, and A.A. Wilde, *Voltage-gated sodium channels: action players with many faces.* Ann Med, 2006. **38**(7): p. 472-82.
14. Lerche, H., K. Jurkat-Rott, and F. Lehmann-Horn, *Ion channels and epilepsy.* Am J Med Genet, 2001. **106**(2): p. 146-59.
15. Jorge, B.S., et al., *Voltage-gated potassium channel KCNV2 (Kv8.2) contributes to epilepsy susceptibility.* Proc Natl Acad Sci U S A, 2011. **108**(13): p. 5443-8.
16. Laitinen, P.J., et al., *Mutations of the cardiac ryanodine receptor (RyR2) gene in familial polymorphic ventricular tachycardia.* Circulation, 2001. **103**(4): p. 485-90.

17. Berne, P. and J. Brugada, *Brugada syndrome 2012.* Circ J, 2012. **76**(7): p. 1563-71.
18. Wilde, A.A. and R. Brugada, *Phenotypical manifestations of mutations in the genes encoding subunits of the cardiac sodium channel.* Circ Res, 2011. **108**(7): p. 884-97.
19. Schwartz, P.J., L. Crotti, and R. Insolia, *Long-QT syndrome: from genetics to management.* Circ Arrhythm Electrophysiol, 2012. **5**(4): p. 868-77.
20. Kass, R.S. and M.P. Davies, *The roles of ion channels in an inherited heart disease: molecular genetics of the long QT syndrome.* Cardiovasc Res, 1996. **32**(3): p. 443-54.
21. Amin, A.S., A. Asghari-Roodsari, and H.L. Tan, *Cardiac sodium channelopathies.* Pflugers Arch, 2010. **460**(2): p. 223-37.
22. Goldhaber, J.I. and K.D. Philipson, *Cardiac sodium-calcium exchange and efficient excitation-contraction coupling: implications for heart disease.* Adv Exp Med Biol, 2013. **961**: p. 355-64.
23. Milberg, P., et al., *Inhibition of the Na+/Ca2+ exchanger suppresses torsades de pointes in an intact heart model of long QT syndrome-2 and long QT syndrome-3.* Heart Rhythm, 2008. **5**(10): p. 1444-52.
24. Roden, D.M., et al., *Cardiac ion channels.* Annu Rev Physiol, 2002. **64**: p. 431-75.
25. Anderson, P.A. and R.M. Greenberg, *Phylogeny of ion channels: clues to structure and function.* Comp Biochem Physiol B Biochem Mol Biol, 2001. **129**(1): p. 17-28.
26. Zakon, H.H., *Adaptive evolution of voltage-gated sodium channels: the first 800 million years.* Proc Natl Acad Sci U S A, 2012. **109 Suppl 1**: p. 10619-25.
27. Liebeskind, B.J., D.M. Hillis, and H.H. Zakon, *Evolution of sodium channels predates the origin of nervous systems in animals.* Proc Natl Acad Sci U S A, 2011. **108**(22): p. 9154-9.
28. Hille, B., *Ion channels of excitable membranes*. 3rd ed. 2001, Sunderland, Mass.: Sinauer. xviii, 814 p.
29. Postlethwait, J.H., et al., *Zebrafish comparative genomics and the origins of vertebrate chromosomes.* Genome Res, 2000. **10**(12): p. 1890-902.
30. Widmark, J., et al., *Differential evolution of voltage-gated sodium channels in tetrapods and teleost fishes.* Mol Biol Evol, 2011. **28**(1): p. 859-71.
31. Goldin, A.L., *Evolution of voltage-gated Na(+) channels.* J Exp Biol, 2002. **205**(Pt 5): p. 575-84.
32. Novak, A.E., et al., *Gene duplications and evolution of vertebrate voltage-gated sodium channels.* J Mol Evol, 2006. **63**(2): p. 208-21.
33. Catterall, W.A., A.L. Goldin, and S.G. Waxman, *International Union of Pharmacology. XLVII. Nomenclature and structure-function relationships of voltage-gated sodium channels.* Pharmacol Rev, 2005. **57**(4): p. 397-409.

34. Flicek, P., et al., *Ensembl 2012.* Nucleic Acids Res, 2012. **40**(Database issue): p. D84-90.
35. Drenth, J.P. and S.G. Waxman, *Mutations in sodium-channel gene SCN9A cause a spectrum of human genetic pain disorders.* J Clin Invest, 2007. **117**(12): p. 3603-9.
36. George, A.L., Jr., et al., *Assignment of a human voltage-dependent sodium channel alpha-subunit gene (SCN6A) to 2q21-q23.* Genomics, 1994. **19**(2): p. 395-7.
37. Hiyama, T.Y., et al., *Na(x) channel involved in CNS sodium-level sensing.* Nat Neurosci, 2002. **5**(6): p. 511-2.
38. Trudeau, M.M., et al., *Heterozygosity for a protein truncation mutation of sodium channel SCN8A in a patient with cerebellar atrophy, ataxia, and mental retardation.* J Med Genet, 2006. **43**(6): p. 527-30.
39. Veeramah, K.R., et al., *De novo pathogenic SCN8A mutation identified by whole-genome sequencing of a family quartet affected by infantile epileptic encephalopathy and SUDEP.* Am J Hum Genet, 2012. **90**(3): p. 502-10.
40. Sharkey, L.M., et al., *The ataxia3 mutation in the N-terminal cytoplasmic domain of sodium channel Na(v)1.6 disrupts intracellular trafficking.* J Neurosci, 2009. **29**(9): p. 2733-41.
41. Kim, H., et al., *Hypokalemic periodic paralysis; two different genes responsible for similar clinical manifestations.* Korean J Pediatr, 2011. **54**(11): p. 473-6.
42. Heine, R., U. Pika, and F. Lehmann-Horn, *A novel SCN4A mutation causing myotonia aggravated by cold and potassium.* Hum Mol Genet, 1993. **2**(9): p. 1349-53.
43. Simkin, D., et al., *Mechanisms underlying a life-threatening skeletal muscle Na+ channel disorder.* J Physiol, 2011. **589**(Pt 13): p. 3115-24.
44. Yang, T., et al., *Blocking Scn10a channels in heart reduces late sodium current and is antiarrhythmic.* Circ Res, 2012. **111**(3): p. 322-32.
45. Denny, J.C., et al., *Identification of genomic predictors of atrioventricular conduction: using electronic medical records as a tool for genome science.* Circulation, 2010. **122**(20): p. 2016-21.
46. Noujaim, S.F., et al., *A null mutation of the neuronal sodium channel NaV1.6 disrupts action potential propagation and excitation-contraction coupling in the mouse heart.* FASEB J, 2012. **26**(1): p. 63-72.
47. Maier, S.K., et al., *An unexpected role for brain-type sodium channels in coupling of cell surface depolarization to contraction in the heart.* Proc Natl Acad Sci U S A, 2002. **99**(6): p. 4073-8.
48. Moric, E., et al., *The implications of genetic mutations in the sodium channel gene (SCN5A).* Europace, 2003. **5**(4): p. 325-34.
49. Gellens, M.E., et al., *Primary structure and functional expression of the human cardiac tetrodotoxin-insensitive voltage-dependent sodium channel.* Proc Natl Acad Sci U S A, 1992. **89**(2): p. 554-8.

50. Murphy, L.L., et al., *Developmentally regulated SCN5A splice variant potentiates dysfunction of a novel mutation associated with severe fetal arrhythmia.* Heart Rhythm, 2012. **9**(4): p. 590-7.
51. Shang, L.L., et al., *Human heart failure is associated with abnormal C-terminal splicing variants in the cardiac sodium channel.* Circ Res, 2007. **101**(11): p. 1146-54.
52. Ou, S.W., et al., *Tetrodotoxin-resistant Na+ channels in human neuroblastoma cells are encoded by new variants of Nav1.5/SCN5A.* Eur J Neurosci, 2005. **22**(4): p. 793-801.
53. Yang, P., S. Kupershmidt, and D.M. Roden, *Cloning and initial characterization of the human cardiac sodium channel (SCN5A) promoter.* Cardiovasc Res, 2004. **61**(1): p. 56-65.
54. Atack, T.C., et al., *Informatic and functional approaches to identifying a regulatory region for the cardiac sodium channel.* Circ Res, 2011. **109**(1): p. 38-46.
55. NCBI. *HomoloGene*. 2013; Available from: http://www.ncbi.nlm.nih.gov/homologene.
56. Novak, A.E., et al., *Embryonic and larval expression of zebrafish voltage-gated sodium channel α-subunit genes.* Developmental Dynamics, 2006. **235**(7): p. 1962-1973.
57. Schoonheim, P.J., et al., *Optogenetic localization and genetic perturbation of saccade-generating neurons in zebrafish.* J Neurosci, 2010. **30**(20): p. 7111-20.
58. Wright, M.A., et al., *In vivo evidence for transdifferentiation of peripheral neurons.* Development, 2010. **137**(18): p. 3047-56.
59. Low, S.E., et al., *Na(v)1.6a is required for normal activation of motor circuits normally excited by tactile stimulation.* Dev Neurobiol, 2010. **70**(7): p. 508-22.
60. Tsai, C.W., et al., *Primary structure and developmental expression of zebrafish sodium channel Na(v)1.6 during neurogenesis.* DNA Cell Biol, 2001. **20**(5): p. 249-55.
61. Chopra, S.S., et al., *Voltage-gated sodium channels are required for heart development in zebrafish.* Circ Res, 2010. **106**(8): p. 1342-50.
62. Roden, D.M. and A.L. George, Jr., *Structure and function of cardiac sodium and potassium channels.* Am J Physiol, 1997. **273**(2 Pt 2): p. H511-25.
63. Balser, J.R., *Structure and function of the cardiac sodium channels.* Cardiovasc Res, 1999. **42**(2): p. 327-38.
64. Perez-Garcia, M.T., et al., *Structure of the sodium channel pore revealed by serial cysteine mutagenesis.* Proc Natl Acad Sci U S A, 1996. **93**(1): p. 300-4.
65. Clatot, J., et al., *Dominant-negative effect of SCN5A N-terminal mutations through the interaction of Na(v)1.5 alpha-subunits.* Cardiovasc Res, 2012. **96**(1): p. 53-63.
66. Herfst, L.J., M.B. Rook, and H.J. Jongsma, *Trafficking and functional expression of cardiac Na+ channels.* J Mol Cell Cardiol, 2004. **36**(2): p. 185-93.

67. Lemaillet, G., B. Walker, and S. Lambert, *Identification of a conserved ankyrin-binding motif in the family of sodium channel alpha subunits.* J Biol Chem, 2003. **278**(30): p. 27333-9.
68. Lowe, J.S., et al., *Voltage-gated Nav channel targeting in the heart requires an ankyrin-G dependent cellular pathway.* J Cell Biol, 2008. **180**(1): p. 173-86.
69. West, J.W., et al., *A cluster of hydrophobic amino acid residues required for fast Na(+)-channel inactivation.* Proc Natl Acad Sci U S A, 1992. **89**(22): p. 10910-4.
70. Chandra, R., C.F. Starmer, and A.O. Grant, *Multiple effects of KPQ deletion mutation on gating of human cardiac Na+ channels expressed in mammalian cells.* Am J Physiol, 1998. **274**(5 Pt 2): p. H1643-54.
71. Bennett, P.B., et al., *Molecular mechanism for an inherited cardiac arrhythmia.* Nature, 1995. **376**(6542): p. 683-5.
72. Yamamura, K., et al., *A novel SCN5A mutation associated with the linker between III and IV domains of Nav1.5 in a neonate with fatal long QT syndrome.* Int J Cardiol, 2010. **145**(1): p. 61-4.
73. Catterall, W.A., *Voltage-gated sodium channels at 60: structure, function and pathophysiology.* J Physiol, 2012. **590**(Pt 11): p. 2577-89.
74. Ashpole, N.M., et al., *Ca2+/calmodulin-dependent protein kinase II (CaMKII) regulates cardiac sodium channel NaV1.5 gating by multiple phosphorylation sites.* J Biol Chem, 2012. **287**(24): p. 19856-69.
75. Gavillet, B., et al., *Cardiac sodium channel Nav1.5 is regulated by a multiprotein complex composed of syntrophins and dystrophin.* Circ Res, 2006. **99**(4): p. 407-14.
76. Gomez-Ospina, N., et al., *The C terminus of the L-type voltage-gated calcium channel Ca(V)1.2 encodes a transcription factor.* Cell, 2006. **127**(3): p. 591-606.
77. Tateyama, M., et al., *Structural effects of an LQT-3 mutation on heart Na+ channel gating.* Biophys J, 2004. **86**(3): p. 1843-51.
78. Cormier, J.W., et al., *Secondary structure of the human cardiac Na+ channel C terminus: evidence for a role of helical structures in modulation of channel inactivation.* J Biol Chem, 2002. **277**(11): p. 9233-41.
79. Wingo, T.L., et al., *An EF-hand in the sodium channel couples intracellular calcium to cardiac excitability.* Nat Struct Mol Biol, 2004. **11**(3): p. 219-25.
80. Liu, C.J., et al., *Modulation of the cardiac sodium channel Nav1.5 by fibroblast growth factor homologous factor 1B.* J Biol Chem, 2003. **278**(2): p. 1029-36.
81. Wang, C., et al., *Crystal structure of the ternary complex of a NaV C-terminal domain, a fibroblast growth factor homologous factor, and calmodulin.* Structure, 2012. **20**(7): p. 1167-76.
82. Abriel, H. and R.S. Kass, *Regulation of the voltage-gated cardiac sodium channel Nav1.5 by interacting proteins.* Trends Cardiovasc Med, 2005. **15**(1): p. 35-40.

83. Fotia, A.B., et al., *Regulation of neuronal voltage-gated sodium channels by the ubiquitin-protein ligases Nedd4 and Nedd4-2.* J Biol Chem, 2004. **279**(28): p. 28930-5.
84. Ou, Y., et al., *Syntrophin gamma 2 regulates SCN5A gating by a PDZ domain-mediated interaction.* J Biol Chem, 2003. **278**(3): p. 1915-23.
85. Ueda, K., et al., *Syntrophin mutation associated with long QT syndrome through activation of the nNOS-SCN5A macromolecular complex.* Proc Natl Acad Sci U S A, 2008. **105**(27): p. 9355-60.
86. Larkin, M.A., et al., *Clustal W and Clustal X version 2.0.* Bioinformatics, 2007. **23**(21): p. 2947-8.
87. Arnold, K., et al., *The SWISS-MODEL workspace: a web-based environment for protein structure homology modelling.* Bioinformatics, 2006. **22**(2): p. 195-201.
88. Patino, G.A. and L.L. Isom, *Electrophysiology and beyond: multiple roles of Na+ channel beta subunits in development and disease.* Neurosci Lett, 2010. **486**(2): p. 53-9.
89. Savio-Galimberti, E., M.H. Gollob, and D. Darbar, *Voltage-gated sodium channels: biophysics, pharmacology, and related channelopathies.* Front Pharmacol, 2012. **3**: p. 124.
90. Brackenbury, W.J. and L.L. Isom, *Na Channel beta Subunits: Overachievers of the Ion Channel Family.* Front Pharmacol, 2011. **2**: p. 53.
91. An, R.H., et al., *Novel LQT-3 mutation affects Na+ channel activity through interactions between alpha- and beta1-subunits.* Circ Res, 1998. **83**(2): p. 141-6.
92. Chopra, S.S., et al., *Molecular cloning and analysis of zebrafish voltage-gated sodium channel beta subunit genes: implications for the evolution of electrical signaling in vertebrates.* BMC Evol Biol, 2007. **7**: p. 113.
93. Sherry, S.T., et al., *dbSNP: the NCBI database of genetic variation.* Nucleic Acids Res, 2001. **29**(1): p. 308-11.
94. Sotoodehnia, N., et al., *Common variants in 22 loci are associated with QRS duration and cardiac ventricular conduction.* Nat Genet, 2010. **42**(12): p. 1068-76.
95. Smith, J.G., et al., *Genome-wide association studies of the PR interval in African Americans.* PLoS Genet, 2011. **7**(2): p. e1001304.
96. Smith, J.G., et al., *Genome-wide association study of electrocardiographic conduction measures in an isolated founder population: Kosrae.* Heart Rhythm, 2009. **6**(5): p. 634-41.
97. Pfeufer, A., et al., *Genome-wide association study of PR interval.* Nat Genet, 2010. **42**(2): p. 153-9.
98. Holm, H., et al., *Several common variants modulate heart rate, PR interval and QRS duration.* Nat Genet, 2010. **42**(2): p. 117-22.

99. George, A.L., Jr., *Molecular and genetic basis of sudden cardiac death.* J Clin Invest, 2013. **123**(1): p. 75-83.
100. Behr, E.R., et al., *Sudden arrhythmic death syndrome: familial evaluation identifies inheritable heart disease in the majority of families.* Eur Heart J, 2008. **29**(13): p. 1670-80.
101. Marchlinski, F., *Chapter 233. The Tachyarrhythmias*, in *Harrison's Principles of Internal Medicine.*, F.A. Longo DL, Kasper DL, Hauser SL, Jameson JL, Loscalzo J, eds, Editor. 2012, McGraw-Hill: New York.
102. Wang, Q., et al., *SCN5A mutations associated with an inherited cardiac arrhythmia, long QT syndrome.* Cell, 1995. **80**(5): p. 805-11.
103. Jiang, C., et al., *Two long QT syndrome loci map to chromosomes 3 and 7 with evidence for further heterogeneity.* Nat Genet, 1994. **8**(2): p. 141-7.
104. Liu, K., et al., *New mechanism contributing to drug-induced arrhythmia: rescue of a misprocessed LQT3 mutant.* Circulation, 2005. **112**(21): p. 3239-46.
105. Hedley, P.L., et al., *The genetic basis of long QT and short QT syndromes: a mutation update.* Hum Mutat, 2009. **30**(11): p. 1486-511.
106. Song, W. and W. Shou, *Cardiac sodium channel Nav1.5 mutations and cardiac arrhythmia.* Pediatr Cardiol, 2012. **33**(6): p. 943-9.
107. George, A.L., Jr., *Restoring repolarization in LQT3.* Heart Rhythm, 2009. **6**(1): p. 107-8.
108. Ackerman, M.J., et al., *Postmortem molecular analysis of SCN5A defects in sudden infant death syndrome.* JAMA, 2001. **286**(18): p. 2264-9.
109. Plant, L.D., et al., *A common cardiac sodium channel variant associated with sudden infant death in African Americans, SCN5A S1103Y.* J Clin Invest, 2006. **116**(2): p. 430-5.
110. Abriel, H. and E.V. Zaklyazminskaya, *Cardiac channelopathies: genetic and molecular mechanisms.* Gene, 2013. **517**(1): p. 1-11.
111. Kapplinger, J.D., et al., *An international compendium of mutations in the SCN5A-encoded cardiac sodium channel in patients referred for Brugada syndrome genetic testing.* Heart Rhythm, 2010. **7**(1): p. 33-46.
112. Riuro, H., et al., *A Missense Mutation in the Sodium Channel beta2 Subunit Reveals SCN2B as a New Candidate Gene for Brugada Syndrome.* Hum Mutat, 2013.
113. Janse, M.J. and A.A. Wilde, *Molecular mechanisms of arrhythmias.* Rev Port Cardiol, 1998. **17 Suppl 2**: p. II41-6.
114. Brugada, R., et al., *Brugada Syndrome*, in *GeneReviews*, R.A. Pagon, et al., Editors. 1993: Seattle (WA).
115. LW Stevenson, J.L., *Chapter 238. Cardiomyopathy and Myocarditis*, in *Harrison's Principles of Internal Medicine*, A.F. DL Longo, DL Kasper, SL Hauser, JL Jameson, J Loscalzo, Editor. 2012, McGraw-Hill: New York.
116. McNair, W.P., et al., *SCN5A mutation associated with dilated cardiomyopathy, conduction disorder, and arrhythmia.* Circulation, 2004. **110**(15): p. 2163-7.

117. Mann, S.A., et al., *R222Q SCN5A mutation is associated with reversible ventricular ectopy and dilated cardiomyopathy.* J Am Coll Cardiol, 2012. **60**(16): p. 1566-73.
118. Shan, L., et al., *SCN5A variants in Japanese patients with left ventricular noncompaction and arrhythmia.* Mol Genet Metab, 2008. **93**(4): p. 468-74.
119. Nguyen, T.P., et al., *Divergent biophysical defects caused by mutant sodium channels in dilated cardiomyopathy with arrhythmia.* Circ Res, 2008. **102**(3): p. 364-71.
120. Watanabe, H., et al., *Striking In vivo phenotype of a disease-associated human SCN5A mutation producing minimal changes in vitro.* Circulation, 2011. **124**(9): p. 1001-11.
121. Zaragoza, M.V., E. Arbustini, and J. Narula, *Noncompaction of the left ventricle: primary cardiomyopathy with an elusive genetic etiology.* Curr Opin Pediatr, 2007. **19**(6): p. 619-27.
122. BB Keller, R.M., JB Hoying, *Chapter 9. Molecular Development of the Heart*, in *Hurst's The Heart*, R.W. V Fuster, RA Harrington, Editor. 2011, McGraw-Hill: New York.
123. Liu, K., et al., *Recombinase-mediated cassette exchange to rapidly and efficiently generate mice with human cardiac sodium channels.* Genesis, 2006. **44**(11): p. 556-64.
124. Papadatos, G.A., et al., *Slowed conduction and ventricular tachycardia after targeted disruption of the cardiac sodium channel gene Scn5a.* Proc Natl Acad Sci U S A, 2002. **99**(9): p. 6210-5.
125. Martin, C.A., et al., *In vivo studies of Scn5a+/- mice modeling Brugada syndrome demonstrate both conduction and repolarization abnormalities.* J Electrocardiol, 2010. **43**(5): p. 433-9.
126. Davies, M.P., et al., *Developmental changes in ionic channel activity in the embryonic murine heart.* Circ Res, 1996. **78**(1): p. 15-25.
127. Rottbauer, W., et al., *Growth and function of the embryonic heart depend upon the cardiac-specific L-type calcium channel alpha1 subunit.* Dev Cell, 2001. **1**(2): p. 265-75.
128. Kimmel, C.B., et al., *Stages of embryonic development of the zebrafish.* Dev Dyn, 1995. **203**(3): p. 253-310.
129. Nasevicius, A. and S.C. Ekker, *Effective targeted gene /`knockdown/' in zebrafish.* Nat Genet, 2000. **26**(2): p. 216-220.
130. Stainier, D.Y., et al., *Mutations affecting the formation and function of the cardiovascular system in the zebrafish embryo.* Development, 1996. **123**: p. 285-92.
131. Chen, J.N., et al., *Mutations affecting the cardiovascular system and other internal organs in zebrafish.* Development, 1996. **123**: p. 293-302.
132. Bakkers, J., *Zebrafish as a model to study cardiac development and human cardiac disease.* Cardiovasc Res, 2011. **91**(2): p. 279-88.

133. Sehnert, A.J., et al., *Cardiac troponin T is essential in sarcomere assembly and cardiac contractility.* Nat Genet, 2002. **31**(1): p. 106-10.
134. Keegan, B.R., D. Meyer, and D. Yelon, *Organization of cardiac chamber progenitors in the zebrafish blastula.* Development, 2004. **131**(13): p. 3081-91.
135. Ueno, S., et al., *Biphasic role for Wnt/beta-catenin signaling in cardiac specification in zebrafish and embryonic stem cells.* Proc Natl Acad Sci U S A, 2007. **104**(23): p. 9685-90.
136. Dohn, T.E. and J.S. Waxman, *Distinct phases of Wnt/β-catenin signaling direct cardiomyocyte formation in zebrafish.* Dev Biol, 2012. **361**(2): p. 364-376.
137. de Pater, E., et al., *Bmp signaling exerts opposite effects on cardiac differentiation.* Circ Res, 2012. **110**(4): p. 578-87.
138. Reifers, F., et al., *Fgf8 is mutated in zebrafish acerebellar (ace) mutants and is required for maintenance of midbrain-hindbrain boundary development and somitogenesis.* Development, 1998. **125**(13): p. 2381-95.
139. Reifers, F., et al., *Induction and differentiation of the zebrafish heart requires fibroblast growth factor 8 (fgf8/acerebellar).* Development, 2000. **127**(2): p. 225-35.
140. Marques, S.R., et al., *Reiterative roles for FGF signaling in the establishment of size and proportion of the zebrafish heart.* Dev Biol, 2008. **321**(2): p. 397-406.
141. Takeuchi, J.K. and B.G. Bruneau, *Directed transdifferentiation of mouse mesoderm to heart tissue by defined factors.* Nature, 2009. **459**(7247): p. 708-11.
142. Lou, X., et al., *Smarcd3b and Gata5 promote a cardiac progenitor fate in the zebrafish embryo.* Development, 2011. **138**(15): p. 3113-23.
143. Ochi, H., S. Hans, and M. Westerfield, *Smarcd3 regulates the timing of zebrafish myogenesis onset.* J Biol Chem, 2008. **283**(6): p. 3529-36.
144. Lee, K.H., Q. Xu, and R.E. Breitbart, *A new tinman-related gene, nkx2.7, anticipates the expression of nkx2.5 and nkx2.3 in zebrafish heart and pharyngeal endoderm.* Dev Biol, 1996. **180**(2): p. 722-31.
145. Bodmer, R., *The gene tinman is required for specification of the heart and visceral muscles in Drosophila.* Development, 1993. **118**(3): p. 719-29.
146. Tanaka, M., et al., *The cardiac homeobox gene Csx/Nkx2.5 lies genetically upstream of multiple genes essential for heart development.* Development, 1999. **126**(6): p. 1269-80.
147. Schott, J.J., et al., *Congenital heart disease caused by mutations in the transcription factor NKX2-5.* Science, 1998. **281**(5373): p. 108-11.
148. Benson, D.W., et al., *Mutations in the cardiac transcription factor NKX2.5 affect diverse cardiac developmental pathways.* J Clin Invest, 1999. **104**(11): p. 1567-73.
149. McElhinney, D.B., et al., *NKX2.5 mutations in patients with congenital heart disease.* J Am Coll Cardiol, 2003. **42**(9): p. 1650-5.

150. Tu, C.-T., T.-C. Yang, and H.-J. Tsai, *Nkx2.7 and Nkx2.5 Function Redundantly and Are Required for Cardiac Morphogenesis of Zebrafish Embryos.* PLoS One, 2009. **4**(1): p. e4249.
151. Targoff, K.L., T. Schell, and D. Yelon, *Nkx genes regulate heart tube extension and exert differential effects on ventricular and atrial cell number.* Dev Biol, 2008. **322**(2): p. 314-321.
152. Heicklen-Klein, A., L.J. McReynolds, and T. Evans, *Using the zebrafish model to study GATA transcription factors.* Semin Cell Dev Biol, 2005. **16**(1): p. 95-106.
153. Reiter, J.F., et al., *Gata5 is required for the development of the heart and endoderm in zebrafish.* Genes Dev, 1999. **13**(22): p. 2983-95.
154. Holtzinger, A. and T. Evans, *Gata4 regulates the formation of multiple organs.* Development, 2005. **132**(17): p. 4005-14.
155. Peterkin, T., A. Gibson, and R. Patient, *GATA-6 maintains BMP-4 and Nkx2 expression during cardiomyocyte precursor maturation.* EMBO J, 2003. **22**(16): p. 4260-73.
156. Reiter, J.F., H. Verkade, and D.Y. Stainier, *Bmp2b and Oep promote early myocardial differentiation through their regulation of gata5.* Dev Biol, 2001. **234**(2): p. 330-8.
157. Jia, H., et al., *Vertebrate heart growth is regulated by functional antagonism between Gridlock and Gata5.* Proc Natl Acad Sci U S A, 2007. **104**(35): p. 14008-13.
158. Maves, L., et al., *Pbx acts with Hand2 in early myocardial differentiation.* Dev Biol, 2009. **333**(2): p. 409-18.
159. Garavito-Aguilar, Z.V., H.E. Riley, and D. Yelon, *Hand2 ensures an appropriate environment for cardiac fusion by limiting Fibronectin function.* Development, 2010. **137**(19): p. 3215-20.
160. Evans, S.M., et al., *Myocardial lineage development.* Circ Res, 2010. **107**(12): p. 1428-44.
161. Chen, Z., et al., *Depletion of zebrafish essential and regulatory myosin light chains reduces cardiac function through distinct mechanisms.* Cardiovasc Res, 2008. **79**(1): p. 97-108.
162. Stainier, D.Y.R., *Zebrafish genetics and vertebrate heart formation.* Nat Rev Genet, 2001. **2**(1): p. 39-48.
163. Hinits, Y., et al., *Zebrafish Mef2ca and Mef2cb are essential for both first and second heart field cardiomyocyte differentiation.* Dev Biol, 2012. **369**(2): p. 199-210.
164. Jin, D., et al., *Promoter analysis of ventricular myosin heavy chain (vmhc) in zebrafish embryos.* Dev Dyn, 2009. **238**(7): p. 1760-7.
165. Sultana, N., et al., *Zebrafish early cardiac connexin, Cx36.7/Ecx, regulates myofibril orientation and heart morphogenesis by establishing Nkx2.5 expression.* Proc Natl Acad Sci U S A, 2008. **105**(12): p. 4763-8.

166. Garrity, D.M., S. Childs, and M.C. Fishman, *The heartstrings mutation in zebrafish causes heart/fin Tbx5 deficiency syndrome.* Development, 2002. **129**(19): p. 4635-45.
167. Chi, N.C., et al., *Genetic and physiologic dissection of the vertebrate cardiac conduction system.* PLoS Biol, 2008. **6**(5): p. e109.
168. Moskowitz, I.P., et al., *The T-Box transcription factor Tbx5 is required for the patterning and maturation of the murine cardiac conduction system.* Development, 2004. **131**(16): p. 4107-16.
169. Arnolds, D.E., et al., *TBX5 drives Scn5a expression to regulate cardiac conduction system function.* J Clin Invest, 2012. **122**(7): p. 2509-18.
170. Moorman, A.F., et al., *The heart-forming fields: one or multiple?* Philos Trans R Soc Lond B Biol Sci, 2007. **362**(1484): p. 1257-65.
171. Hami, D., et al., *Zebrafish cardiac development requires a conserved secondary heart field.* Development, 2011. **138**(11): p. 2389-2398.
172. Kelly, R.G., *The second heart field.* Curr Top Dev Biol, 2012. **100**: p. 33-65.
173. Clark, C.D., et al., *Evolutionary conservation of Nkx2.5 autoregulation in the second heart field.* Dev Biol, 2013. **374**(1): p. 198-209.
174. Zaffran, S. and R.G. Kelly, *New developments in the second heart field.* Differentiation, 2012. **84**(1): p. 17-24.
175. de Pater, E., et al., *Distinct phases of cardiomyocyte differentiation regulate growth of the zebrafish heart.* Development, 2009. **136**(10): p. 1633-41.
176. Ando, R., et al., *An optical marker based on the UV-induced green-to-red photoconversion of a fluorescent protein.* Proc Natl Acad Sci U S A, 2002. **99**(20): p. 12651-6.
177. Furthauer, M., et al., *sprouty4 acts in vivo as a feedback-induced antagonist of FGF signaling in zebrafish.* Development, 2001. **128**(12): p. 2175-86.
178. Lazic, S. and I.C. Scott, *Mef2cb regulates late myocardial cell addition from a second heart field-like population of progenitors in zebrafish.* Dev Biol, 2011. **354**(1): p. 123-133.
179. Zhou, Y., et al., *Latent TGF-beta binding protein 3 identifies a second heart field in zebrafish.* Nature, 2011. **474**(7353): p. 645-8.
180. Robu, M.E., et al., *p53 activation by knockdown technologies.* PLoS Genet, 2007. **3**(5): p. e78.
181. Westerfield, M., *The zebrafish book. A guide for the laboratory use of Zebrafish (Danio rerio).* 4th ed. 2000, Eugene: Univ. of Oregon Press.
182. Ao, A., et al., *DMH1, a novel BMP small molecule inhibitor, increases cardiomyocyte progenitors and promotes cardiac differentiation in mouse embryonic stem cells.* PLoS One, 2012. **7**(7): p. e41627.
183. Sato, N., et al., *Maintenance of pluripotency in human and mouse embryonic stem cells through activation of Wnt signaling by a pharmacological GSK-3-specific inhibitor.* Nat Med, 2004. **10**(1): p. 55-63.

184. Ro, H., et al., *Novel vector systems optimized for injecting in vitro-synthesized mRNA into zebrafish embryos.* Mol Cells, 2004. **17**(2): p. 373-6.
185. Kwan, K.M., et al., *The Tol2kit: a multisite gateway-based construction kit for Tol2 transposon transgenesis constructs.* Dev Dyn, 2007. **236**(11): p. 3088-99.
186. Yu, P.B., et al., *Dorsomorphin inhibits BMP signals required for embryogenesis and iron metabolism.* Nat Chem Biol, 2008. **4**(1): p. 33-41.
187. Brown, C.O., 3rd, et al., *The cardiac determination factor, Nkx2-5, is activated by mutual cofactors GATA-4 and Smad1/4 via a novel upstream enhancer.* J Biol Chem, 2004. **279**(11): p. 10659-69.
188. Little, S.C. and M.C. Mullins, *Twisted gastrulation promotes BMP signaling in zebrafish dorsal-ventral axial patterning.* Development, 2004. **131**(23): p. 5825-35.
189. Coverdale, L.E., L.E. Burton, and C.C. Martin, *High-throughput whole mount in situ hybridization of zebrafish embryos for analysis of tissue-specific gene expression changes after environmental perturbation.* Methods Mol Biol, 2008. **410**: p. 3-14.
190. Verkerk, A.O. and C.A. Remme, *Zebrafish: a novel research tool for cardiac (patho)electrophysiology and ion channel disorders.* Front Physiol, 2012. **3**: p. 255.
191. Barrionuevo, W.R. and W.W. Burggren, *O2 consumption and heart rate in developing zebrafish (Danio rerio): influence of temperature and ambient O2.* Am J Physiol, 1999. **276**(2 Pt 2): p. R505-13.
192. Baker, K., et al., *Defective "pacemaker" current (Ih) in a zebrafish mutant with a slow heart rate.* Proc Natl Acad Sci U S A, 1997. **94**(9): p. 4554-9.
193. Leong, I.U., et al., *Zebrafish as a model for long QT syndrome: the evidence and the means of manipulating zebrafish gene expression.* Acta Physiol (Oxf), 2010. **199**(3): p. 257-76.
194. Sedmera, D., et al., *Functional and morphological evidence for a ventricular conduction system in zebrafish and Xenopus hearts.* Am J Physiol Heart Circ Physiol, 2003. **284**(4): p. H1152-60.
195. Milan, D.J., et al., *In vivo recording of adult zebrafish electrocardiogram and assessment of drug-induced QT prolongation.* Am J Physiol Heart Circ Physiol, 2006. **291**(1): p. H269-73.
196. Brette, F., et al., *Characterization of isolated ventricular myocytes from adult zebrafish (Danio rerio).* Biochem Biophys Res Commun, 2008. **374**(1): p. 143-6.
197. Chi, N.C., et al., *Cardiac conduction is required to preserve cardiac chamber morphology.* Proc Natl Acad Sci U S A, 2010. **107**(33): p. 14662-7.
198. Auman, H.J., et al., *Functional modulation of cardiac form through regionally confined cell shape changes.* PLoS Biol, 2007. **5**(3): p. e53.
199. DiFrancesco, D., *Pacemaker mechanisms in cardiac tissue.* Annu Rev Physiol, 1993. **55**: p. 455-72.

200. Warren, K.S., K. Baker, and M.C. Fishman, *The slow mo mutation reduces pacemaker current and heart rate in adult zebrafish.* Am J Physiol Heart Circ Physiol, 2001. **281**(4): p. H1711-9.
201. Hassel, D., et al., *Deficient zebrafish ether-a-go-go-related gene channel gating causes short-QT syndrome in zebrafish reggae mutants.* Circulation, 2008. **117**(7): p. 866-75.
202. Kopp, R., T. Schwerte, and B. Pelster, *Cardiac performance in the zebrafish breakdance mutant.* J Exp Biol, 2005. **208**(Pt 11): p. 2123-34.
203. Mittelstadt, S.W., et al., *Evaluation of zebrafish embryos as a model for assessing inhibition of hERG.* J Pharmacol Toxicol Methods, 2008. **57**(2): p. 100-5.
204. Milan, D.J., et al., *Drug-sensitized zebrafish screen identifies multiple genes, including GINS3, as regulators of myocardial repolarization.* Circulation, 2009. **120**(7): p. 553-9.
205. Meder, B., et al., *Reconstitution of defective protein trafficking rescues Long-QT syndrome in zebrafish.* Biochem Biophys Res Commun, 2011. **408**(2): p. 218-24.
206. Menick, D.R., et al., *Transcriptional pathways and potential therapeutic targets in the regulation of Ncx1 expression in cardiac hypertrophy and failure.* Adv Exp Med Biol, 2013. **961**: p. 125-35.
207. Kessler, M., S. Just, and W. Rottbauer, *Ion flux dependent and independent functions of ion channels in the vertebrate heart: lessons learned from zebrafish.* Stem Cells Int, 2012. **2012**: p. 462161.
208. Ebert, A.M., et al., *Calcium extrusion is critical for cardiac morphogenesis and rhythm in embryonic zebrafish hearts.* Proc Natl Acad Sci U S A, 2005. **102**(49): p. 17705-10.
209. Langenbacher, A.D., et al., *Mutation in sodium-calcium exchanger 1 (NCX1) causes cardiac fibrillation in zebrafish.* Proc Natl Acad Sci U S A, 2005. **102**(49): p. 17699-704.
210. Kim, J.W., et al., *A common variant in SLC8A1 is associated with the duration of the electrocardiographic QT interval.* Am J Hum Genet, 2012. **91**(1): p. 180-4.
211. Hasenfuss, G. and W. Schillinger, *Is modulation of sodium-calcium exchange a therapeutic option in heart failure?* Circ Res, 2004. **95**(3): p. 225-7.
212. Shu, X., et al., *Na,K-ATPase is essential for embryonic heart development in the zebrafish.* Development, 2003. **130**(25): p. 6165-73.
213. Shu, X., et al., *Na,K-ATPase alpha2 and Ncx4a regulate zebrafish left-right patterning.* Development, 2007. **134**(10): p. 1921-30.
214. Chernyavskaya, Y., et al., *Voltage-gated calcium channel CACNB2 (beta2.1) protein is required in the heart for control of cell proliferation and heart tube integrity.* Dev Dyn, 2012. **241**(4): p. 648-62.
215. Burns, C.G., et al., *High-throughput assay for small molecules that modulate zebrafish embryonic heart rate.* Nat Chem Biol, 2005. **1**(5): p. 263-4.

216. el-Sherif, N., H.A. Fozzard, and D.A. Hanck, *Dose-dependent modulation of the cardiac sodium channel by sea anemone toxin ATXII.* Circ Res, 1992. **70**(2): p. 285-301.
217. Ulbricht, W. and J. Schmidtmayer, *Modification of sodium channels in myelinated nerve by Anemonia sulcata toxin II.* J Physiol (Paris), 1981. **77**(9): p. 1103-11.
218. Shigenobu, K. and N. Sperelakis, *Development of sensitivity to tetrodotoxin of chick embryonic hearts with age.* J Mol Cell Cardiol, 1971. **3**(3): p. 271-86.
219. Vornanen, M., M. Hassinen, and J. Haverinen, *Tetrodotoxin sensitivity of the vertebrate cardiac Na+ current.* Mar Drugs, 2011. **9**(11): p. 2409-22.
220. Isogai, S., M. Horiguchi, and B.M. Weinstein, *The vascular anatomy of the developing zebrafish: an atlas of embryonic and early larval development.* Dev Biol, 2001. **230**(2): p. 278-301.
221. Link, V., A. Shevchenko, and C.P. Heisenberg, *Proteomics of early zebrafish embryos.* BMC Dev Biol, 2006. **6**: p. 1.
222. Csernoch, L., et al., *Effects of tetracaine on sarcoplasmic calcium release in mammalian skeletal muscle fibres.* J Physiol, 1999. **515 (Pt 3)**: p. 843-57.
223. Salkoff, L.B. and M.A. Tanouye, *Genetics of ion channels.* Physiol Rev, 1986. **66**(2): p. 301-29.
224. Fiske, J.L., et al., *Voltage-sensitive ion channels and cancer.* Cancer Metastasis Rev, 2006. **25**(3): p. 493-500.
225. Gao, R., et al., *Expression of voltage-gated sodium channel alpha subunit in human ovarian cancer.* Oncol Rep, 2010. **23**(5): p. 1293-9.
226. Yang, M., et al., *Therapeutic potential for phenytoin: targeting Na(v)1.5 sodium channels to reduce migration and invasion in metastatic breast cancer.* Breast Cancer Res Treat, 2012. **134**(2): p. 603-15.
227. Levin, M., *Molecular bioelectricity in developmental biology: new tools and recent discoveries: control of cell behavior and pattern formation by transmembrane potential gradients.* Bioessays, 2012. **34**(3): p. 205-17.
228. Blackiston, D.J., K.A. McLaughlin, and M. Levin, *Bioelectric controls of cell proliferation: ion channels, membrane voltage and the cell cycle.* Cell Cycle, 2009. **8**(21): p. 3519-28.
229. Freedman, B.D., M.A. Price, and C.J. Deutsch, *Evidence for voltage modulation of IL-2 production in mitogen-stimulated human peripheral blood lymphocytes.* J Immunol, 1992. **149**(12): p. 3784-94.
230. Adams, D.S. and M. Levin, *Endogenous voltage gradients as mediators of cell-cell communication: strategies for investigating bioelectrical signals during pattern formation.* Cell Tissue Res, 2013. **352**(1): p. 95-122.
231. Lynagh, T., et al., *Molecular determinants of ivermectin sensitivity at the glycine receptor chloride channel.* J Biol Chem, 2011. **286**(51): p. 43913-24.

232. Zhang, R. and X. Xu, *Transient and transgenic analysis of the zebrafish ventricular myosin heavy chain (vmhc) promoter: an inhibitory mechanism of ventricle-specific gene expression.* Dev Dyn, 2009. **238**(6): p. 1564-73.
233. Sabeh, M.K., H. Kekhia, and C.A. Macrae, *Optical mapping in the developing zebrafish heart.* Pediatr Cardiol, 2012. **33**(6): p. 916-22.
234. Poss, K.D., L.G. Wilson, and M.T. Keating, *Heart regeneration in zebrafish.* Science, 2002. **298**(5601): p. 2188-90.
235. Jopling, C., et al., *Zebrafish heart regeneration occurs by cardiomyocyte dedifferentiation and proliferation.* Nature, 2010. **464**(7288): p. 606-9.
236. Lien, C.L., et al., *Gene expression analysis of zebrafish heart regeneration.* PLoS Biol, 2006. **4**(8): p. e260.
237. Ribeiro, I., et al., *Tbx2 and Tbx3 regulate the dynamics of cell proliferation during heart remodeling.* PLoS One, 2007. **2**(4): p. e398.
238. Chen, J.N. and M.C. Fishman, *Zebrafish tinman homolog demarcates the heart field and initiates myocardial differentiation.* Development, 1996. **122**(12): p. 3809-16.
239. Qu, X., et al., *Ndrg4 is required for normal myocyte proliferation during early cardiac development in zebrafish.* Dev Biol, 2008. **317**(2): p. 486-96.
240. Lam, N.T., et al., *Nerve growth factor stimulates cardiac regeneration via cardiomyocyte proliferation in experimental heart failure.* PLoS One, 2012. **7**(12): p. e53210.
241. Glickman, N.S. and D. Yelon, *Cardiac development in zebrafish: coordination of form and function.* Semin Cell Dev Biol, 2002. **13**(6): p. 507-13.
242. Rohr, S., N. Bit-Avragim, and S. Abdelilah-Seyfried, *Heart and soul/PRKCi and nagie oko/Mpp5 regulate myocardial coherence and remodeling during cardiac morphogenesis.* Development, 2006. **133**(1): p. 107-15.
243. Mably, J.D., et al., *santa and valentine pattern concentric growth of cardiac myocardium in the zebrafish.* Development, 2006. **133**(16): p. 3139-46.
244. Mably, J.D., et al., *heart of glass regulates the concentric growth of the heart in zebrafish.* Curr Biol, 2003. **13**(24): p. 2138-47.
245. Kleaveland, B., et al., *Regulation of cardiovascular development and integrity by the heart of glass-cerebral cavernous malformation protein pathway.* Nat Med, 2009. **15**(2): p. 169-76.
246. Rosen, J.N., et al., *ccm2-like is required for cardiovascular development as a novel component of the Heg-CCM pathway.* Dev Biol, 2013. **376**(1): p. 74-85.
247. Peshkovsky, C., R. Totong, and D. Yelon, *Dependence of cardiac trabeculation on neuregulin signaling and blood flow in zebrafish.* Dev Dyn, 2011. **240**(2): p. 446-56.
248. Sato, T., M. Takahoko, and H. Okamoto, *HuC:Kaede, a useful tool to label neural morphologies in networks in vivo.* Genesis, 2006. **44**(3): p. 136-42.

249. Huang, C.J., et al., *Germ-line transmission of a myocardium-specific GFP transgene reveals critical regulatory elements in the cardiac myosin light chain 2 promoter of zebrafish.* Dev Dyn, 2003. **228**(1): p. 30-40.
250. Scott, E.K., et al., *Targeting neural circuitry in zebrafish using GAL4 enhancer trapping.* Nat Meth, 2007. **4**(4): p. 323-326.
251. Abramoff, M.D., P.J. Magalhaes, and S.J. Ram, *Image Processing with ImageJ.* Biophotonics International, 2004. **11**(7): p. 36-42.
252. Arnaout, R., et al., *Zebrafish model for human long QT syndrome.* Proc Natl Acad Sci U S A, 2007. **104**(27): p. 11316-21.
253. Lin, Y.F., I. Swinburne, and D. Yelon, *Multiple influences of blood flow on cardiomyocyte hypertrophy in the embryonic zebrafish heart.* Dev Biol, 2012. **362**(2): p. 242-53.
254. Rottbauer, W., et al., *Cardiac myosin light chain-2: a novel essential component of thick-myofilament assembly and contractility of the heart.* Circ Res, 2006. **99**(3): p. 323-31.
255. Balasuriya, D., et al., *The sigma-1 receptor binds to the Nav1.5 voltage-gated Na+ channel with 4-fold symmetry.* J Biol Chem, 2012. **287**(44): p. 37021-9.
256. Lin, S.L., J.D. Miller, and S.Y. Ying, *Intronic microRNA (miRNA).* J Biomed Biotechnol, 2006. **2006**(4): p. 26818.
257. Mercier, A., et al., *The beta1-subunit of Na(v)1.5 cardiac sodium channel is required for a dominant negative effect through alpha-alpha interaction.* PLoS One, 2012. **7**(11): p. e48690.
258. Chazin, W.J., *Relating form and function of EF-hand calcium binding proteins.* Acc Chem Res, 2011. **44**(3): p. 171-9.
259. van Bemmelen, M.X., et al., *Cardiac voltage-gated sodium channel Nav1.5 is regulated by Nedd4-2 mediated ubiquitination.* Circ Res, 2004. **95**(3): p. 284-91.
260. Olsen, S.K., et al., *Fibroblast growth factor (FGF) homologous factors share structural but not functional homology with FGFs.* J Biol Chem, 2003. **278**(36): p. 34226-36.
261. Brookfield, R., et al., *Unsuccessful attempt at gene-editing by homologous recombination in the zebrafish germ line using the approach of "Rong and Golic".* Transgenic Res, 2012. **21**(5): p. 1125-36.
262. Streisinger, G., et al., *Production of clones of homozygous diploid zebra fish (Brachydanio rerio).* Nature, 1981. **291**(5813): p. 293-6.
263. Driever, W., et al., *A genetic screen for mutations affecting embryogenesis in zebrafish.* Development, 1996. **123**: p. 37-46.
264. Wang, D., et al., *Efficient genome-wide mutagenesis of zebrafish genes by retroviral insertions.* Proc Natl Acad Sci U S A, 2007. **104**(30): p. 12428-33.
265. Amsterdam, A., G.K. Varshney, and S.M. Burgess, *Retroviral-mediated Insertional Mutagenesis in Zebrafish.* Methods Cell Biol, 2011. **104**: p. 59-82.

266. Kettleborough, R.N., et al., *A systematic genome-wide analysis of zebrafish protein-coding gene function.* Nature, 2013.
267. Porteus, M.H. and D. Carroll, *Gene targeting using zinc finger nucleases.* Nat Biotechnol, 2005. **23**(8): p. 967-73.
268. Meng, X., et al., *Targeted gene inactivation in zebrafish using engineered zinc-finger nucleases.* Nat Biotechnol, 2008. **26**(6): p. 695-701.
269. Gaj, T., C.A. Gersbach, and C.F. Barbas, 3rd, *ZFN, TALEN, and CRISPR/Cas-based methods for genome engineering.* Trends Biotechnol, 2013.
270. Reyon, D., et al., *FLASH assembly of TALENs for high-throughput genome editing.* Nat Biotechnol, 2012. **30**(5): p. 460-5.
271. Cong, L., et al., *Multiplex genome engineering using CRISPR/Cas systems.* Science, 2013. **339**(6121): p. 819-23.
272. Hwang, W.Y., et al., *Efficient genome editing in zebrafish using a CRISPR-Cas system.* Nat Biotechnol, 2013. **31**(3): p. 227-9.
273. Abriel, H., *Cardiac sodium channel Na(v)1.5 and interacting proteins: Physiology and pathophysiology.* J Mol Cell Cardiol, 2010. **48**(1): p. 2-11.
274. Mortazavi, A., et al., *Mapping and quantifying mammalian transcriptomes by RNA-Seq.* Nat Methods, 2008. **5**(7): p. 621-8.
275. Manduchi, E., et al., *Comparison of different labeling methods for two-channel high-density microarray experiments.* Physiol Genomics, 2002. **10**(3): p. 169-79.
276. Diboun, I., et al., *Microarray analysis after RNA amplification can detect pronounced differences in gene expression using limma.* BMC Genomics, 2006. **7**: p. 252.
277. Mutz, K.O., et al., *Transcriptome analysis using next-generation sequencing.* Curr Opin Biotechnol, 2013. **24**(1): p. 22-30.
278. Wang, Z., M. Gerstein, and M. Snyder, *RNA-Seq: a revolutionary tool for transcriptomics.* Nat Rev Genet, 2009. **10**(1): p. 57-63.